

Geosciences 2016

Annual Conference of the Geoscience Society of
New Zealand, Wanaka

Field Trip 1
25-28 November 2016

Tectonics of the Pacific-Australian Plate Boundary

Leader: Virginia Toy
University of Otago

Bibliographic reference:

Toy, V.G., Norris, R.J., Cooper, A.F., Sibson, R.H., Little, T., Sutherland, R., Langridge, R., Berryman, K. (2016). Tectonics of the Pacific Australian Plate Boundary. *In*: Smillie, R. (compiler). Fieldtrip Guides, Geosciences 2016 Conference, Wanaka, New Zealand. Geoscience Society of New Zealand Miscellaneous Publication 145B, 86p.

ISBN 978-1-877480-53-9

ISSN (print) : 2230-4487

ISSN (online) : 2230-4495



Frontispiece: Near-surface displacement on the Alpine Fault has been localised in an ~1cm thick gouge zone exposed in the bed of Hare Mare Creek. Photo by D.J. Prior.

INTRODUCTION

This guide contains background geological information about sites that we hope to visit on this field trip. It is based primarily on the one that has been used for University of Otago Geology Department West Coast Field Trips for the last 30 years, partially updated to reflect recently published research. Copies of relevant recent publications will also be made available. Flexibility with respect to weather, driving times, and participant interest may mean that we do not see all of these sites. Stops are denoted by letters, and their locations indicated on Figure 1.

List of stops and milestones						
Date	Time start	Time stop	Location	Stop letter	Aim of stop	Notes
25-Nov	800	930	N Door Geol Dept, Dunedin		Food delivery	
	930	1015	N Door Geology, Dunedin		VT, AV, Nathaniel Chandrakumar go to Hansens in Kai Valley to collect van	
	1015	1100	New World, Dunedin		Shopping for last food supplies	
	1115	1130	N Door		Pick up Gilbert van Reenen	
	1130	1700	<i>Dud-Chch</i>		Drive to Chch airport to collect other participants	
	1700	1900	<i>Chch-Flockhill</i>		Drive Chch Airport - Flockhill Lodge	Stop at a shop so people can buy beer/wine/snacks
26-Nov	1900		Flockhill Lodge		Overnight accommodation; cook meal (nachos); sleep	Flockhill Lodge: SH 73, Arthur's Pass 7875. Ph: (03) 318 8196. Email: mail@flockhill.co.nz
	900	945	<i>Flockhill - Arthur's Pass</i>	A	Overview; road infrastructure	Stop in Arthur's Pass village for toilets
	945	1030	<i>Arthur's Pass - Taramakau</i>			
	1030	1045	Taramakau	B	Standing on the AF! View up and down valley	
	1045	1130	<i>Taramakau - Hokitika</i>		Toilet break; coffee break; souvenir shopping	
	1130	1200	<i>Hokitika - Mt Harry</i>			
	1200	1300	Mt Harry	C	Terrace offsets, trenches, mylonite type section, Round Top debris avalanche	
	1300	1315	Mt Harry - Hokitika Gorge			
	1315	1400	Hokitika Gorge	D	Scenery, Fraser Complex, lunch stop	
	1400	1445	<i>Hokitika Gorge - Ross</i>			
	1445	1530	Ross	E	Alluvial gold mining history	
	1530	1630	<i>Ross - Harold Creek</i>			
	1630	1700	Harold Creek	F	Pseudotachylyte	We <i>could</i> visit natural hot springs in the Wanganui River Valley if people are keen
	1715		Hari Hari		Overnight accommodation; pub; cook meal (sausages and spuds); sleep	Hari Hari field station U Canterbury); 75 Wanganui Flat Rd, Hari Hari 7884; Ph 3642987 extn 8355; 0276867260 Obtain key from Jeanette Orłowski at 36 Wanganui Flat Rd; Phone in advance = 03 753 3112 or 021 173 6738
27-Nov	800	845	<i>Hari Hari - Whataroa</i>			
	845	900	Whataroa	G	DFDP-2 site	
	930	1300	Gaunt Creek	H	Alpine Fault + lunch stop	Access to Gaunt Ck via Alpine Fault Tours (http://alpinefaulttours.co.nz)
	1300	1330	<i>Whataroa - Franz Josef</i>			
	1330	1515	Franz Josef	I	Schist, glacier	
	1515	1600	<i>Franz Josef - Doughboy Creek</i>		Stop en route at Doughboy Creek for pegmatites	
	1600	1615	Doughboy Creek	J	Pegmatites; amphibolites	
	1615	1630	<i>Doughboy Creek - Knight's Pt</i>			
	1630	1645	Knight's Pt	K	Uplifted terraces; K-T sequence	
	1645	1700	<i>Knight's Pt - Ship Creek</i>			
	1700	1730	Ship Creek	L	Basalts associated with Tasman rifting	
	1730	1745	<i>Ship Creek - Haast</i>			
	1745	1800	Haast area	M	Overview / discussion of uplift rates and terraces	
1800		Haast Lodge		Overnight accommodation, cook meal (stir fry), sleep	Haast Lodge: Marks Rd, Haast 7886; Ph: (03) 750 0703; haastlodge@ruralinzone.net	
28-Nov	830	845	<i>Haast Lodge - Snapshot Creek</i>			
	845	850	Snapshot Creek	N	Alpine Fault	
	850	920	<i>Snapshot Creek - 18 Mile Bluff</i>			
	920	945	18 Mile Bluff	O	Haast Schist	
	945	1000	<i>18 Mile Bluff - Pivot Creek</i>			
	1000	1045	Pivot Creek	P	Volcanism associated with initiation of AF; greenschist facies Haast Schist lithologies	
	1045	1100	<i>Pivot Creek - Gates of Haast</i>			
	1100	1115	Gates of Haast	Q	Haast Schist structure	
	1115	1200	<i>Gates of Haast - Makarora</i>			
	1200	1300	Makarora		Toilet stop and lunch	
	1300	1330	<i>Makarora - The Neck</i>			
	1330	1400	The Neck	R	Higher textural zone Otago Schist	
	1400	1430	<i>The Neck - L Hawea shore</i>			
1430	1600	L Hawea shores	S	Lower textural zone Otago Schist; general structure		

OVERVIEW INFORMATION ABOUT STOPS:

Further detailed info on some sites can be found from page 7 of this guide, or in papers, reports and maps that will be printed and bought on the trip, and made available electronically.

STOP A: ARTHUR'S PASS

Pre-2001 the road through this pass crossed over an active landslide. It was a constant maintenance headache and not very safe to drive. The current viaduct was constructed in c. 2001. This is a great place for a discussion of highway engineering in NZ, and to say 'hi' to keas.

STOP B: TARAMAKAU RIVER

The Taramakau River valley follows the trace of the Alpine Fault, and the topographic expression is dramatic. We may also stop at roadside outcrops of Alpine Fault mylonites, to get our first view of the tectonite fabrics that are characteristic of these.

STOP C: MT. HARRY AREA

Paleoseismic trenches were dug across recent surface traces of the Alpine Fault, on the south bank of the Toaroha River, east of Hokitika, in 2009. The purpose of these trenches was to expose recent faulting related to the last few displacement events, and to demonstrate the recent structure and shallow mechanics of the Alpine Fault for the first Alpine Fault Drilling Project planning workshop. The trenches are located at the northern end of the 'aseismic' part of the fault, near the intersection with the Kelly Fault, which is the first of a series of active strike-slip structures (the Marlborough Fault system) that distribute plate boundary deformation away from the single structure observed further south.

The Lake Arthur Road loops around Mt Harry (Figure B.1). The type section of Alpine Fault rocks (both mylonites and cataclasites) is located in the valley between Mt Harry and the main range front to the SE. The section is unique because both hangingwall protolith 'schist-derived mylonites', and footwall protolith 'granitoid-derived mylonites' are exposed. Unfortunately, most of the outcrops are quite overgrown. Scattered exposure of feldspar augen-bearing granitoid mylonites can be found on farm tracks to the SE of the road.

The range front to the SE was subject to a large debris avalanche c. 930AD, and debris deposits from this avalanche are scattered across the area around Mt Harry (Figure B.5).

STOP D: HOKITIKA GORGE

The outcrops are of gneissic rocks of the Fraser Complex (Rattenbury, 1991). It is rare to find these so beautifully exposed. The natural scenery is also spectacular.

STOP E: ROSS

This is the home of the largest alluvial gold mine I know of in NZ. The alluvium is still being worked over. We will tour the historic workings and find out about the history of mining here from the awesome information provided on all the signs and in the museum.

STOP F: HAROLD CREEK

Harold Creek is renowned for being one of the best 'easy access' pseudotachylyte localities on the Alpine Fault, and as a result much of the published literature about Alpine Fault pseudotachylytes is derived from samples collected here. The creek is located at the southern termination of the surface trace of the Cretaceous Fraser Fault against the Alpine Fault and perhaps due to this, footwall-derived mylonites have been complexly intercalated with the normal mylonite sequence in this area. The protolith for many pseudotachylytes is not clearly defined. The point of the stop is to examine boulders in the creek beside the road, which contain the entire range of mylonites found anywhere along the fault, and some beautiful pseudotachylytes.

STOP G: DFDP-2 DRILLSITE

DFDP-2A and DFDP-2B boreholes were drilled to depths of ~250 and 893m respectively in 2014-2015 at this location. Copies of the Borehole Completion Report (Sutherland et al., 2015) contain a summary of the project.

The site in the Whataroa valley was chosen because it offers easy relatively access to the Alpine Fault hanging wall and spectacular exposures of fault rocks at Gaunt Creek are directly up-slip-vector from a potential drill site in the valley.

STOP H: GAUNT CREEK

Gaunt Creek is perhaps the best-known exposure of the Alpine Fault in South Westland. Here, the fault itself is exposed in a large slip where mylonitic fault rocks exhumed from depths of <35 km are thrust out over a hanging wall composed primarily of fluvio-glacial gravels. The thickest body of altered cataclasite yet found on the fault is exposed along parts of the overthrust plane. The outcrop is directly up-slip of the proposed intersection of the fault at depth if a 4 km deep borehole is put down in the Whataroa River, so is likely representative of the fault rock sequence we could expect to encounter at depth.

DFDP-1A and DFDP-1B boreholes were drilled to depths of ~100 and ~150m respectively in 2011 at this location. DFDP-1A cored a hangingwall mylonite sequence containing cataclasite zones that increase in frequency downward; 20-30 m of cemented and hydrothermally altered cataclasites; a >5 cm-thick principal slip surface of ultracataclasite and gouge at 90 m; and footwall fluvial gravels to a total depth of 101 m. DFDP-1B cored a similar hangingwall sequence; encountered a principal slip surface with a thickness of about 20 cm at a depth of 128 m; then penetrated a footwall sequence of quartz and feldspar-rich, extensively altered and variably cataclased rock containing an additional possible principal slip surface at 144 m, to a total depth of 151 m. A complete suite of downhole geophysical logs were collected and borehole observatories were installed. Further information about the outcomes of this project can be found in Boulton et al., (2014), Carpenter et al., (2014), Niemeijer et al., (2016), Schleicher et al. (2015), Sutherland et al., (2013), Townend et al. (2013), Toy et al. (2015).

STOP I: WAIHO VALLEY AND FRANZ JOSEF GLACIER

The spectacular Franz Josef and Fox glaciers have advanced and retreated numerous times over the last few thousand years, leaving scoured rock outcrops at their toes. The Alpine Schists of the Waiho Valley, below the terminus of the Franz Josef Glacier, occur in the hangingwall of the Alpine Fault (Figure I.1). The car park is near the oligoclase (albite-out)

isograd, about 4 km east of the recent fault trace and outcrops within the valley are composed of garnet zone schist. At this stop we will learn how the Mesozoic and Cenozoic deformation sequence is preserved in these schist outcrops. We will also examine vein systems within the schist, and consider the implications of fluid inclusion and stable isotope data derived from them for thermal structure and fluid transport within the fault hanging wall.

STOP J: DOUGHBOY CREEK

The float in Doughboy Creek contains protomylonitic pegmatites used to define the ductile strain gradient across the Alpine Fault (Norris & Cooper, 2003). The sequence is also very rich in amphibolite and pelitic lithologies.

STOP K: KNIGHT'S PT.

Uplifted marine terraces here demonstrate the footwall of the Alpine Fault is not actually being downthrust.

The view up and down the coast reveals the Cretaceous-Tertiary sequence of this region and this is the perfect place for a brief discussion of the nature of this sequence and its tectonic significance.

STOP L: SHIP CREEK

We will visit outcrops of Arnott Basalt on the beach.

STOP M: HAAST BRIDGE OR VISITOR'S CENTRE

Here we will discuss the relationship between dramatic geomorphology and tectonics in this area, focusing on how rates of deformation have been determined from offset of Quaternary features.

STOP N: SNAPSHOT CREEK

The most recent trace of the Alpine Fault crosses farm paddocks and SH6 at this location. Paleoseismic trenches were dug here in 1998 and the results recently published (Berryman et al., 2009).

STOP O: 18 MILE BLUFF

The oligoclase zone Haast Schist exposed here has a flat-lying foliation, demonstrating it is part of the Haast Antiform/Thomas Synform sequence of post-metamorphic folds characteristic of this area.

STOP P: PIVOT CREEK

This creek samples a variety of lithologies characteristic of the Haast region, but different from the Alpine Schists and mylonites we encountered further North. Additionally, there are a suite of post-metamorphic igneous rocks of peculiar chemistry that provide clues about timing and mechanics of initiation of the Alpine Fault.

STOP Q: GATES OF HAAST

This spectacular site also contains outcrops of typical TZ IV Haast Schist, and is a good place to observe their tectonite fabrics and consider the relationship of these to those of the Alpine Schist.

STOP R: THE NECK, LAKES HAWEA-WANAKA

Here again we see TZ III – IV Haast Schist.

STOP S: LAKE HAWEA SHORELINE

Lower textural zone schists (II-III) outcrop here. We will particularly focus on the timing and mechanism of development of their tectonite fabrics (Turnbull et al., 2001).

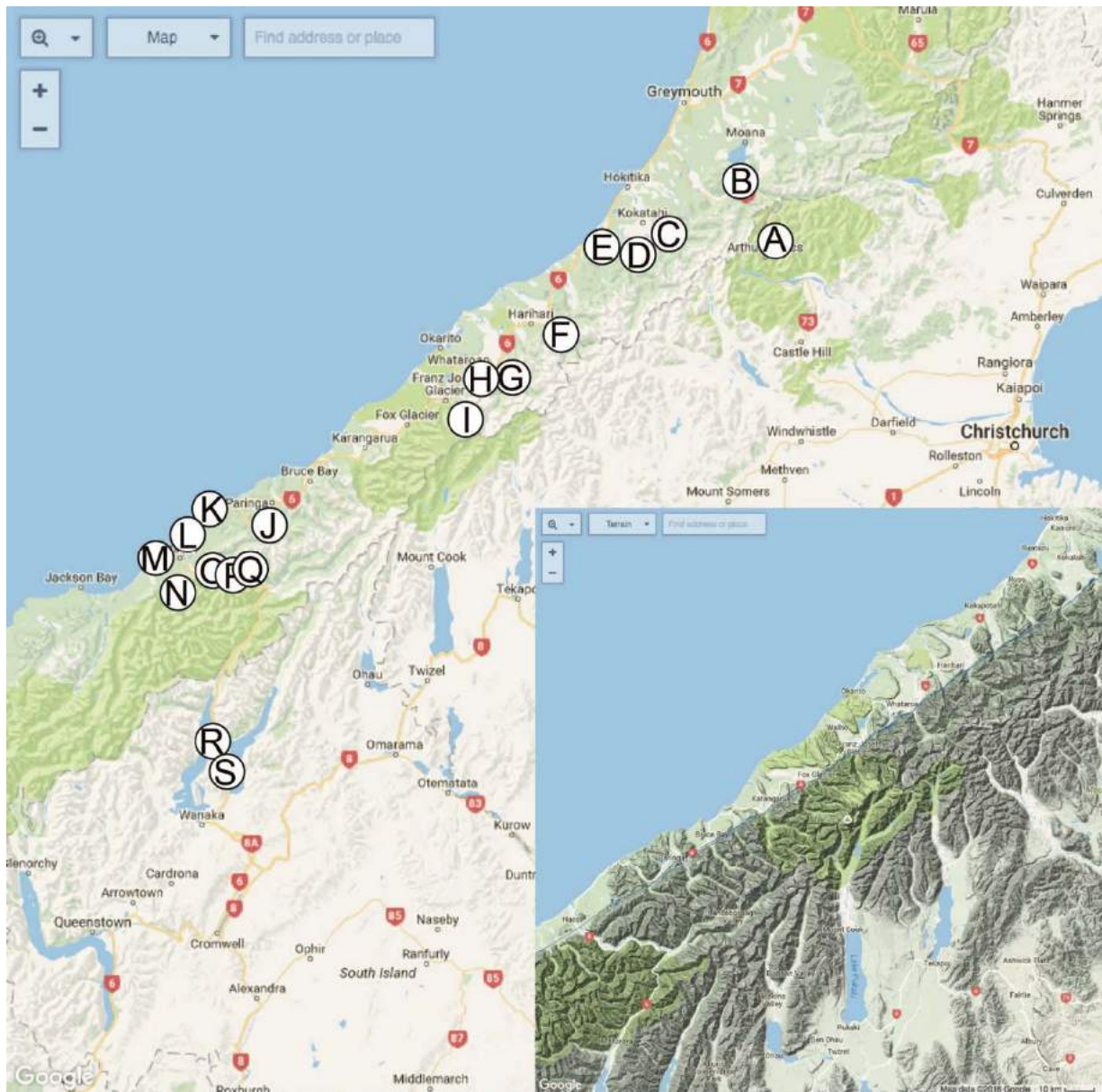


Figure 1. Overview of stops

PURPOSE OF THIS FIELD TRIP:

The field trip aims to examine the geological features and products of two plate collisional events in New Zealand's history. The first event saw the collision of the Torlesse and Caples terranes during the Rangitata Orogeny, the dynamo-thermal consequences of which were the formation of the Haast Schist. The inception of the Alpine Fault



plate boundary in the mid-Cenozoic heralded the onset of the Kaikoura Orogeny, with the tempo of deformation increasing to the present day, where oblique collision between the Pacific and Australian plates results in uplift on the Alpine Fault and formation of the mountain range of the Southern Alps.

It is run in commemoration of Professor Richard Norris, who designed it with Prof. Alan Cooper, and for 30 years bought Otago undergraduates on a similar annual field trip.

FURTHER INFORMATION ABOUT SELECTED STOPS

STOP C: TOAROHA RIVER – RECENT ALPINE FAULT TRACES AND TRENCHES

Robert Langridge

As part of the first Alpine Fault Drilling Project Workshop in 2009, we opened two new paleoseismic trenches across the Alpine Fault, near the True Left bank of the Toaroha River, east of Hokitika (grid ref. J33/567100). The site can be reached off Lake Arthur Road from Hokitika (Figure B.1), and is close to the Saddle Creek and Round Top localities on Staples' farm (Stop B). The purpose of these trenches was to expose recent faulting related to the last few displacement events, and to demonstrate the recent structure of the Alpine Fault to those interested in the mechanics of Alpine Fault deformation.

The "Staples" site was previously studied during the late 1990's by Mark Yetton, who re-mapped the site after Berryman (1975) and Cutten (1985). Yetton excavated two trenches here across low alluvial surface where the strike-slip and vertical components of slip are relatively small and measurable (Yetton 2000; Yetton et al. 1998).

The Alpine Fault offers considerable challenges for paleoseismologists, none more so than the terrain, bush cover and rainfall that are part and parcel of West Coast geology. The stretch of the Alpine Fault between the Hokitika and Styx rivers is one of the more open portions of the landscape along the fault, where it can be easily mapped and access for paleoseismic trenching is feasible. In addition, the Staples site occurs at the NE end of the high-slip rate (c. 25 mm/yr) 'Cook' segment of the fault, almost coincident with the area where traces of the Kelly Fault approach the Alpine Fault from the east, down the Styx River. To the NE of this site, the plate margin is characterised by distributed strike-slip deformation related to the Marlborough Fault System, with the Alpine Fault playing a diminished role in the overall strain release budget through South Island. Thus, at the Toaroha River we should expect the slip rate and earthquake record to be broadly equivalent to the rest of the Cook segment to the SW, e.g. as seen near Whataroa and Franz Josef.

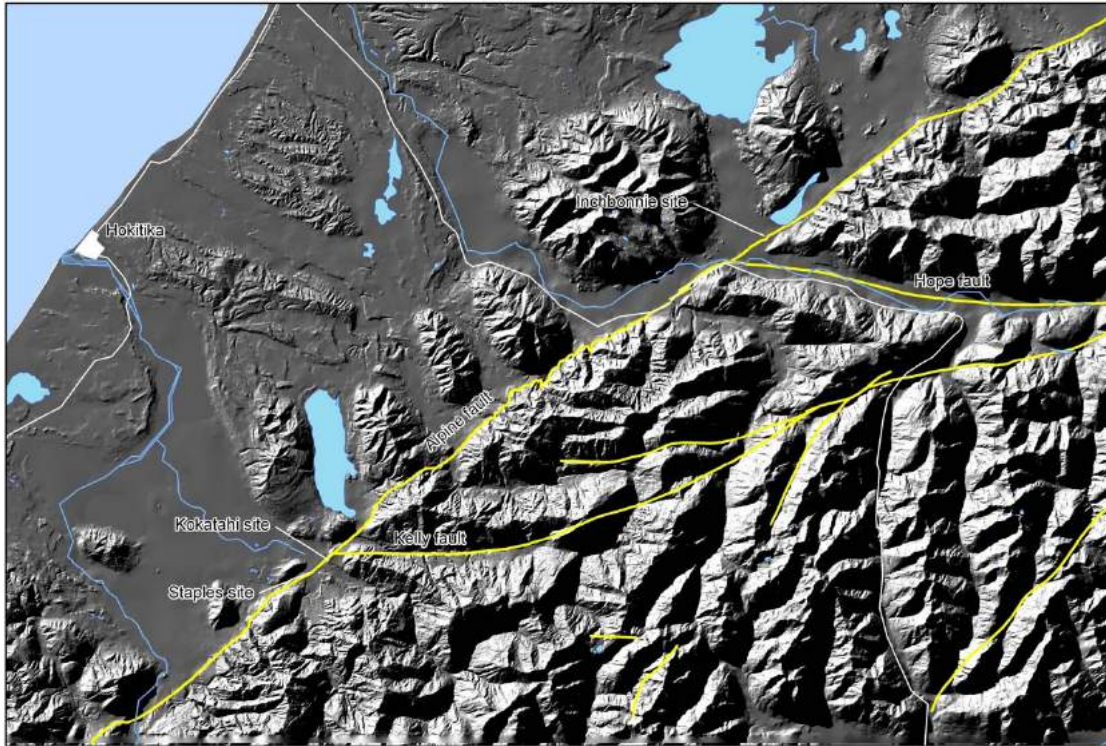


Figure B.1. Location map of the Alpine Fault in central Westland. The Staples and Kokatahi sites are located to the SE of Hokitika.

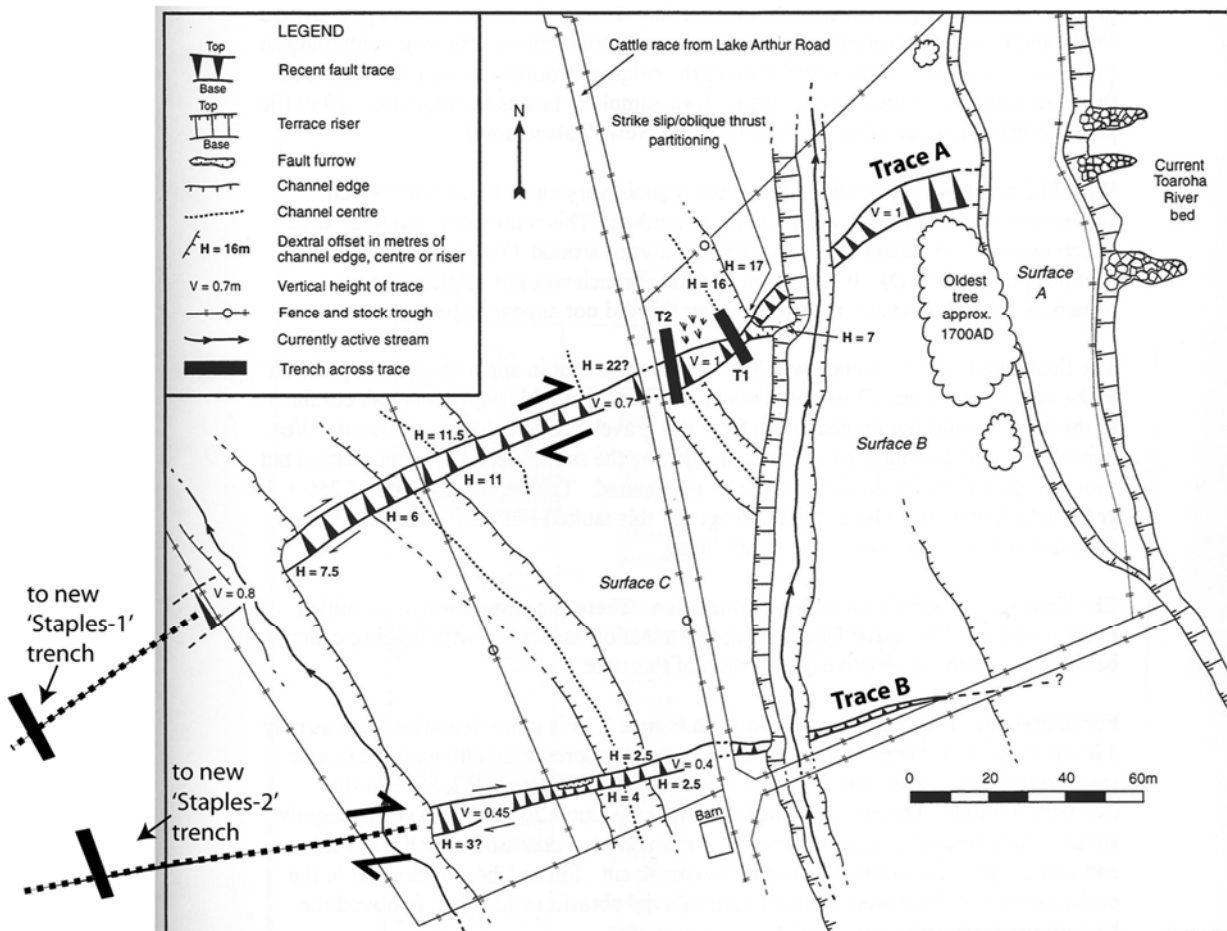


Figure B.2. Sketch map of the Alpine Fault at the Staples farm site, SE of Hokitika (after Yetton 2000). The Toaroha River (at right) has constructed a number of fluvial terraces that preserve displacements relating to Alpine Fault deformation. Note: Surface A is unfaulted and the trees shown on Surface B probably colonised this surface since the AD 1717 earthquake.

The following are a series of preliminary observations from the Staples site. Berryman (1975) and Cutten (1985) mapped two fault traces (A and B) across a continuous low fluvial terrace on the true left bank of the Toaroha River where we will trench. These traces converge to the SW. The main trace (Trace A; Figure A.2) strikes at c. 065° and is characterised by a vertical scarp with heights of 0.6-1.2 m, and dextrally offset alluvial channels and risers of generally c. 5-8 m in size. It is considered that these may represent single-event displacements related to the most recent event. A single measurement of 16 m dextral on a small riser was also identified on this surface, implying that multiple events had occurred on this surface. The secondary trace (Trace B) strikes at c. 076° (2.5-3.9 m RL; 0.3 m V). Collectively, and in concert with trenching results (below), it seems likely that the sum of the displacements on both traces represents the product of at least two earthquake displacements.

A new map of this lower terrace sequence was produced by Yetton (2000). This map documents dextral displacements of generally c. 6-17 m across Trace A and also 2-4 m across Trace B (Figure A.2). As part of the 2009 study a detailed microtopographic map of the site was produced using a GPS-RTK system to better assess the displacements across the lower terraces, and to include the higher surface where the trenches were located.

In addition, Yetton (2000) presents the results of two paleoseismic trenches from this site. Trenches T1 and T2 were excavated across the two portions of the former channel separated dextrally by c. 16 m (Figure A.2). The trenches show evidence for a recent rupture and possibly at least one or two older events (Yetton 2000). Based on radiocarbon dates from within the trenches, the most recent faulting event is believed to have occurred since 1700 AD – this is the event usually referred to as the AD 1717 rupture. This was supported by a program of tree coring from a cohort of trees that colonised the lowest faulted terrace to the east of the trenches, and to other dates from nearby trenches at the Kokatahi River. The ages of the older events are not known, though the penultimate event at the nearby Kokatahi trenches probably also occurred within the last c. 500 yr

What did we hope to learn from two new trenches? The trenches (Staples-1 and -2) were sited on a higher terrace close to where the main trace (A) and secondary trace (B) converge. Here, Berryman (1975) estimated a vertical scarp height of c. 3.6 m on the main trace. At this location Trace B runs at the base of a higher and older surface. Recently the farmer has created an exposure into the fault zone which cuts the edge of Trace A (Figure A.3).

We hope to expose the structure of the fault zone in an area where at least three earthquake events have occurred. The deposits seen in the exposure thus far are typically pebbly schistose fluvial deposits derived from the Toaroha River. These are interbedded with sands and some silt beds. The interbedded stratigraphy and the differing material properties help define the locations of faults and deformation. These types of deposits are typically poor in datable material – though we will remain hopeful! We hope to display the style and possibly the amount of deformation related to the high alluvial surface.

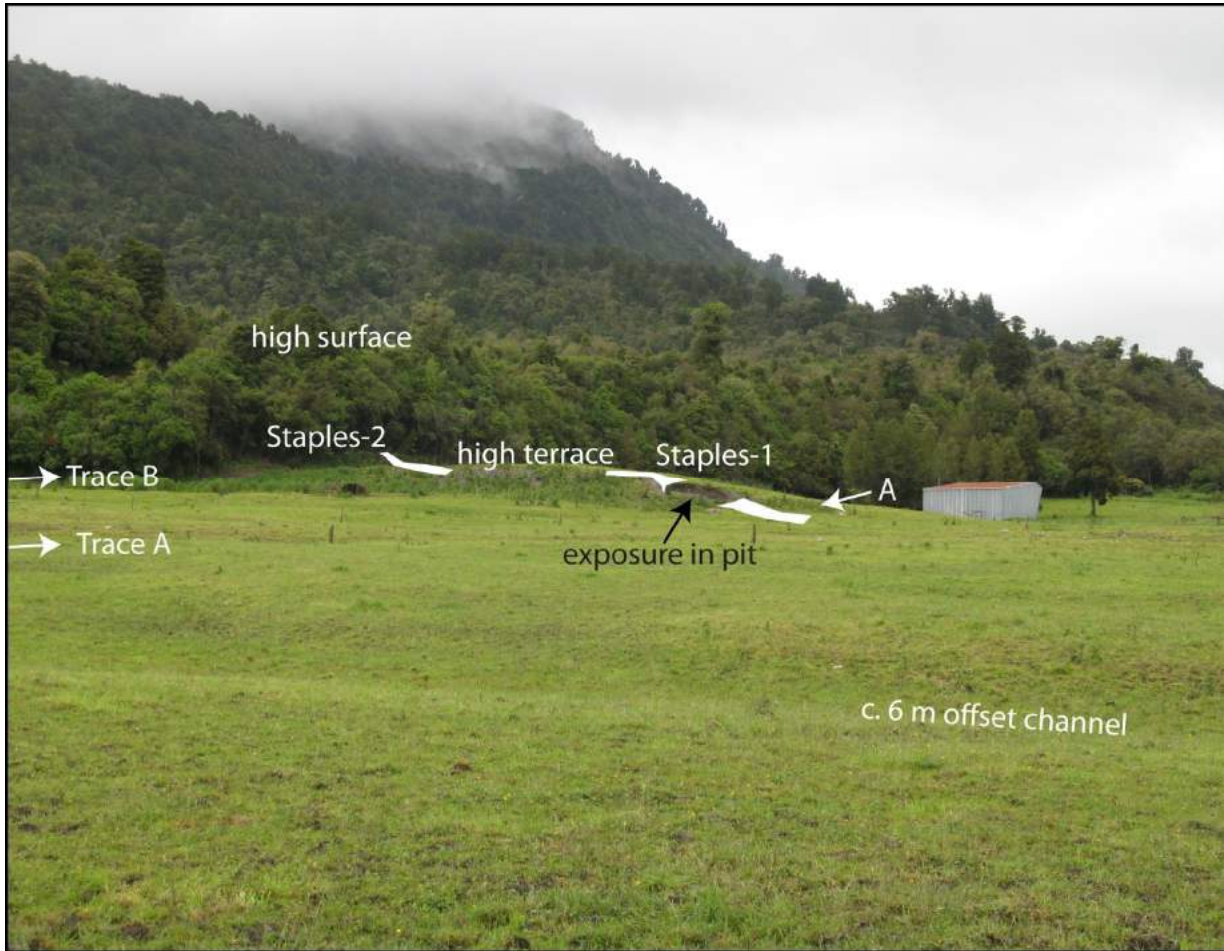


Figure B.3. Photo looking to the south of the Alpine Fault as expressed at the Staples farm site. In the background is the range front of the fault and Southern Alps, with a high abandoned surface in the midground that defines Trace B. In the foreground are the lower terraces, previously studied by Yetton. The new trenches - Staples-1 and -2 (in white) - were excavated across both fault traces on the high abandoned terrace behind the farm barn.

STOP C: KOKATAHI RIVER

Rick Sibson

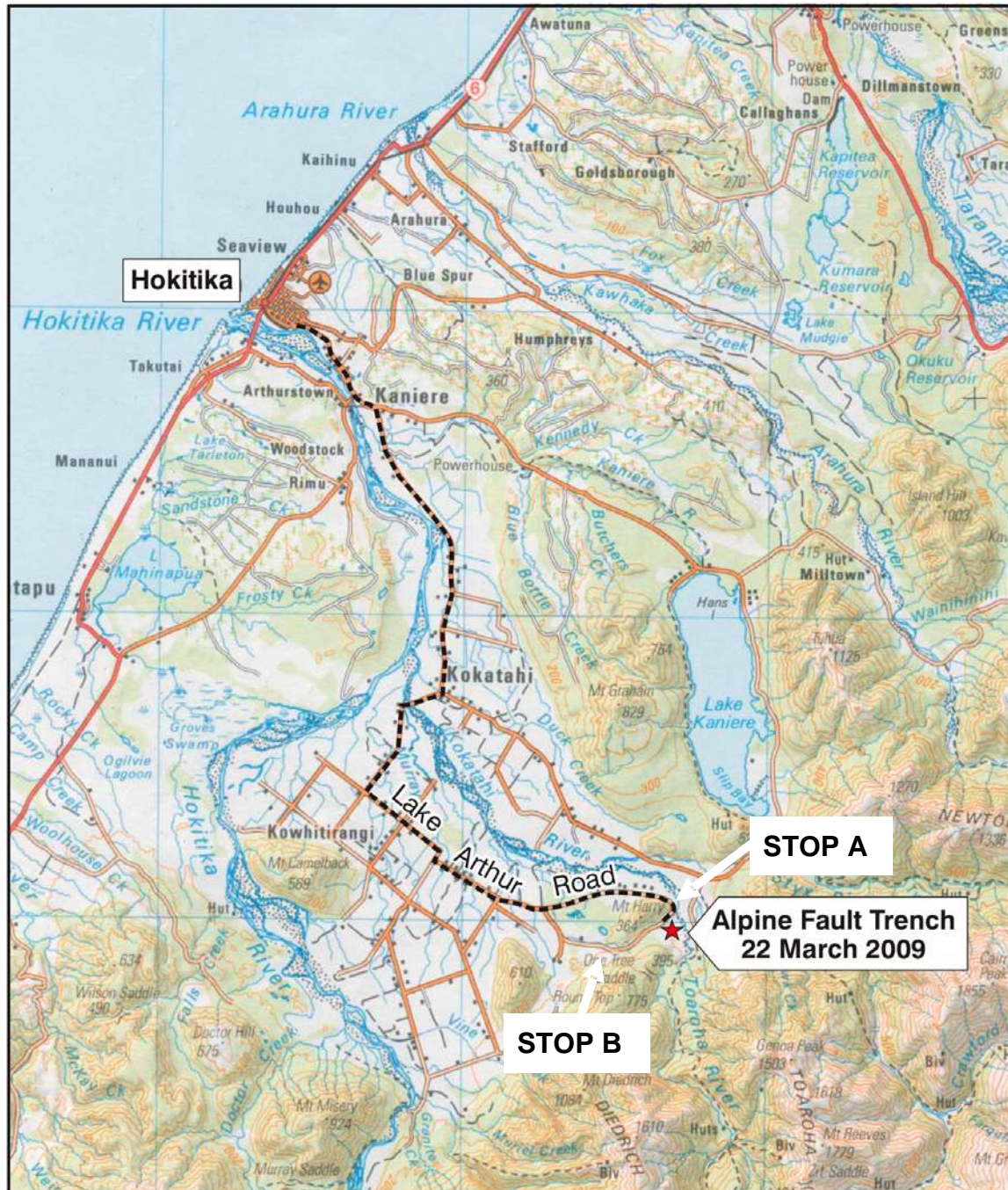


Figure B.1. Map of the Kokotahi Valley area, illustrating the locations of Stops A and B, and the appropriated route to drive there.

GEOLOGICAL SETTING

In this area (Figure B.1), the Alpine Fault zone strikes $\sim 050^\circ$ and is defined by active surface traces offsetting terrace gravels in the valley of the Toaroha and Kokotahi Rivers, and also by the lithological juxtaposition across the narrow valley between Mt Harry and Sunshine Spur, of Fraser Complex assemblages to the northwest against Alpine Schists (garnet-oligoclase assemblages) to the southeast (Warren 1967; Nathan et al. 2002). Mt Harry and

The Doughboy are made up of variably mylonitised and cataclastically deformed granites (of probable Devonian and/or Cretaceous age?; Waight et al. 1997) contained within the Fraser Complex (Rattenbury 1991) which is bounded to the west of Mt Harry by the buried trace of the SE-dipping Fraser Fault.

SADDLE CREEK TRANSECT

First described by Reed (1964), the transect from Mt Harry along Saddle Creek (GR: 555092 – Figures B.2 and B.3), provides one of the more continuous exposures through the Alpine Fault zone. Deformed granite (cataclasite-ultracataclasite with possible minor relict pseudotachylyte) is locally exposed in the creek at the extreme northeastern corner of Mt Harry. Saddle Creek itself exposes a semi-continuous section of mylonites with foliation generally dipping moderately (40-50°) to the southeast, though locally affected by folding. A transition from granitoid-derived mylonites to mylonites derived from the Alpine Schist is apparent about halfway up the transect. Mylonites in the upper part of the transect have an L-S tectonite fabric with a stretch lineation plunging approximately east, consistent with dextral-reverse oblique shearing across the fault zone (Figure B.4).

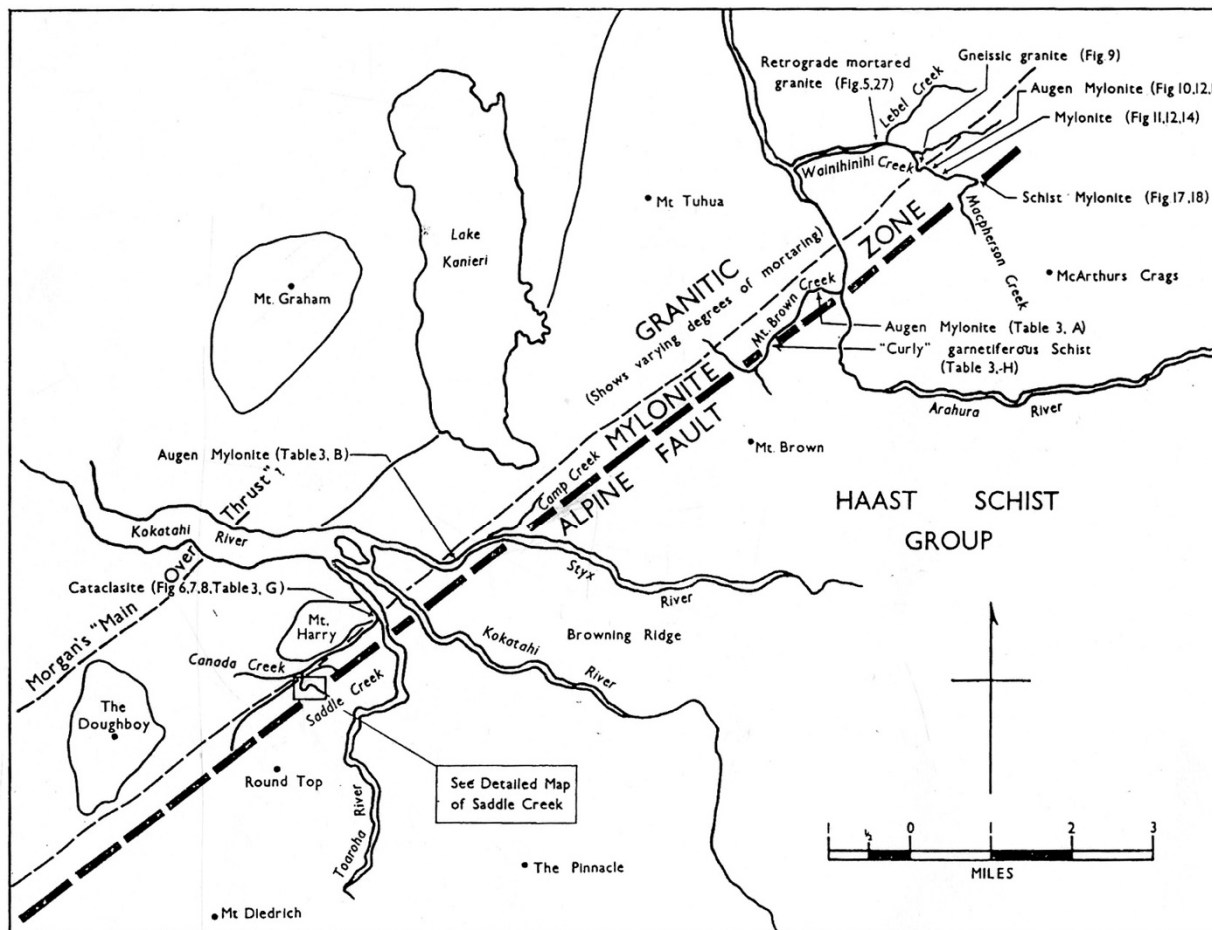


FIG. 28—Map of part of Sheet S58 showing key outcrops in the Wainihinihi Cr and Canada Creek regions.

Figure B.2. Map of the Alpine Fault and localities in the upper Kokatahi Valley around Mt. Harry. From Reed (1964).

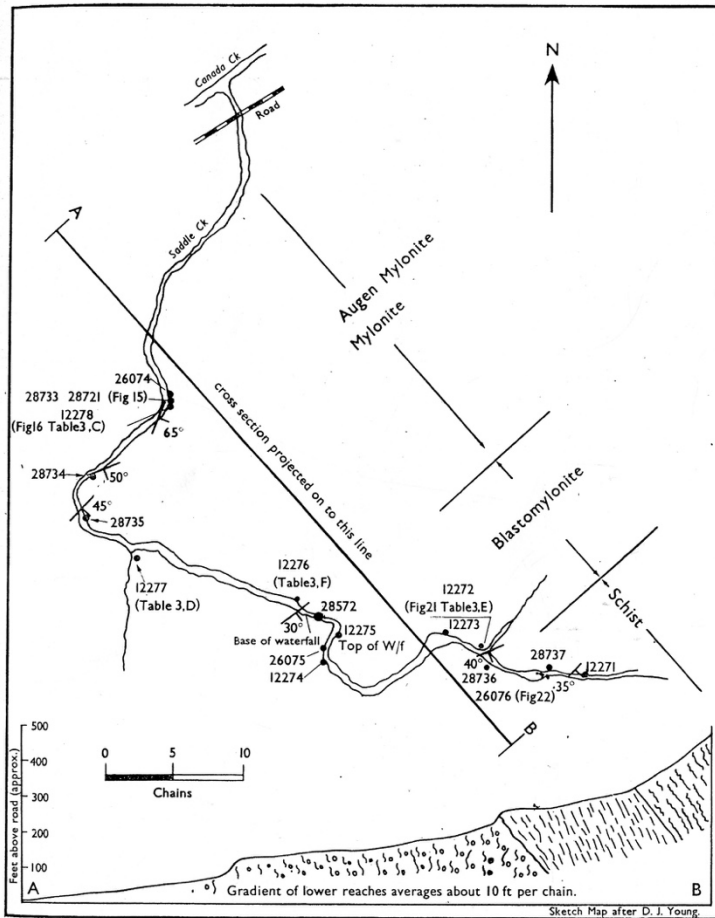


FIG. 29—Detailed map of Saddle Creek showing sample locations.

Figure B.3. Detailed map of Saddle Creek, type section for the Alpine Fault mylonites as described by Reed (1964)

A critical issue is whether all of the mylonitic fabrics are derived from Alpine Fault deformation, or whether some of the fabrics are inherited from Fraser Complex deformation. Not long ago the creek transect was obscured by dense rain-forest, but recent farm clearing has provided comparatively easy access to the mylonitic assemblage. This transect has also been influential in the generation of subsequent composite cross-sections through the Alpine Fault zone (e.g. Sibson et al. 1979).

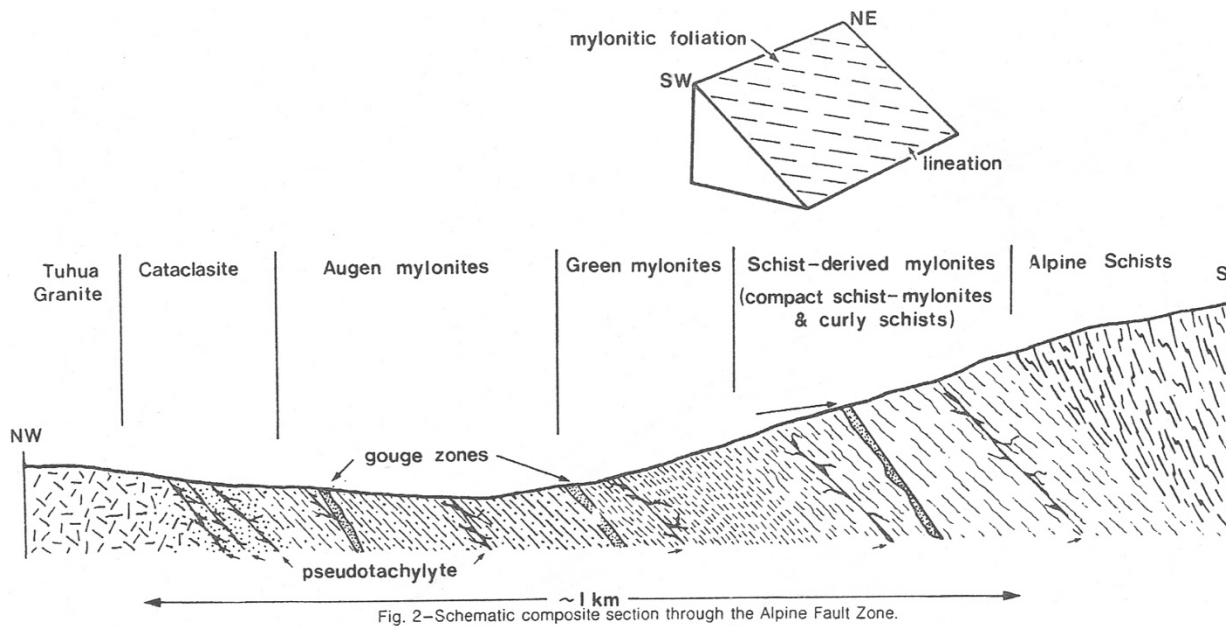


Fig. 2—Schematic composite section through the Alpine Fault Zone.

Figure B.4. Composite cross section through the Alpine Fault mylonites. From Sibson et al. (1979)

DOWRICK'S DILEMMA CREEK

This tributary to the Styx River (GR: 587115 – Figure B.1) is incised into Samuel Spur above the projection of an active fault trace and provides a continual exposure of mylonites with foliation dipping c. 50° SE for upwards of 100 m upstream from the road bridge.

ROUND TOP DEBRIS AVALANCHE

A major debris avalanche deposit (Figure B.5) made up of blocks of Alpine Schist derived from the multi-scalloped western face of Round Top (775 m) covers a lobate region of >5 km² with characteristically hummocky topography to the west and southwest of Mt Harry (Wright 1994). The volume of the debris avalanche, which has flowed more than 4 km northwest of the range-front over the alluvial plain, is estimated at ~45 million cubic metres. Dating of wood contained within the debris suggests an emplacement age of c. 930 AD. The avalanche was likely triggered by rupturing along the Alpine Fault.

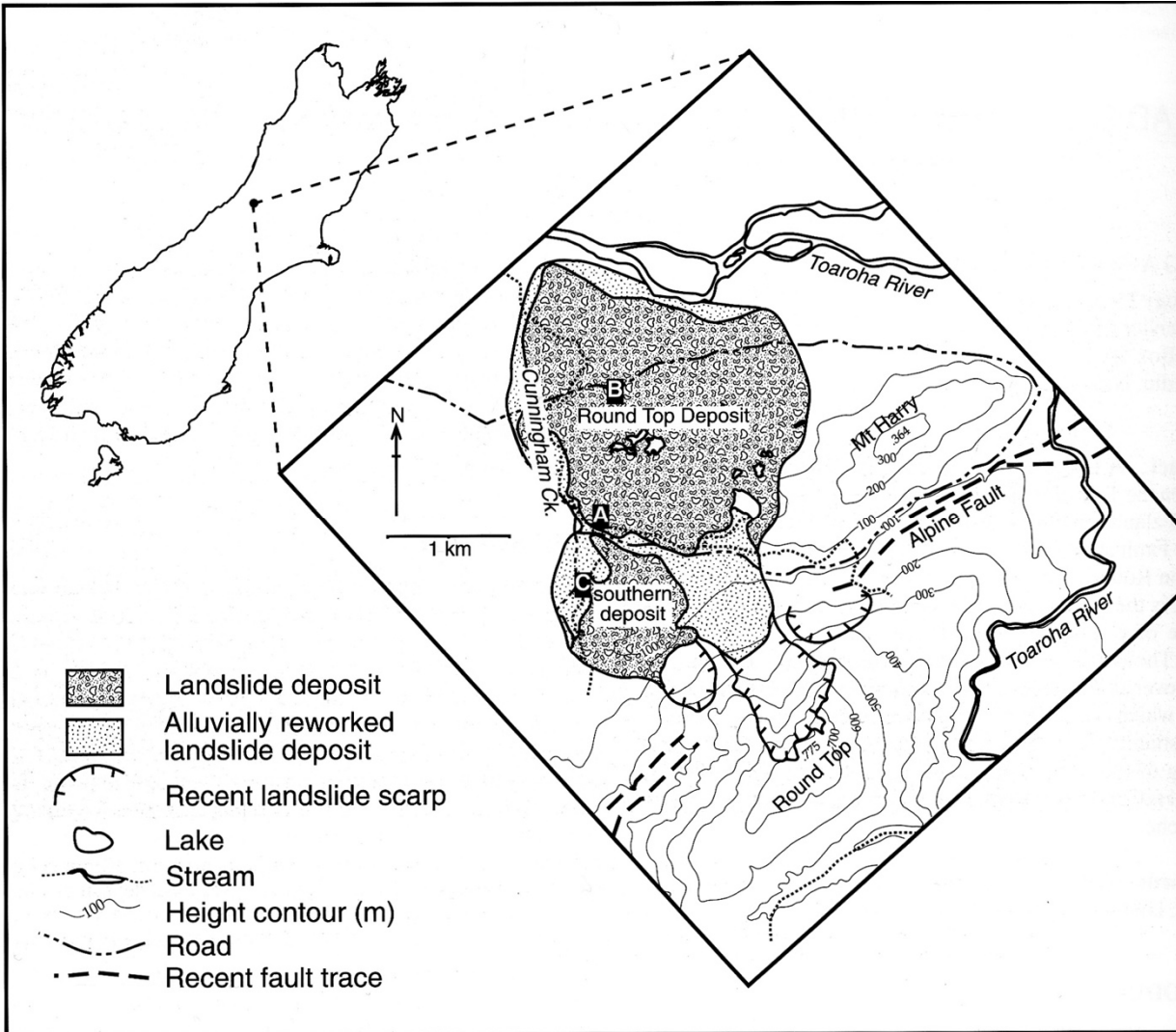


Figure B.5. Map of landslide deposits near Round Top. From Wright (1998b)

STOP F: HAROLD CREEK

Virginia Toy

SH6 crosses Harold Creek between Hari Hari and the Wanganui River road bridge. Park at the south end of the road bridge and descend into the river bed to examine boulders.

Cataclased mylonites are thrust over glacial gravels where the recent trace of the Alpine Fault is exposed at the base of the range-front in Harold Creek (at A; Figure D.2). Behind this thrust fault, augen mylonites derived from a Western Province protolith are intercalated with slivers of Alpine Schist-derived mylonite in a pattern that cannot be attributed to partitioning on brittle faults at the near surface (Wright 1998a; Toy 2008). Instead, this complex intercalation indicates footwall and hangingwall material are sheared together at depth.



Figure F.1. Pseudotachylyte in a boulder from Harold Creek

Pseudotachylytes are particularly numerous both in float and in outcrop in this creek (Sibson et al. 1979). These pseudotachylytes have yielded Ar-Ar ages of 1.1 Ma and 570 ka (Warr et al. 2003; Warr et al. 2007). An outcrop containing abundant *in situ* pseudotachylyte was, in the past, visible in the bed of the creek at an elevation of approximately 200masl but this outcrop has since been obscured due to aggradation of the creek bed. Numerous pseudotachylytes can still be found in different host rocks in float and more rarely in outcrop. We will examine float samples from near the road

Most pseudotachylytes in Harold Creek are hosted in mylonites with a Western Province-protolith (possibly those yielding Carboniferous ages described by Warr et al. 2007), or material that may be derived from metabasic layers in the Alpine Schist. The pseudotachylytes are relatively voluminous compared to those found in schist-derived mylonites elsewhere. The host rocks have mostly developed a greenschist facies mineral assemblage (chlorite+epidote+albite); which is uncharacteristic for the bulk of the Alpine Fault mylonites (Toy 2008). The presence of these hydrated assemblages may have

promoted formation of friction melt since incorporation of volatiles from breakdown of hydrous minerals lowers the melting point of silicates (Spray 1987). This may also be related to the absence of a strong anisotropic foliation. The host rock can readily fracture in a variety of orientations as the stress field varies during dynamic rupture propagation. These fractures provide pathways along which friction melt can be tapped from the fault plane, so that shear resistance is not reduced and production of friction melt continues throughout the slip event (Swanson 1992).

Pseudotachylytes were formed in a variety of environments in the Alpine Fault zone, as summarised in Figure D.3. We will see pseudotachylytes hosted in the cataclastic fault core, and in quartzofeldspathic schist-derived mylonites at Gaunt Creek.

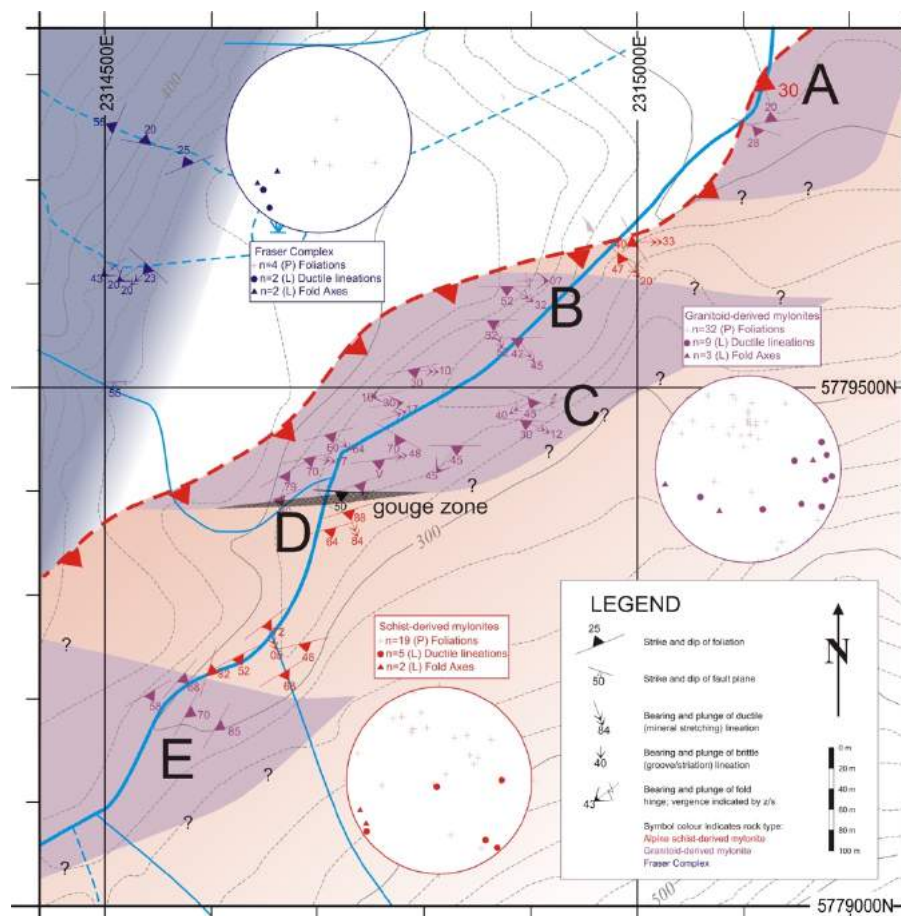


Figure F.2. Map of lower Harold Creek, showing intercalation of Alpine Schist and footwall granitoid-derived mylonites. From Toy (2008).

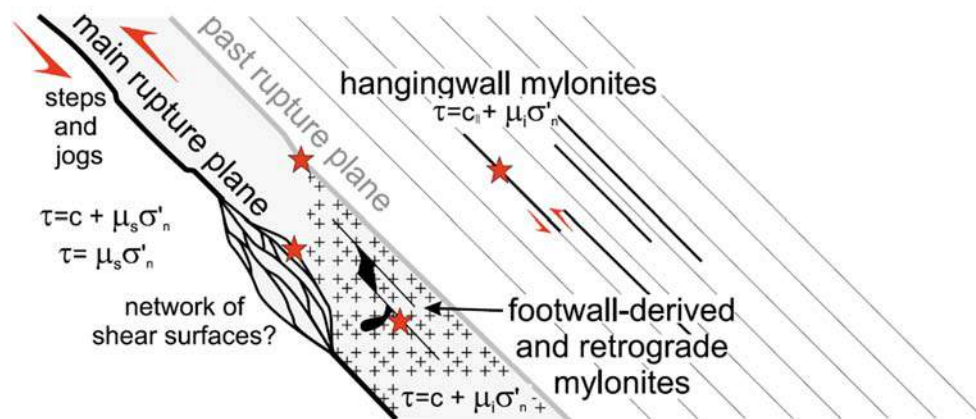


Figure F.3. Schematic cross-section illustrating the settings in which we infer pseudotachylyte was formed within the Alpine Fault rocks. Red stars show places pseudotachylyte has been found. Failure conditions in each case are indicated. From Toy (2007).

STOP G: WHATAROA RIVER

QUATERNARY PROCESSES AND ALPINE FAULT TRACE, WHATAROA RIVER

R. Sutherland and K. Berryman

On the northeast side of Whataroa River, turn west onto a farm track just before road turns next to the river. Drive down and park next to the river.

QUATERNARY SEDIMENTS AND EARTHQUAKE HISTORY

The Whataroa River is one of the larger rivers crossing the Alpine Fault. It has a mean discharge of 140 cumecs, a mean annual flood of 2822 cumecs, and drains 445 km² of mountainous terrain extending from the Tasman Sea to the main divide of the Southern Alps (don't fall in). The lower plain of the Whataroa River lies between lateral moraines of probable ages 18-28 ka and 60-80 ka that extend to the present coastline, and offshore (Figure E.1) (Suggate 1990; Sutherland et al. 2007; Cox and Barrell 2007). Seismic reflection data (SIGHT project 1996, 1998) show that there is >1 km thickness of post-glacial sediment downstream of the Alpine Fault.

Small rangefront tributaries of the Whataroa River form fans that have been eroded by the Whataroa River northeast of the road bridge (Figure E.2). These fans reveal a c. 2000 year stratigraphy of alternate buried soils and fining upward fan alluvium, with many in-situ tree stumps rooted in buried soil horizons, that record episodic rangefront collapse (Figure E.3). Six significant landscape-change events are identified during the last 1600 yrs: 1717 AD, c. 1625 AD, c. 1425 AD, c. 1300 AD, c. 900 AD, and c. 400 AD. In the coastal plain, tree ring dating studies reveal episodes of re-establishment of vegetation following aggradation episodes in 1717 and 1620 AD (Cullen et al. 2003), and rangefront fans grade to aggradation levels in the main valley (Figure E.2). Some events surely result from rupture of the Alpine Fault at Whataroa, while others may correlate with rupture of more distant segments of the Alpine Fault, or possibly with other large earthquakes in the region (Berryman et al. 2009).

The elapsed time since the last major Alpine Fault earthquake to impact on the catchment is almost 300 years. The landscape is now in its "most stable" condition with soil development

on stable fan surfaces, mature forest cover over much of the catchment, and river incision (the river carries $5.1 \times 10^6 \text{ m}^3/\text{yr}$ of sediment (Griffiths 1979, but it is currently undersupplied, resulting in downcutting). Past events indicate a future $M_w 8$ earthquake will result in widespread landsliding in the alps and along the rangefront, river aggradation, and coastal progradation, with associated widespread sedimentation and flooding hazards.

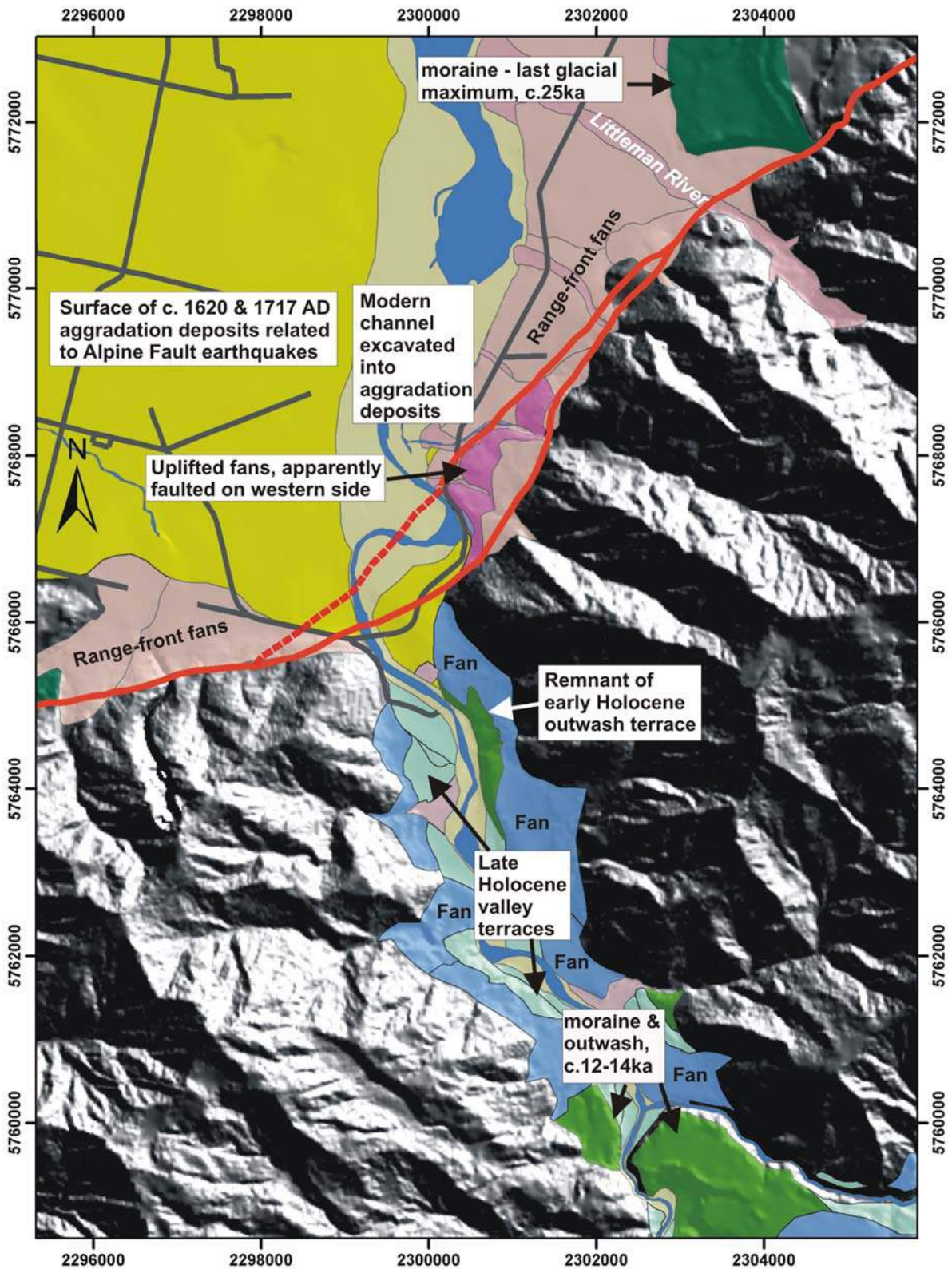


Figure D.1. Map of Quaternary deposits of the Whataroa River area. Alpine Fault traces are shown as red lines along the range front. Their location is inferred from topographic and geological considerations. The only possible geomorphic trace of the fault is west of the apparently uplifted fans northeast of the Whataroa River bridge. Grid marks are 2 km apart. Based on mapping by Cox and Barrell (2007) and unpublished data of Berryman and Almond, et al.

LOCATION OF THE ALPINE FAULT

The location of the Alpine Fault is constrained by the distribution of faulted and uplifted late Quaternary deposits, seismic-reflection data, mapping and assumed thickness of the hanging-wall mylonite zone, and geomorphologic interpretation.

Northeast of Whataroa River, large (>1 m) glacially-derived greywacke boulders (transported from headwaters of the valley) are contained within a coarse fluvial deposit exposed next to the road and reworked into the river. They probably represent late-glacial (c. 18-14 ka) deposits that are recessional moraine and till reworked by fluvial action, and they have subsequently been uplifted and exposed by throw on the Alpine Fault to c. 80 m above river level. Their distribution is consistent with geomorphic evidence for uplift across the more westerly fault trace shown on Figure E.1. This interpretation is consistent with the location of the topographic break in slope towards the base of the fans to the northeast (Figure E.2). The interpreted position also corresponds with that of the strongest seismic reflection identified above 0.5 s twt (middle reflection on Figure E.4, outer side of meander bend of river).

An oblique-thrust segment NE of the river has been mapped closer to the range front by R. Norris, A. Cooper and S. Read (Figure 1). This interpretation is supported by the occurrence and thickness of the mylonite zone exposed within the hanging wall (Figures E.5, E.6, E.7). It is also consistent with the NNE-trending range front reflecting slip on the inferred oblique-thrust segment and there is a possible Holocene scarp near to the road.

On the SW side of the river, an ENE-striking segment of the fault, passing south of Whataroa township is inferred by Norris and coworkers to be chiefly dextral strike-slip; and two active strike-slip strands (Figure E.5) were mapped by Read (1994). Such near-surface segmentation of the fault has been described at many other locations in the central part of the Southern Alps, and the traces are inferred to merge at depth into a single oblique-slip master fault dipping 45-50 degrees (Norris and Cooper 1995). Little's mapping of the bedrock exposures near the fault supports the view that that the strike-slip strand has offset Alpine Fault's mylonite zone, omitting parts that sequence at the surface near the mouth of the river.

Seismic reflection data (Figure E.4) are low-fold and certainly open to alternate interpretations, but a preliminary analysis identifies three possible reflections that could be associated with Alpine Fault displacement. The strongest reflection event near to the surface is evident near the outer meander bend of the river and approximately corresponds to the more westerly fault trace identified from geological mapping (Figure E.1; Cox and Barrell 2007). A weak reflection identified upstream of the road bridge has an interpolated surface position that corresponds to the trace mapped by Norris and coworkers just downstream of the road bridge. An additional even weaker and less continuous reflection event surfaces in the most westward location and approximately corresponds to where the late Quaternary sediments substantially increase in thickness downstream. It is suggested that, if this most

westerly reflection represents a fault, then it is no longer an active trace, but may have undergone activity while the valley was glaciated and shortly afterwards.

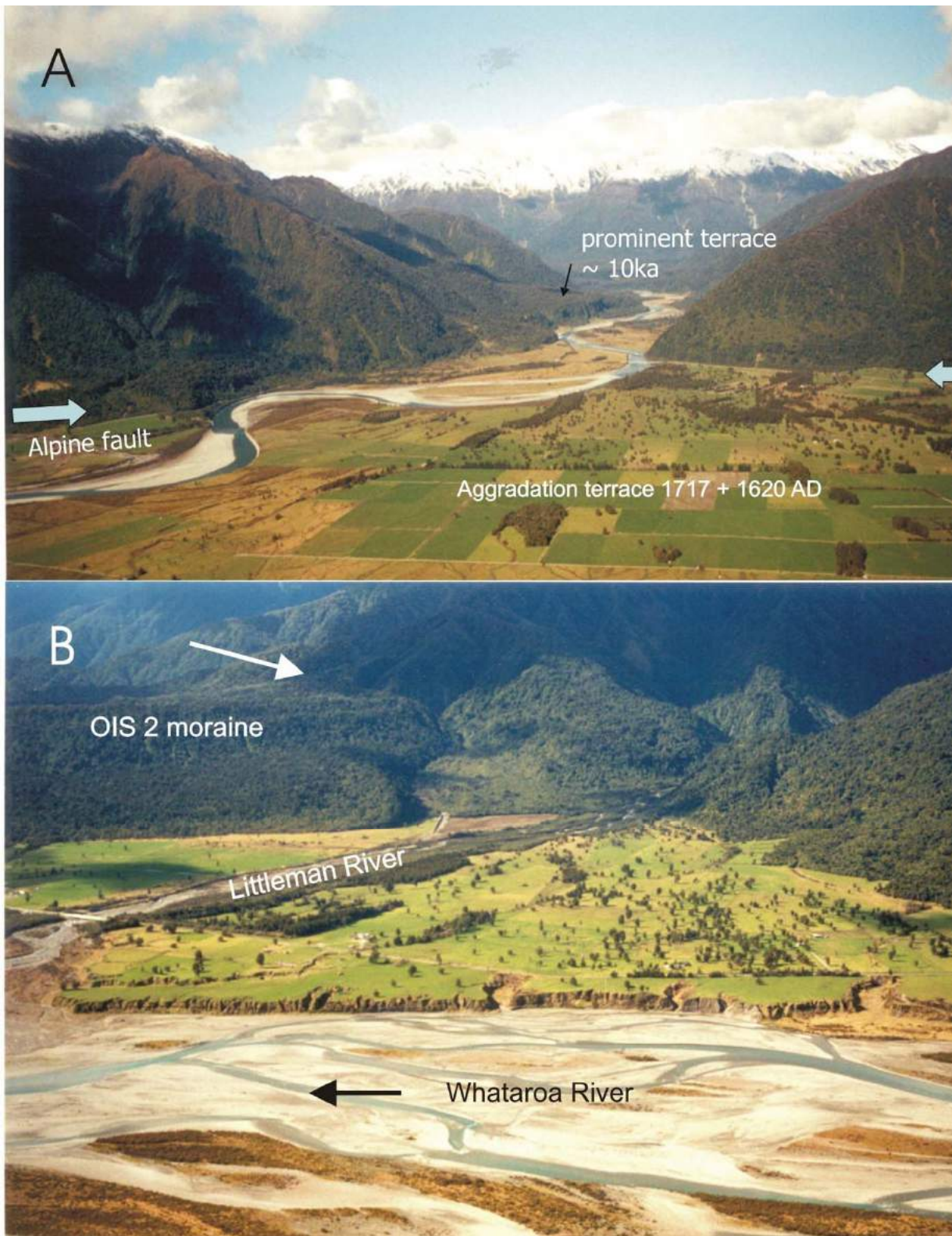
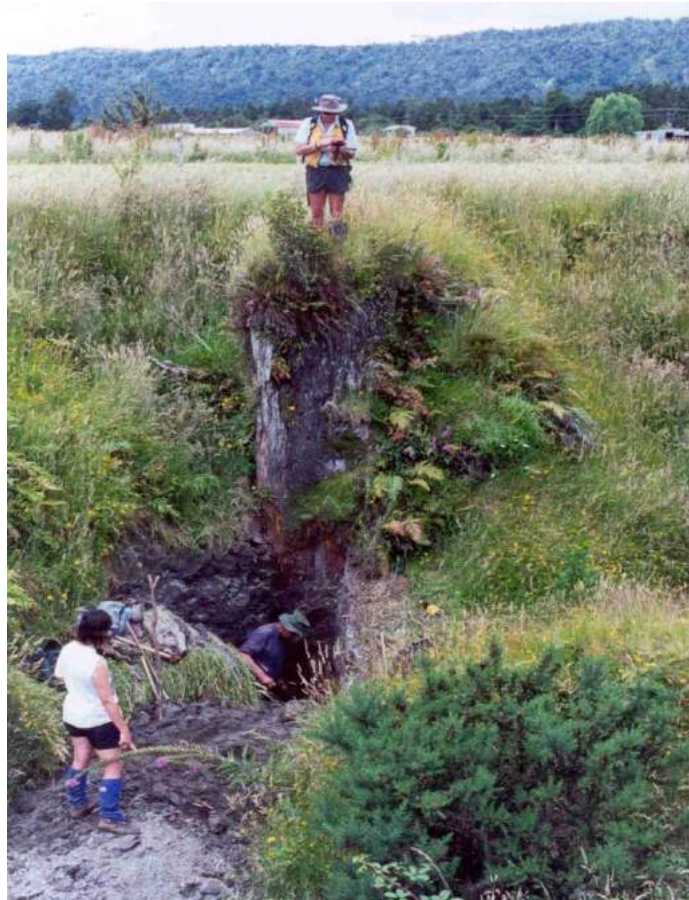


Figure D.2. A. Looking upstream into Whataroa valley. The modern channel of the river has downcut about 10 m into the aggradation fill dating from 1717 and 1620 AD events. The approximate line of the Alpine Fault is shown by blue arrows along the range front. B. Aerial

view of rangefront fans trimmed by the Whataroa River in the vicinity of the Littleman River. The approximate position of the Alpine Fault is shown by white arrow at the rangefront. Exposures of the rangefront fans, as depicted in Figure E.2, occur along the riverbank sections. Photos: Graham Hancox, GNS Science.

A



B

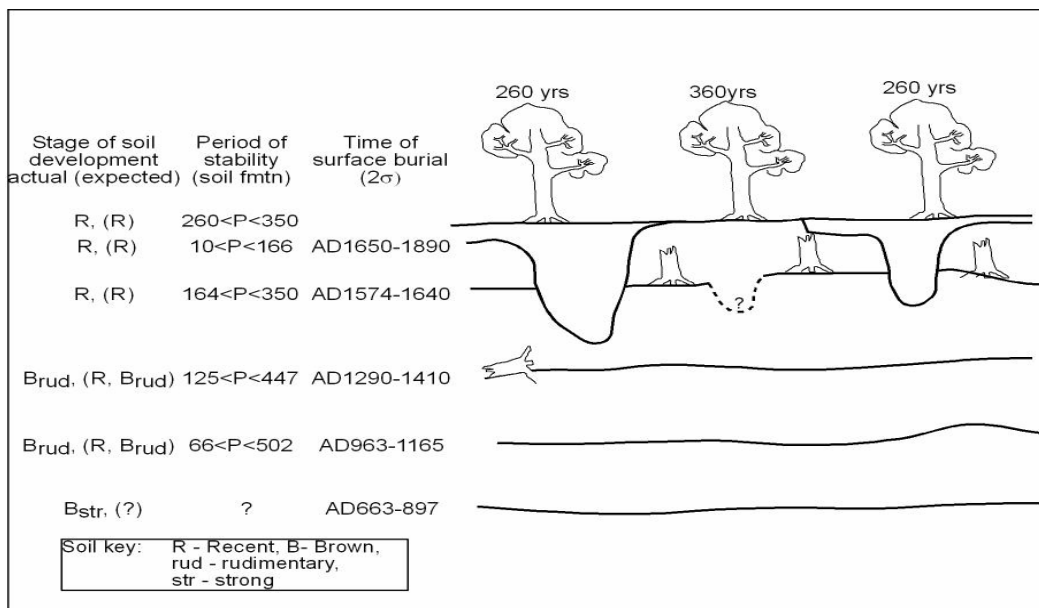
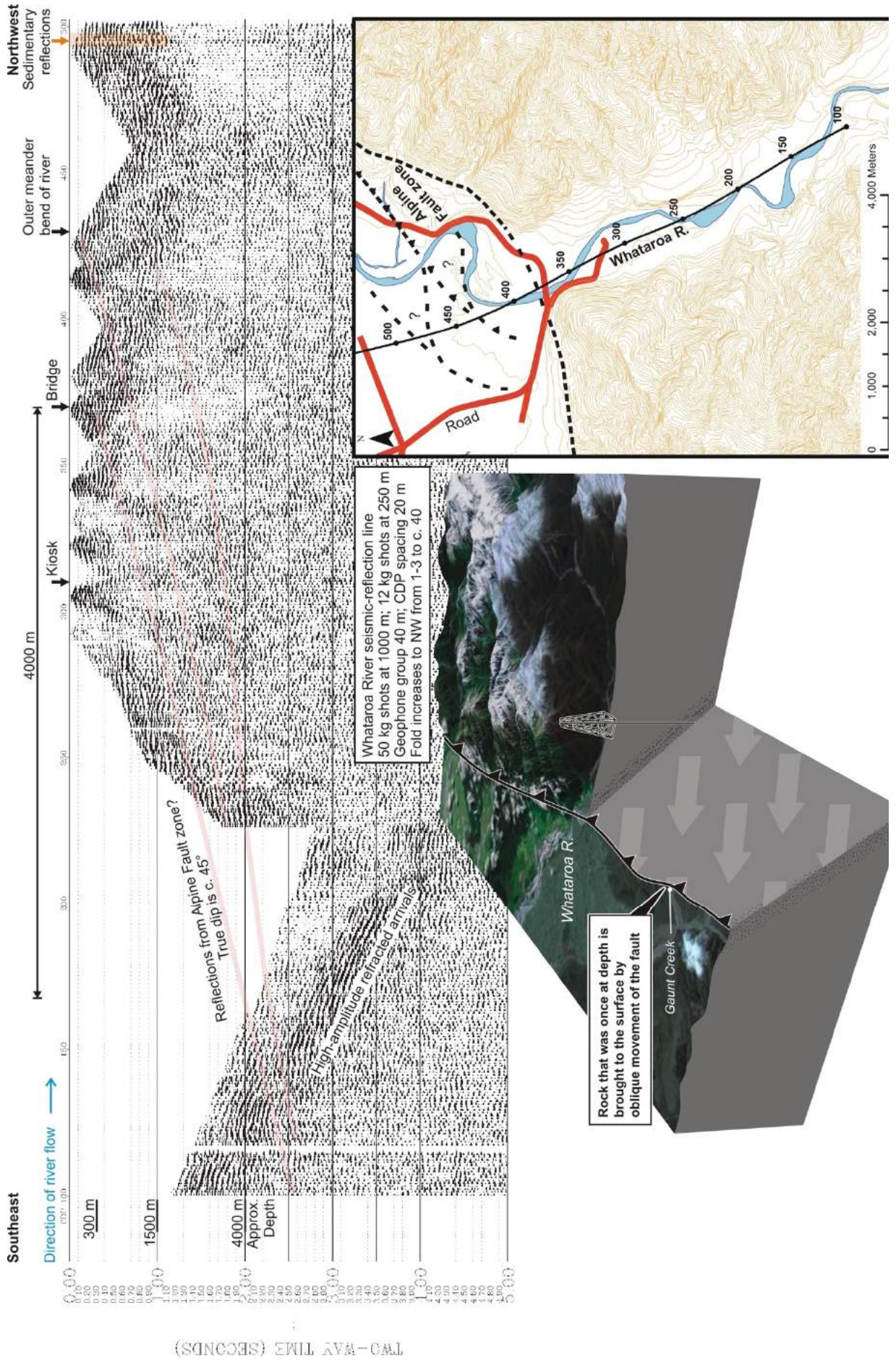


Figure D.3. A. Tree stump rooted in soil unit on the fan of Littleman River. B. Schematic showing relationships between fan units, buried soils, and insitu tree stumps. These

relationships provide estimates of time of burial of soils (earthquakes induced range front collapse), the period of stability between fan-building episodes, and a basis for soil chronosequence studies. The sequence has now been extended to 2000 years. (Berryman et al. 2009)



TWO-WAY TIME (SECONDS)

Figure D.4.

ALPINE FAULT HANGING WALL AND DFD-2 DRILLSITE, WHATAROA RIVER

T. Little, R. Sutherland and K. Berryman

Location map of Whataroa River Stop

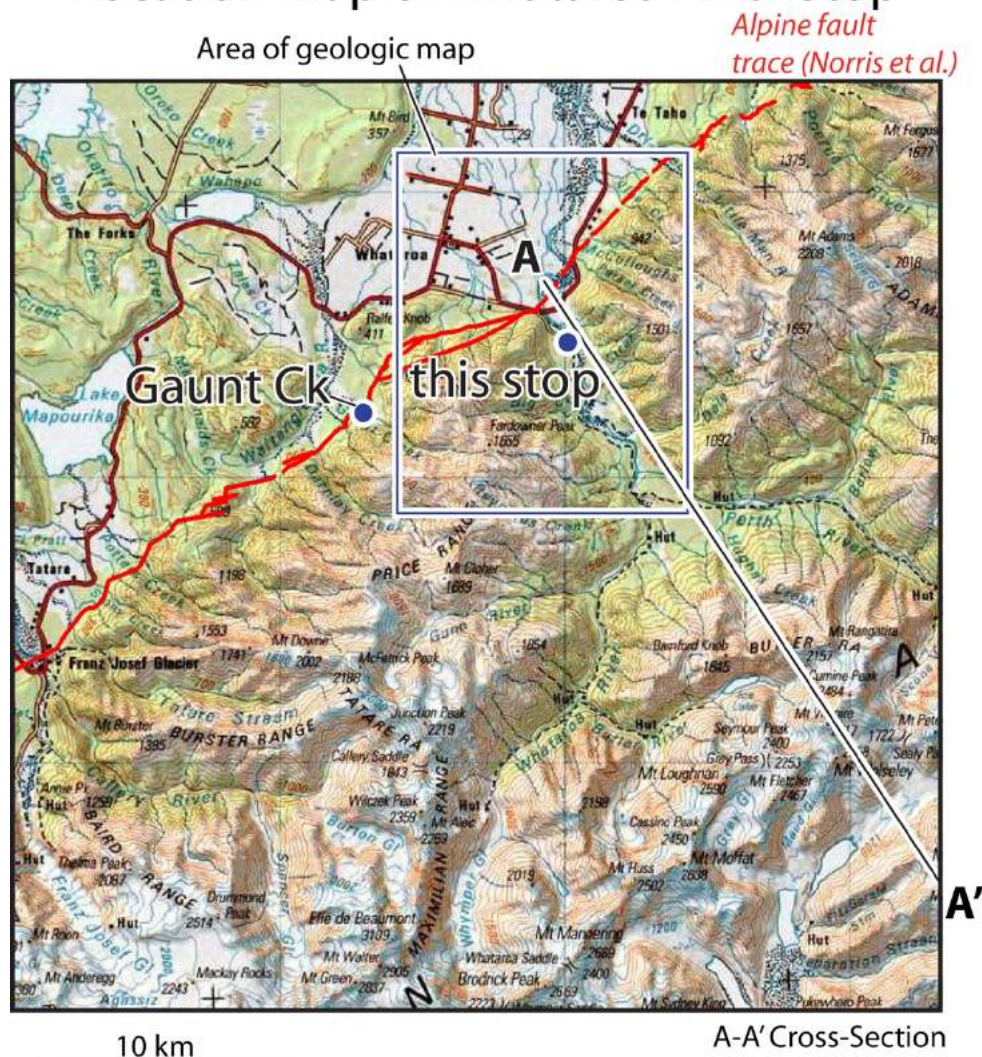


Figure D.5. Location of fieldtrip stop upstream of Whataroa road bridge, and of the detailed geological map and cross-section.

QUATERNARY SEDIMENTS

Upstream of the Alpine Fault, the landscape is inferred to be entirely younger than 18 ka (Cox and Barrell, 2007).

A terminal moraine of probable latest Pleistocene age (c. 12-14 ka) occurs at about 280 m above sea level near the confluence of the Perth and Whataroa Rivers, and outwash terraces at similar elevation occur nearby and are inferred to have formed contemporaneously or shortly after (Figure E.1). About 2 km upstream of the Whataroa River bridge a remnant of a high terrace composed principally of greywacke gravel and overlain by

schist fan gravel is at about 220 m elevation and correlated with the moraine and outwash farther upstream. Trevor Chinn obtained a radiocarbon age of 10489 ± 88 yr B.P. from a wood sample from the terrace gravels. The well-developed terrace is substantially above river level because of continued uplift of the Alpine Fault hanging wall and erosion to establish a stable profile of the Whataroa River.

Boulders that are present in the river bed near to the kiosk are assumed to be a lag deposit from beneath the terrace gravels and may be late glacial (c. 18-14 ka) deposits correlative with those exposed by the road near to the river northeast of the bridge (previous stop).

The river valley floor is flat and covered in late Holocene sediment, but Holocene sediment is unlikely to be very thick, for the uplift reason given above. The Holocene terrace is probably a similar age to aggradation surfaces associated with the amalgamated 1717 AD and 1620 AD (probable earthquake) surfaces identified farther downstream. The Holocene terrace provides easy access and is not prone to flooding.

Based upon the exposure of late glacial deposits at river level, we suggest that the total thickness of sedimentary deposits within the valley is unlikely to be very large (<100 m) and is largely bouldery or conglomeratic in nature. In some valleys farther south (e.g. Paringa) lake or/and marine silts were deposited immediately following glacial retreat, but there is no evidence (e.g. seismic: Figure E.4) for such deposits upstream of the Alpine Fault in the Whataroa valley.

SEISMIC-REFLECTION LOCATION OF THE ALPINE FAULT

Wide-angle reflections from the Alpine Fault are tentatively identified at 4-5 km depth, 4-5 km upstream of the road bridge. These reflection events are identified from a single large shot farther upstream and cut across strong refracted arrivals (Figure E.4). There are several weak and discontinuous reflection events that occur at depths of c. 1500-3500 m beneath the kiosk. These reflections are approximately between possible surface traces of the fault (above) and the deeper reflections, and yield a similar dip (c. 45°) to regional geological and geophysical estimates (Stern et al. 2007; Norris et al. 1990). In summary, existing low-fold seismic-reflection data suggest that the Alpine Fault can be imaged and that it dips moderately southeastward, but new data with acquisition parameters optimised for this type of imaging are required.

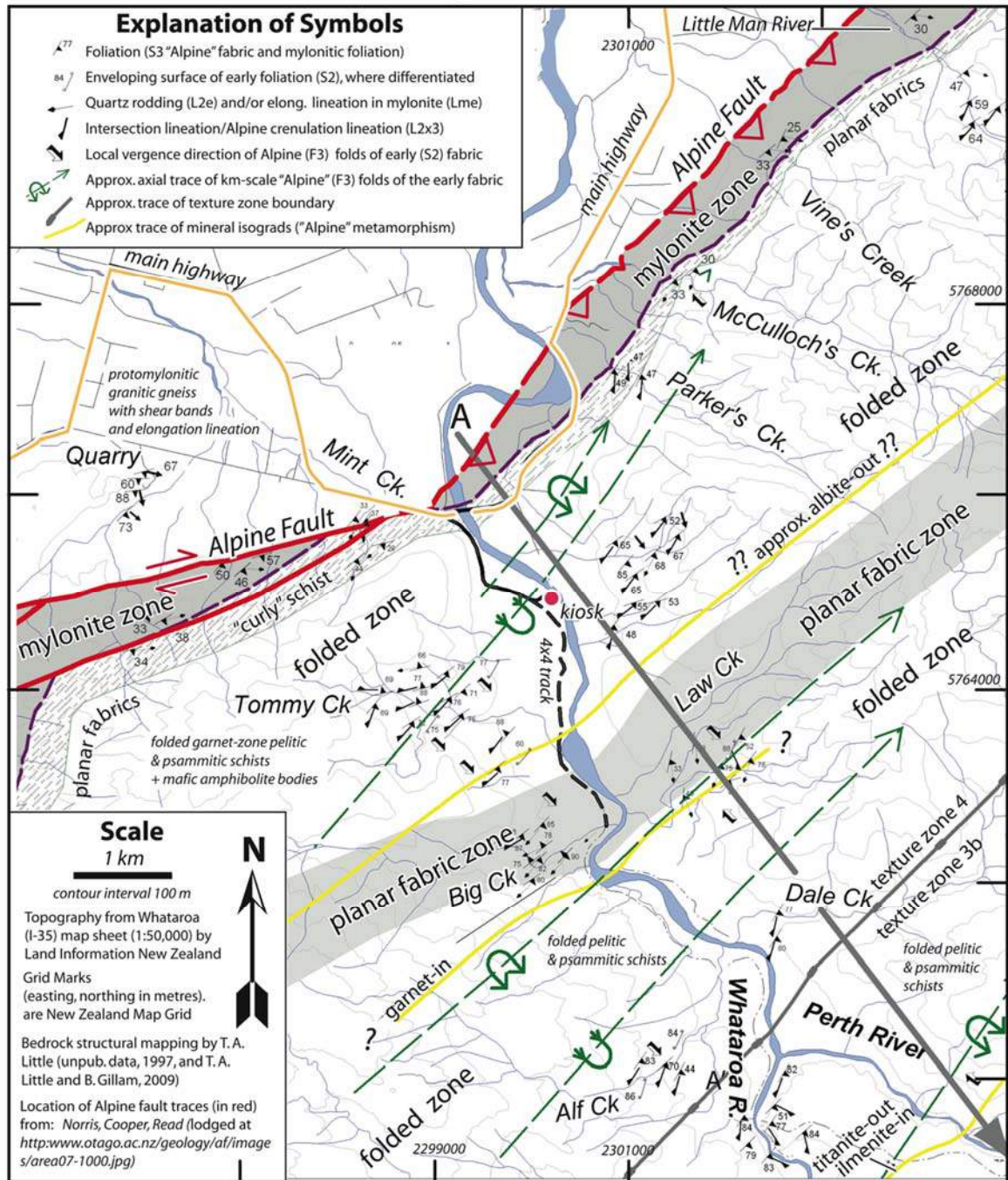
GEOLOGY OF THE ALPINE FAULT HANGING WALL

Located about 10 km to the east of the Waitangitanao River and its tributary, Gaunt Creek, the glacially incised Whataroa River Valley (Figure E.5) provides deep access into the hangingwall of the Alpine Fault, and is a potential target for deep drilling of that structure. Beyond our stopping point, the 4-wheel drive track on the west side of the river continues as far as Big Creek, a distance of about 4 km into the Alpine Fault's hangingwall. If a drill hole was undertaken at this point to intersect the Alpine Fault vertically at a depth of ~4 m, this point of intersection would occur approximately tectonically "upstream" of the Gaunt Creek outcrop (Figures E.4 and E.5). Provided that the protoliths are similar, any systematic differences between fault zone materials sampled in the drill hole and those now exposed at Gaunt Creek might be attributed to the additional fault transport distance through the upper crust that the exposed rocks must have experienced on their obliquely upward path to the surface. The flat valley floor is buried in alluvial gravel from the coast to just upstream of the junction between the Perth and Whataroa Rivers. Above this junction, both of rivers are

typically incised directly into Alpine Schist bedrock with little or no alluvial cover. The geomorphic contrast between the Waiho Valley, with its sheer bedrock flanks cut by the Franz Josef Glacier; and the lower Whataroa Valley, with its deep alluvial infill and dense bush cover is conspicuous. Glaciers retreated from the Whataroa Valley >10 ka, leaving behind a thick outwash terrace, the fluviially dissected (and heavily forested) remnants of which we will see raised above the modern river from our stop on the edge of the river bluff.

Ductilely deformed granitic rocks of New Zealand's Western Province occur on the NW (Australian Plate) side of the Alpine fault. Protomylonitic metagranite and gneiss of the footwall, probably part of the Cretaceous Fraser Complex, are exposed in a quarry just south of Whataroa township. These chloritically altered and cataclastically deformed meta-granitic rocks have a strong down-dip or steeply NE-plunging stretching lineation defined by elongate feldspar augen and other deformed mineral aggregates, and are cut by anastomosing brittle-ductile shear bands (T. A. Little unpub data). This deformation is likely to be at least in part pre-Cenozoic (Cretaceous) in age (Rattenbury 1991).

Selected Bedrock Geology of Lower Whataroa River Area



to A'

Figure D.6.

The Pacific Plate crustal section is tilted to the SE against the fault, so that higher structural levels and successively lower-temperature Barrovian metamorphic isograds (e.g. garnet-in, biotite-in) occur with increasing distance away from the fault to the SE. Amphibolite-facies Alpine Schist within a few km of the Alpine Fault consist chiefly of interlayered pelitic and psammitic (greywacke sandstone-derived) metasediments and minor bodies of coarse-grained amphibolite (meta-mafic rocks). Pelitic schist is unusually common farther upstream and in the Whataroa-Perth River gorges. These rock types suggest a derivation of these structurally deepest rocks from the Aspiring Terrane rather than greywacke-dominated

Torlesse Terrane (which is exposed closer to the Main Divide). Sandstone beds in the sequence are tightly folded and pervasively boudinaged into lenticles, and relict bedding becomes increasingly recognizable at higher structural levels and in lower grade rocks.

Little et al. (2002a) discussed the ductile structural geology of the Alpine Fault's hangingwall in the Whataroa and Perth Rivers, work that has recently been supplemented by further field work (Figure E.6). The Alpine mylonite zone is characterized by a NE-pitching elongation lineations and strongly laminar foliation. Upstream of it, the "curly schist" is transitional into the structurally higher non-mylonitic part of the Alpine Schist. The "curly schist" is characterized by pervasive (mm-cm scale) development of dextral-reverse, extensional (C') shear bands garnet-zone that cut an otherwise mostly planar foliation that is inherited from the non-mylonitic part of the Alpine Schist, and which commonly retains the moderately SW-plunging lineation that is characteristic of most of the non-mylonitic Schist in this part of the Southern Alps.

In the non-mylonitic part of the Alpine Schist, a highly segregated, laminar high-strain early foliation (S2) is the dominant fabric element in Alpine Fault's hangingwall. It has been interpreted to be equivalent to the (typically nearly flat-lying) foliation in the Otago Schist, of probable Jurassic age, and to the strongly laminated foliation that has been steeply tilted near the terminus of the Franz Josef Glacier (Little et al. 2002a). The early foliation was later folded and crenulated during the "Alpine" deformation and regional metamorphism in the Late Cretaceous. The "Alpine" foliation (S3) strikes NE, slightly anticlockwise of the strike of the Alpine Fault, and dips more steeply than that structure, commonly to the SE. The dominant lineation in the non-mylonitic schists is an intersection lineation between the early and "Alpine" foliations that pitches moderately to the SW. This L23 lineation marks the hinge-lines of mm-cm scale (F3) fold hinges (crenulations). The folds are defined by deformation of an early foliation (S2) in the rocks, and include km-scale, SW-plunging folds that can be mapped by tracking changes the vergence of the "Alpine" structures.

The early foliation is parallel to mm-scale segregations in the rock, and contains a strong quartz rodding - elongation lineation. During the "Alpine" and Cenozoic folding, this foliation was not everywhere shortened and crenulated, but locally retained its laminated and planar character (also for example, at Franz Josef Glacier). In some panels, typically the inverted limbs of km-scale "Alpine folds," the early fabric was rotated to steep dips without undergoing significant shortening or folding during the "Alpine" event. On these steep limbs, S2 was further stretched along the layering, but little folded or crenulated during the "Alpine" deformation. The strongly laminated high-strain fabrics preserved in these "planar zones" are largely inherited from the early (Otago Schist-related) foliation; they do not represent zones of younger (Alpine age or Cenozoic) shearing or transposition.

During the late Cenozoic, the early foliation (S2) was tilted SE as a result of uplift along the Alpine Fault, and the "Alpine" foliation (S3) and its folds were modestly reinforced and tightened, and some renewed mineral growth took place (e.g. probably of biotite). At this time, ductile deformation became strongly localized into the Alpine mylonite zone with "far-field" shearing extending several kilometres up-section from that zone.

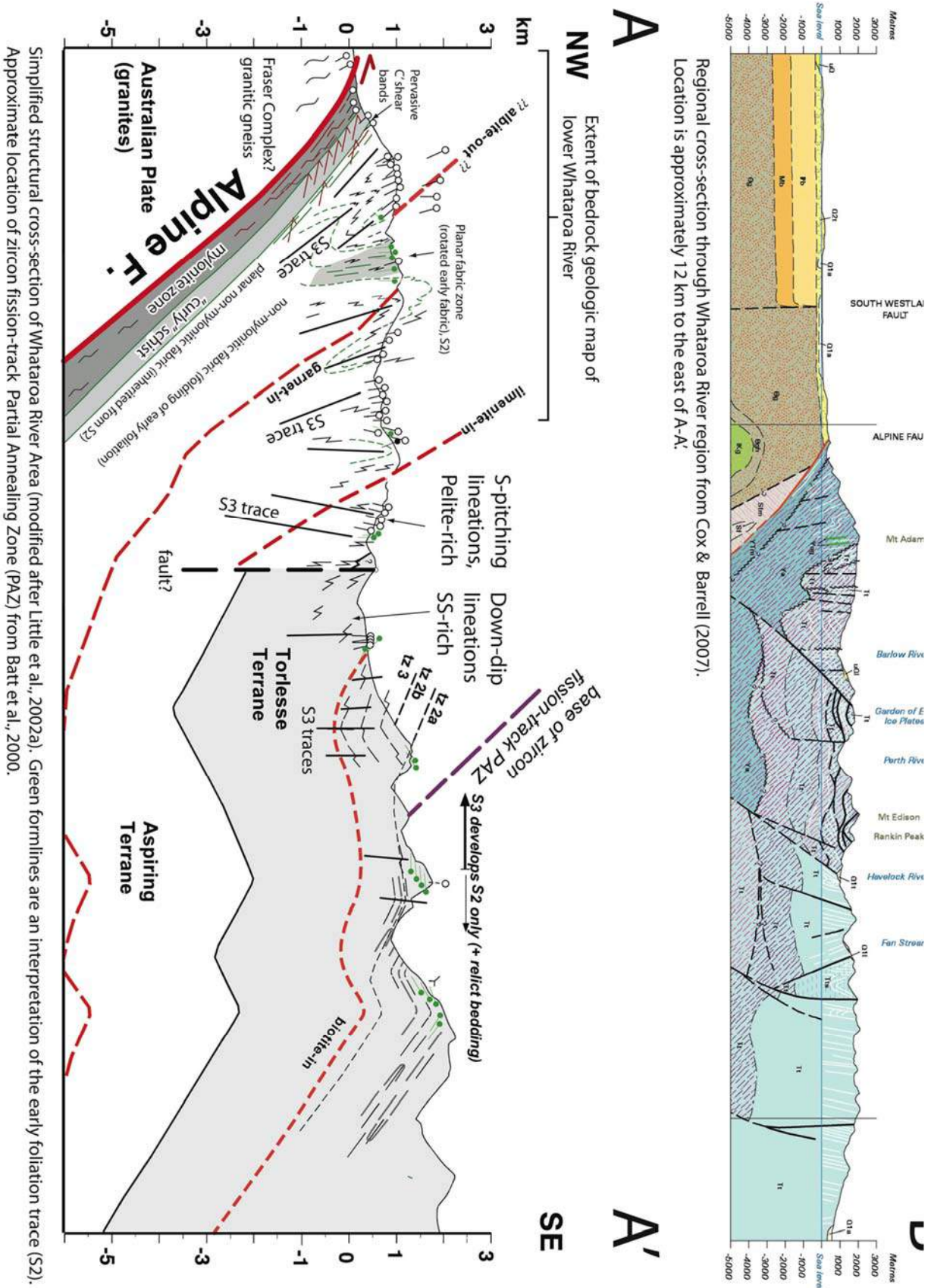


Figure D.7.

The cross-section A-A' (Figure E.7) depicts a fanning of the steep Alpine (S3) foliation and related folds away from the Alpine Fault, and a pattern of decreasing foliation dips in

proximity to the Alpine fault. Near the Main Divide, the early fabric (S2) remains gently dipping, S3 is weak or absent, and relict bedding is conspicuous. A planar panel of the early foliation (S2) borders the mylonite zone. Farther NW, that foliation, and relicts of its associated quartz rodding lineation (L2) have been swept into the mylonite zone, where those and other pre-Cenozoic inherited fabric elements, such as garnet porphyroblasts, have been re-oriented by shearing within the Alpine mylonite zone. The profile B-B' (Figure E.7) is a smaller scale cross-section from Cox and Barrell along a line about 12 km to the east of A-A' (beyond the area of the geological map included in this guide).

STOP H: ALPINE FAULT OVERTHRUST AT GAUNT CREEK

Richard Norris; Alan Cooper; Virginia Toy; Carolyn Boulton

We will be transported to Gaunt Creek by Grey and Vicky Eatwell of Alpine Fault Tours, who have a concession to operate tours to the site. Access crosses their land and they need to be contacted to arrange access if you return to this site in future. If you wish to examine the mylonite and cataclasite sequence exposed above the Alpine Fault plane, you will need to cross Gaunt Creek so expect to get your feet wet!

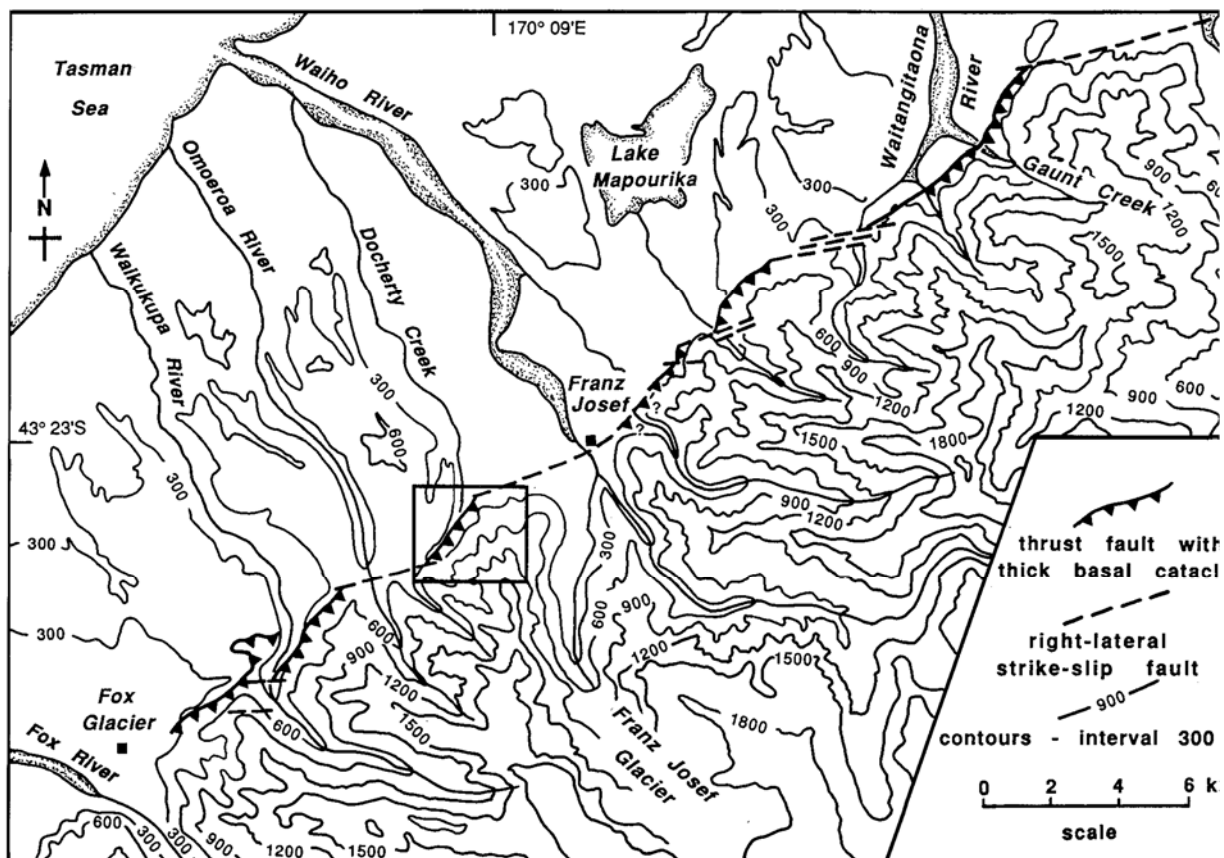


Figure E.1. Map of the central section the Alpine Fault between Gaunt Creek and Fox Glacier (Norris and Cooper 1995)

In historic time, the Waitangitaona River (Figures F.1, F.2) has aggraded more than any other similar sized West Coast river. In the 1950s, concern at the aggradation prompted investigation when it was found that most of the material was being supplied from Gaunt Creek, a tributary that cuts across the Alpine Fault. Gaunt Creek was then, and still is, eroding the base of a large face more than a 100 m high that exposes shattered and

brecciated schist mylonites thrust over schist gravels. The continued aggradation of the Waitangitaona River led in 1967 to the anticipated shift from its original course, across the lower Whataroa flats, to its present one through Lake Wahapo.

On the north bank of the River, immediately after descending from the stop bank (start of the 4WD access road), there is an exposure of foliated granite cut by shear zones and by mafic dykes. The rock is part of the West Coast basement and is probably best included in the Fraser Complex (Rattenbury 1987). The dykes cut the foliation in the granitoids but are themselves deformed by cataclastic shear zones. The age of similar dykes further north is equivocal but probably late Cretaceous (Adams and Nathan 1978; Rattenbury et al. 1988).

The large slip at Gaunt Creek is illustrated in Figure F.3 (Cooper and Norris 1994), which is a **map of the face** projected onto a vertical plane trending 140° and scaled by radial-line plotting from a set of overlapping photographs (N.B. It is **not** a true cross-section).

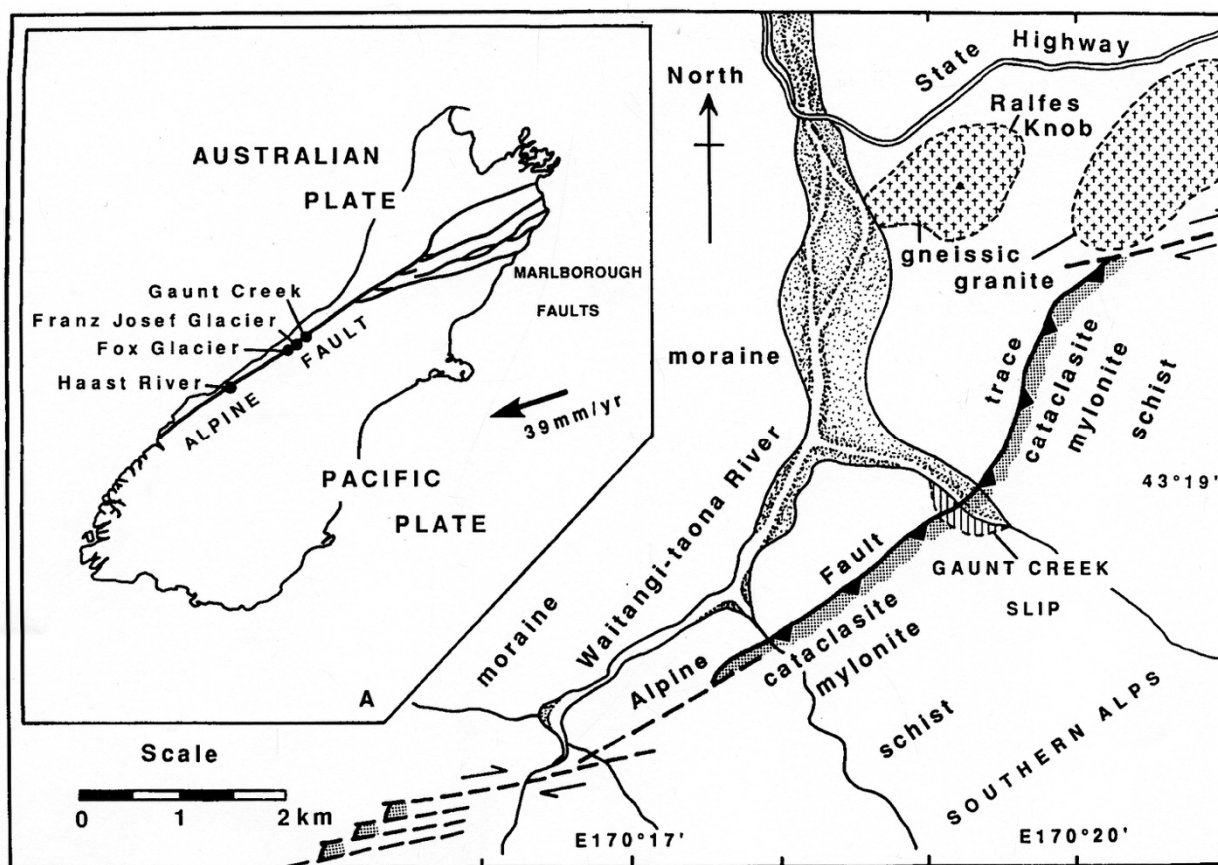


Figure E.2. Geological map of the Waitangi-taona River catchment, illustrating the segmented nature of the Alpine Fault trace and Gaunt Creek locality (Cooper and Norris 1994)

The main feature of the exposure is the overthrust of cataclastic mylonites over gravels. At the base of the overthrust is a zone up to 30 m thick of **pale-green cataclasites** overlying a 10-40 cm thick **grey gouge** (the fault principal slip zone, p.s.z.) above gravels. The base of the cataclasite has a mean strike of 059° and dip of 38° SE, although it is cut by higher-angle shears, and contains a steep east-dipping internal fabric. Slickensides on the grey gouge are variable in orientation - the mean of the dominant set trends almost due east, although at the

level of Gaunt Creek a prominent lineation plunges gently to the SW. All these are quite oblique to the dip direction of the thrust plane (Figure F.4).

In detail, the p.s.z. is composed of sub-planar layers of slightly different colour and particle size range, ranging from 5-60 mm in thickness. The thickest layer is sometimes injected as flame-like structures into the overlying cataclasite. Individual layers contain C-like shears of much finer-grained material, and calcite laminae. The latter indicate fluids passed through the gouge after its formation. Particle sizes within the gouge have been measured using a laser particle size analyzer (Boulton and Toy, 2008). The resulting particle size distributions (Figure F.5) are not fractal, indicating either that the gouge was not formed by constrained comminution during cataclasis (c.f. Sammis et al. 1986), or that finer particles in the C-shears were not sufficiently represented in the analyses.

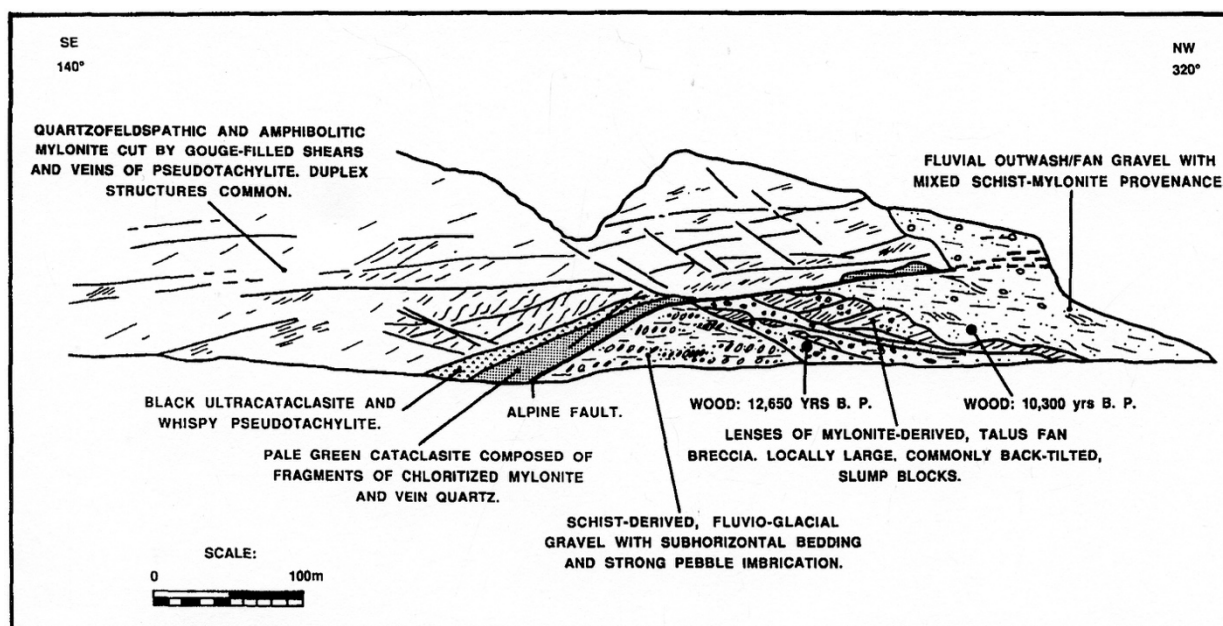


Figure E.3. Map of the Gaunt Creek outcrop face (Cooper and Norris 1994)

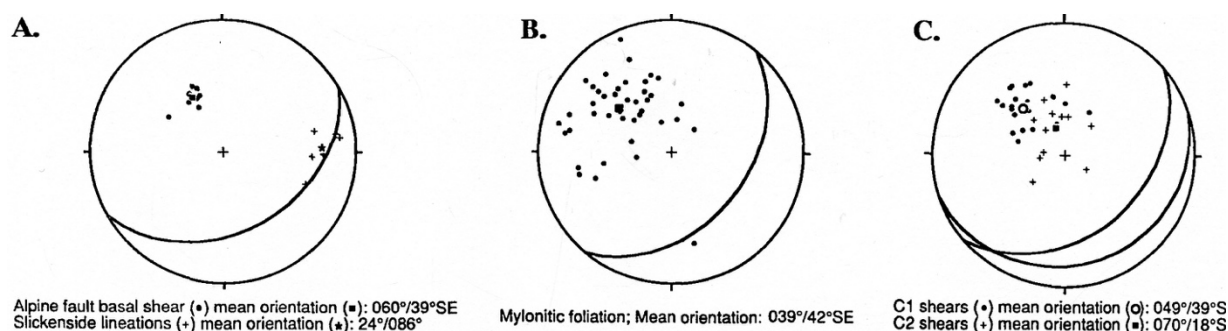


Figure E.4. Equal area plots of structural features in rocks of the Alpine Fault zone, Gaunt Creek (Cooper and Norris 1994)

The overlying pale-green cataclasites contain abundant pseudotachylite, within which the glassy matrix has mostly been devitrified or altered to a mixture of clay minerals and sericite (Toy 2008). In outcrop the pseudotachylites now appear a blue-grey, pale grey, or brown. Some of the more voluminous pseudotachylite bodies contain quartz and carbonate-filled amygdyles, and late calcitic cements are common. Formation of these pseudotachylites within the cataclasite mass indicates that co-seismic slip was well-localised (i.e. the mass

probably did not deform by distributed cataclastic flow), and that fluids were only locally present during seismic events.

Stable isotope data have been obtained from carbonate cements in the p.s.z. and both carbonate cements and cross-cutting calcite veins in the immediately overlying gouge both here and at the Hare Mare Creek locality (Stop K); (Figure F.5). In both cases, the carbon-oxygen isotopic ratios are consistent with an increasingly rock-exchanged fluid source with the transition from cross-cutting veins to cataclasite to p.s.z. cement. This may indicate that the p.s.z. offers the highest permeability pathway for fluid transport from depth within the fault rocks.

The basal cataclasite thins and is cut out upwards, but then reappears at the base of the overthrust further out to the west. The dip of the basal contact here is quite different, being about 30°S on a strike of 120°. This change is almost certainly due to the thrust reaching the surface and rotating under gravity to parallel the ground. It coincides with a change in the overthrust material from sub-horizontally bedded **schist-derived fluvial gravels** to **mylonite- and cataclasite-derived fan gravels** on a depositional slope of approximately 30°W. The latter contain large **slump masses** of mylonite and cataclasite derived by gravitational collapse of the thrust front - they have been subsequently overthrust themselves by the mylonites. The slumped masses preserve the mylonitic foliation, with some back-tilting and imbricate slide zones. The base of the slump packets in places overlie a weathered silt horizon with fine-scale cross-beds - presumably the surface of the shingle fan at that time. The upper surfaces of the slump packets are eroded and overlain by angular mylonitic fan debris. The occurrence of pale green cataclasite amongst the slump masses indicates that the basal thrust zone was exposed at the surface. In contrast, the fluvial gravels below the fan sequence are dominantly schist-derived, suggesting that the thrust zone was not locally exposed at the time of their formation. The thrust cuts through these gravels at a moderate angle of dip.

Several pieces of wood have been obtained from the fan gravel sequence and have been dated by ¹⁴C methods as 12,650 ± 90 and 10,300 ± 130 y BP. Approximately 180 and 110 m respectively of displacement has occurred since the deposition of these gravels, indicating a minimum displacement rate along plate vector-parallel slickenside trends of between 18 and 24 mm/yr.

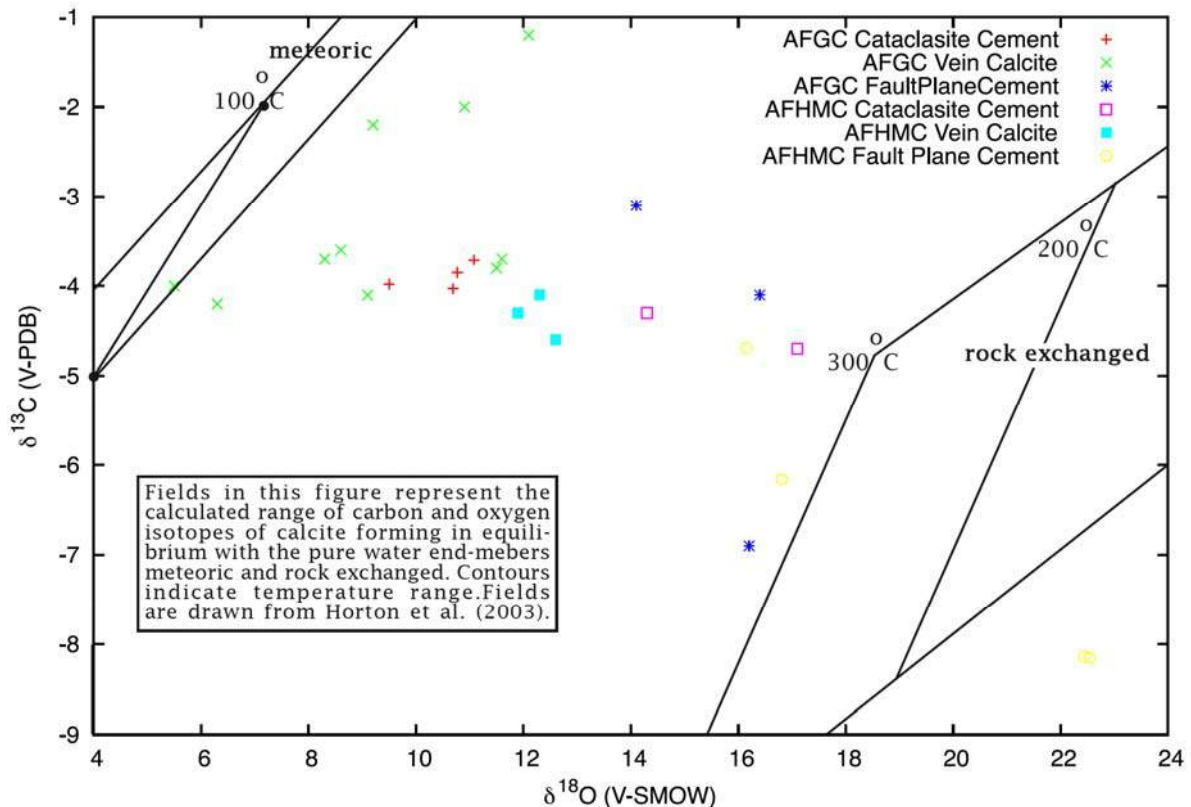


Figure E.5. Carbon-oxygen isotopic data from cataclasite cements and cross-cutting veins within a few metres of the Alpine Fault plane at Gaunt and Hare Mare Creeks (from Boulton and Toy 2008)

Above the pale green cataclasite zone is a zone of black and olive green **cataclased ultramylonites**. These materials contain abundant seams of **pseudotachylyte**, commonly generated by slip along shears juxtaposing olive green and black materials, and oblique to the ultramylonite foliation. Injection structures up to 10 cm long attest to the fact these melts were highly mobile / low viscosity. Fresh pseudotachylyte glass has been obtained from this zone (see Norris and Cooper 2008) but the matrix of most pseudotachylytes is now composed of an alteration or devitrification assemblage (commonly felted masses of sericite) as in the underlying pale green cataclasites. The ultramylonite has a pervasively-developed greenschist-facies mineral assemblage, in which sericitised feldspar porphyroclasts are embedded in a generally fine-grained matrix of chlorite+quartz+muscovite with minor titanite+opaques+clay minerals. Banding of these minerals defines a disjunctive cleavage suggesting pressure solution processes were involved in this deformation. Allanite, with clinozoisite rims, is relatively common suggesting some of these rocks are derived from a footwall, granitoid protolith. The rock is full of anastomosing minor shears, generally filled with incohesive gouge, which are both steeper and shallower than the main thrust.

Further upstream, the cataclasites pass into **schist-derived mylonites**, also containing large numbers of anastomosing gouge zones. The general attitude of the mylonitic foliation is parallel to the basal thrust. However, in many places, it has been imbricated on shears to form steep dipping packets, i.e. a series of duplex structures developed between major thrust zones parallel to the basal thrust. Pseudotachylytes occur on bounding faults between metabasic and quartzo-feldspathic layers and mm-thick foliation-parallel, mixed pseudotachylyte and cataclasite veins are also found in this zone (Toy 2008). Further

upstream, where Gaunt Creek enters its gorge, the foliation is more regular at 40° to 50° SE, with fewer shears and duplex development. A 40° to 50° dip is similar to that recorded from most creek sections in the area (Sibson et al. 1979) and is considered to represent the approximate dip of the main Alpine Fault plane. Mylonites derived from both amphibolites and quartzofeldspathic schists may be observed. Analysis of the imbricated shears and rotated mylonitic foliation suggests a thrust direction to the NW (Figure F.4).

Numerous steep, cross-cutting faults and gouge zones may be observed in the outcrop. A prominent series of normal faults dipping to the west can be seen cutting the mylonite sheet above the gravel face - these were presumably developed during the rotation of the thrust sheet as it thrust out onto the surface. Many of the fault gouges and shears contain carbonate deposits and sulphide minerals, attesting to the percolation of warm fluids through the fractures. Zones of hydrothermal alteration can be seen around many fractures. In the mylonites, quartz veins cross-cut the mylonitic foliation, indicating fracturing and fluid flow above the brittle-ductile transition. Studies of fluid inclusions in veins within the schists and mylonites have been undertaken at Otago University (Craw 1988; Holm et al. 1989; Craw 1997; Toy 2008) – more details are presented below.

Our interpretation of the structural history at Gaunt Creek is (see Figure F.6):

1. The main fault plane dips southeast at about 40°-50°.
2. During a period of aggradation, the basal fault plane together with its associated mylonites and cataclasites was buried by schist-derived fluvial gravels. While the fault may have continued to cut up through the gravels during this period, the cataclasites would not be exposed at the surface provided aggradation kept pace with fault movement.
3. Aggradation ceased and erosional downcutting began. The fault zone became exposed at the surface. Mylonitic and cataclastic debris formed talus fans in front of the advancing thrust front. Blocks of mylonite and cataclasite slumped off the scarp down the fan surface. The thrust wedge continued to advance across the fan gravels, its attitude rotating to conform with the ground surface.
4. The slope of the aggrading fan lessened, and gravels again covered the thrust plane. More recently, extensive downcutting by Gaunt Creek has exposed the fault zone in the present slip.

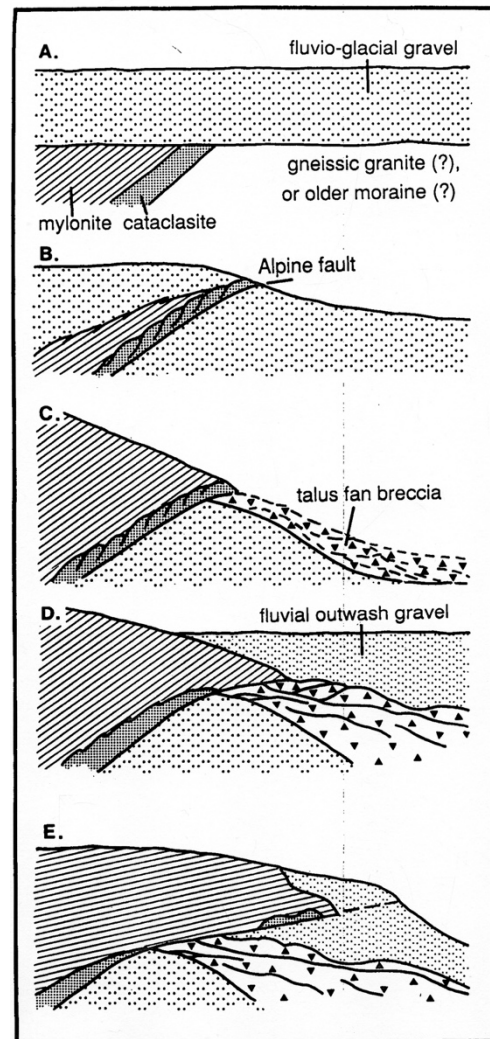


Figure E.6. Sequential structural development of the Alpine Fault zone, Gaunt Creek (Cooper and Norris 1994)

CLUES ABOUT THE THERMAL STRUCTURE OF THE ALPINE FAULT AT DEPTH FROM STUDIES OF THE EXHUMED SEQUENCE AT GAUNT CREEK

Quartz veins within the fault rocks were formed and deformed at temperatures ranging from $>500^{\circ}\text{C}$ to immediately above that of the brittle-viscous transition ($\sim 325^{\circ}\text{C}$), illustrating that fluids are present throughout the fault zone. Mixed $\text{CO}_2\text{-H}_2\text{O}$ fluid inclusions are hosted in quartz veins in foliation boudinage structures in the mylonites here. The structures represent transitional ductile-brittle behaviour. These inclusions were trapped from immiscible fluids so P and T at the time of trapping can be estimated from them via microthermometric studies. These results indicate trapping conditions of $\sim 325 \pm 15^{\circ}\text{C}$ and ~ 0.35 kbar. Vein microstructures indicate fluid temperatures were equal to rock temperatures. Assuming hydrostatic fluid pressure, the veins were trapped at depths of <8 km for an average density of mixed $\text{H}_2\text{O-CO}_2$ fluids in the shallower crust of >500 kg m^{-3} .

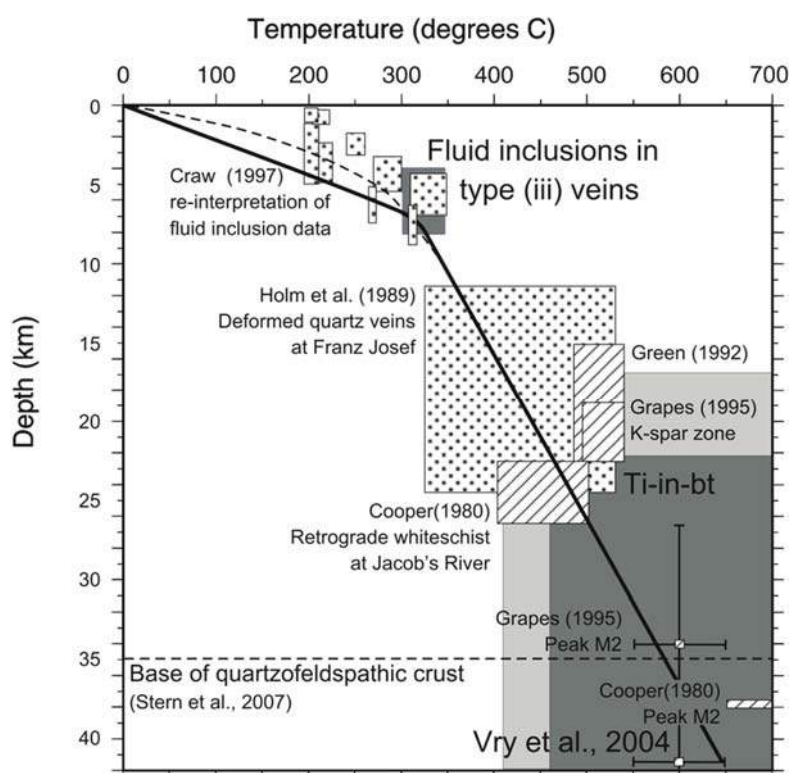


Figure E.7. Summary of existing constraints on thermal structure of the Alpine Fault zone and a proposed 'best-fit' thermal profile (Toy et al. in prep)

Considering this result in the context of pre-existing thermobarometric estimates in the fault rocks and the immediate hangingwall allows definition of a most likely uplift path P-T profile within the fault zone (Figure F.7). In this model, the uplift path P-T gradient of fault zone rocks above the brittle-viscous transition is of the order of $40^{\circ}\text{C km}^{-1}$. Below the brittle-viscous transition, the uplift path P-T gradient is $8\text{-}14^{\circ}\text{C km}^{-1}$. The P-T profile within the fault rocks is comparable to that in the immediate hanging wall Alpine Schist, indicating there is no peak in the crustal isotherms in the fault hangingwall, as was indicated by previous numerical models, and analyses that did not consider data from the fault rocks themselves.

QUARTZ CRYSTALLOGRAPHIC PREFERRED ORIENTATIONS (CPOs) IN THE MYLONITES – IMPLICATIONS FOR DEFORMATION HISTORY AND SHEAR ZONE KINEMATICS

Quartz-rich layers in the mylonite zone at Gaunt Creek contain strong quartz crystallographic preferred orientations (CPOs). The CPOs have a consistent asymmetry indicating a high ratio of simple to pure shear strain, with a shear sense of dextral-up to the NW that is consistent with the mesoscopic shear sense indicators and with the slip on the active fault. There is a transition from Y-maxima and asymmetric single girdles in mylonites and ultramylonites within 300 m of the present fault trace, to cross-girdle fabrics in the protomylonites further from the fault (Figure F.12). The strong Y-maxima or single girdle CPOs are ascribed to high ductile shear strains under amphibolite facies conditions while the cross-girdle patterns found in the protomylonites are interpreted to represent deformation under lower temperature conditions. However, the observed fabric transition cannot logically be attributed to variations in temperature during the last increment of deformation. The highly oriented Y-maximum fabrics formed at high temperature contain very few grains suitably oriented for basal slip, so that the slip systems activated during subsequent shear at lower temperatures during exhumation were prism or rhomb. Further from the fault, where shear strains under high temperature conditions were lower, weaker fabrics developed under these conditions were modified at higher levels in the crust into crossed girdle patterns. This evolutionary path is explained further in Figure F.8. An implication of this interpretation is that intense localisation of shear strain along the fault zone within the lower crust must have occurred in order for the high-temperature fabrics to become sufficiently intense to be preserved. This in turn implies that deep-seated localised shear was taking place early during the evolution of the current oblique-slip plate boundary fault (Toy et al. 2008).

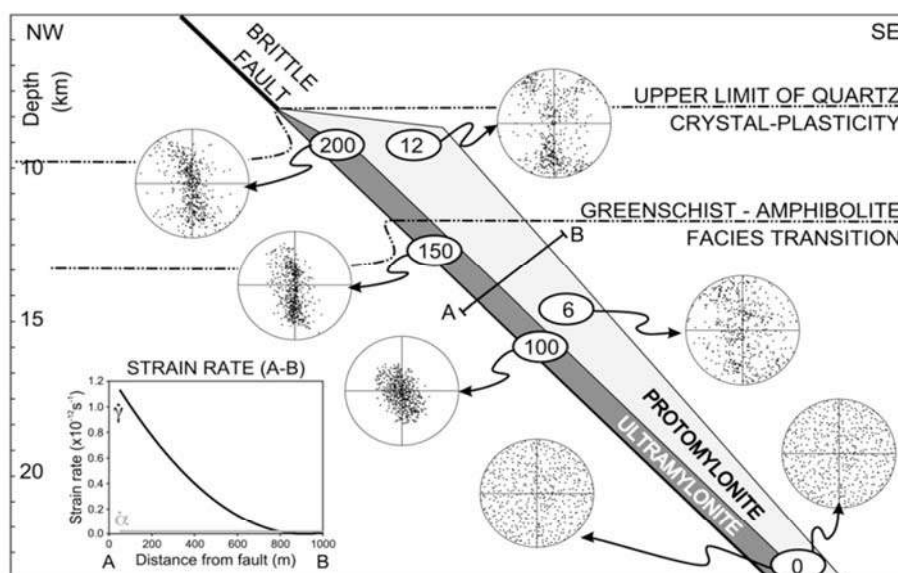


Fig. 11. Cartoon illustrating progressive development of CPOs in quartzites during deformation and exhumation in the Alpine Fault mylonite zone. Numbers in ellipses represent the total strain experienced during uplift to that level of the mylonite zone. Adjacent CPO figures are representative of the pattern that could develop with that strain amount and temperature from the starting CPO that is exhumed from deeper levels. Notice how the amount of strain at high temperatures in the protomylonites is insufficient to form a highly oriented fabric, whereas the ultramylonites exhumed through the amphibolite–greenschist facies transition already contain a strong Y-maximum pattern that is not easily destroyed during subsequent low temperature deformation. Strain rate graph is constructed using the finite strain estimates of Norris and Cooper (2003), evenly distributed over a period of 5 million years. In this cartoon the starting CPO is shown as random. In reality the Alpine schist has a weak pre-existing CPO. All areas of orientation space are represented in these weak fabrics and the pre-existing CPOs do not share the same finite strain axes as the mylonites; so for purposes of general understanding representing the pre-existing fabric as random is a reasonable simplification.

Figure E.8. Cartoon illustrating process of development of quartz CPOs in the Alpine Fault mylonite zone (Toy et al. 2008)

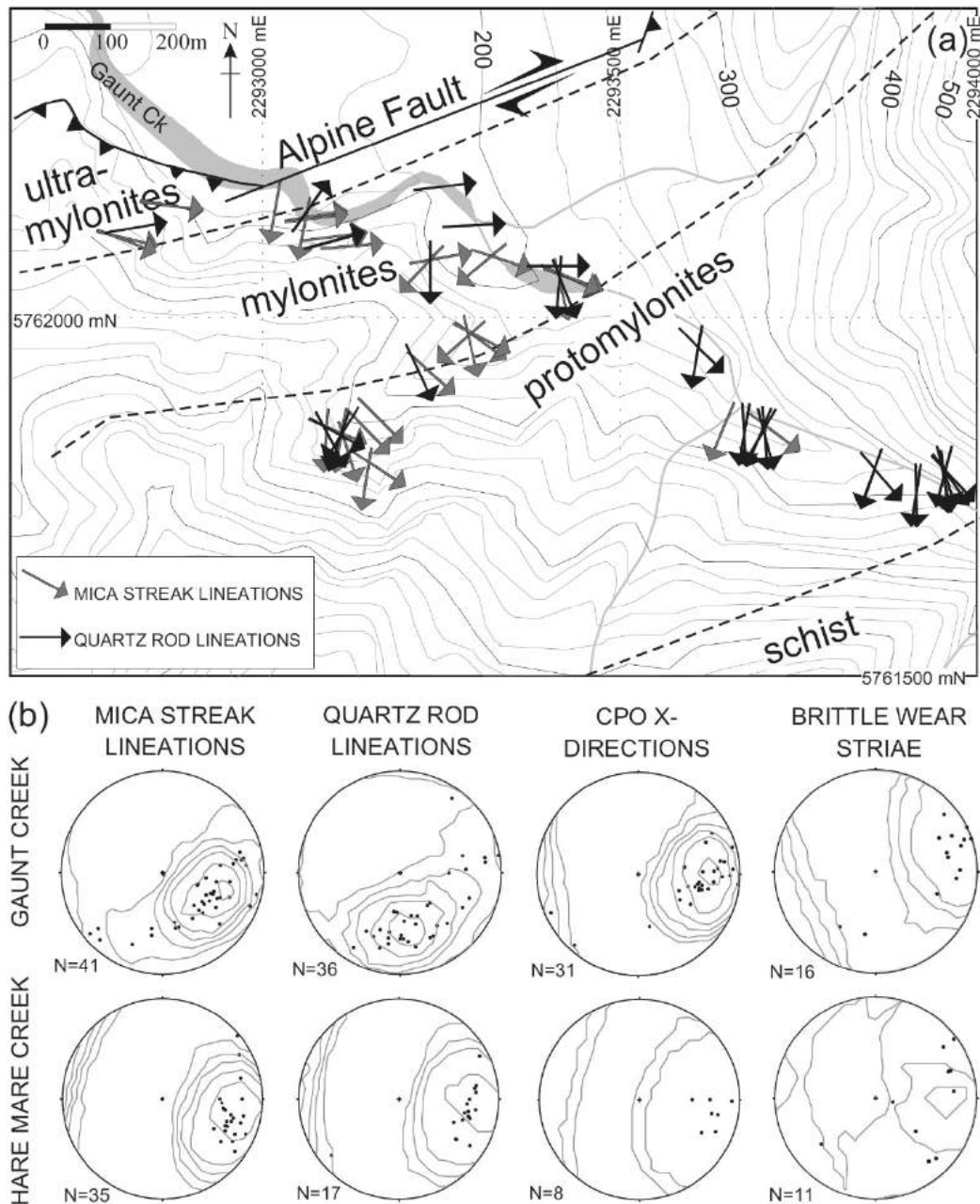


Figure E.9. Summary of mica streak, quartz rod and brittle lineations, and CPO fabric data from Gaunt Creek and Hare Mare Creek. (a) Map shows variation in distribution and orientation of quartz rod and mica streak lineations in the Gaunt Creek section. (b) Plots of lineation data are equal area lower hemispheres Schmidt projections. Kamb contour intervals are 2.0 in all plots.

KINEMATIC HISTORY OF THE MYLONITE ZONE

Asymmetric shear sense indicators, shear band and S-C fabrics, quartz CPO 'X'-axes and various types of lineations that occur within the exhumed mylonites have triclinic symmetry (i.e. the finite stretching direction is not perpendicular to the vorticity vector). In particular, macroscopic object lineations are not usually parallel to the simple shear direction, despite high total simple shear strains ($\epsilon \geq 150$). The various fabric elements record different proportions of the total strain experienced by the mylonites and reflect different aspects of the kinematics of the deforming zone, but collectively record a progressive evolution of

strain. During uplift and exhumation the simple shear strain component became more dominant and progressively more localized into shear bands cross-cutting the mylonitic foliation (as, for example, you may see in the Tartare Stream section, Stop H).

Many object lineations preserved in the mylonites are inherited from the pre-mylonitic fabrics and this has affected the distribution of their orientations. In particular, SW-plunging quartz rodding lineations are commonly preserved in the distal mylonite zone. In places these lineations have been only partially rotated into parallelism with the mylonitic stretching direction during shear focused within mylonitic shear bands (Figure F.11).

We have used models of transpressive deformation in an oblique triclinic shear zone (model of Lin et al. 1998) – see Toy et al. (in revision) for further details. In order to obtain parallelism between the finite stretching direction calculated from transpression models and the mylonitic lineations, a pure shear component of $\epsilon \sim 3.5$ is required for total simple shear strains of $11.7 < \epsilon < 150$. The observations and numerical models also show that rotation of linear features during simple shear is slow and inherited fabric components may not be destroyed until very high simple shear strains have been attained.

RHEOLOGIC EVOLUTION OF THE FAULT ZONE

Quartz CPO data, estimates from Ti-in-biotite thermometry and observations of rheological behaviour of the various constituent minerals in the polyphase materials here provide evidence that deformation at the shallowest levels of the viscous regime was localized to the very core, and the margins of the mylonite zone (Toy et al. 2008). The intervening material may have experienced strain hardening and have been exhumed while experiencing little deformation. Is it possible that we might be able to observe such a localized zone of deformation in the core of the fault? Toy (2008) suggested that fault rock rheology in the shallowest parts of the viscous regime is controlled by a polyphase/composite flow law rather than being quartz-dominated. This flow law results in significant weakening if fluids are present (Figure F.10). However, we as yet have few observational constraints on the amount of fluid present during mylonitic deformation – this is a focus of future research.

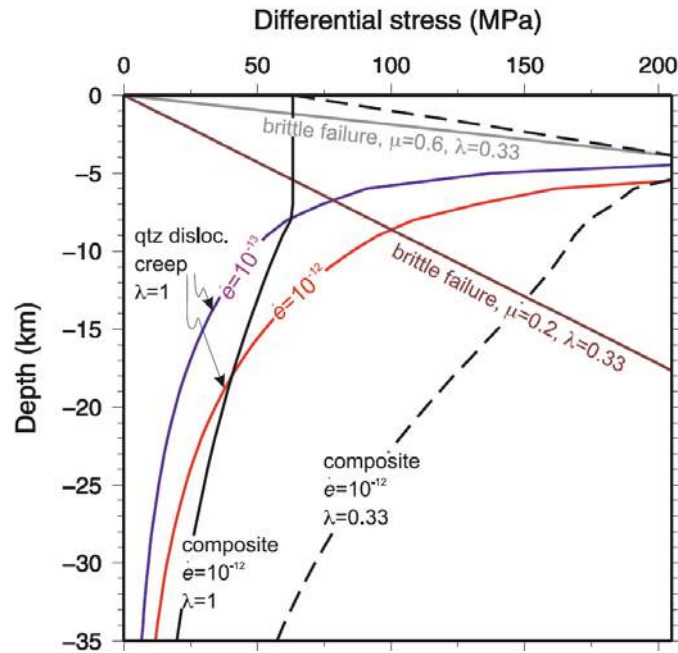


Figure E.10. Strength profiles for the Alpine Fault zone, incorporating a composite frictional-viscous flow law. Purple and red lines are flow stresses for dislocation creep of quartz at the indicated strain rates. Black lines are a composite brittle-viscous flow law constructed using the generalized mixing law of Ji and Xia (2002). Brown and grey lines show brittle failure envelopes. Only the weakest and strongest brittle failure envelopes for the main Alpine Fault plane (ie. $\mu = 0.2$ in an Andersonian strike-slip stress regime; brown lines, and $\mu = 0.6$ in an Andersonian thrust regime; grey lines) for hydrostatic fluid pressure conditions are shown in order to simplify the diagram.

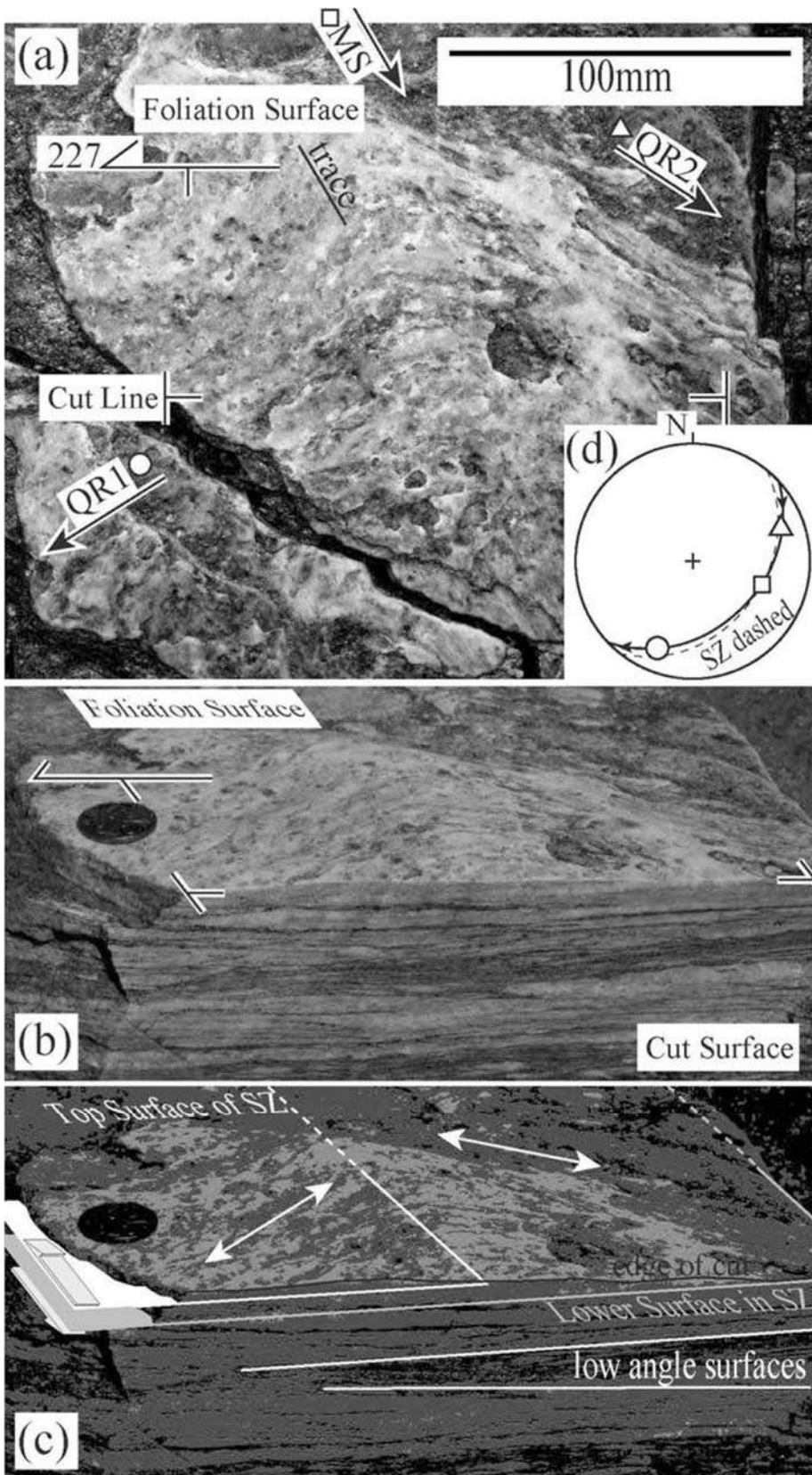


Figure E.11.

Variations in orientation of quartz rodding lineation in the mylonites and possible relationships to shear zones. (a) Quartz rodding lineations on a single quartz layer/ foliation surface (227/42SE) in protomylonites of Hare Mare Creek. Quartz rodding lineations (QR1) on the left are oriented 21/202. These start to bend, across a trace (marked) that pitches 60-70° from the east, into an orientation plunging at 21/071 (QR2). A mica streak lineation at 38/108, from a layer 2mm beneath the quartz rodded surface (MS) is seen 5cm above the top of the photo. (b) Sample of outcrop shown in (a), cut perpendicular to foliation along the line shown in A, to illustrate relationships to internal structures. (c) Three tone rendering of (b) to

highlight geometry. Traces of several surfaces, at low angles to the foliation shown in (a), are visible in the cut surface. A shear zone model to explain the bending of the lineations is shown. The top surface of the shear zone contains the trace marked in (a) and has a trace in the cut surface that is steeper than the trace of surface foliation. A lower surface in the shear zone is shown. Since the outcrop in (a) does not continue to the right, the bottom boundary

of the shear zone is not constrained. A line of paler quartz is visible in the cut surface in (b) parallel to the postulated shear zone trace. The mica streak lineation is used as the movement vector. (d) Stereonet to show measured orientations and the shear zone geometry shown in (c). Solid great circle is the foliation surface in (a). Symbols correspond to the lineations marked in (a). Arrows show rotation sense (clockwise) of lineation. Dashed great circle is the proposed shear zone plane with a shear vector parallel to the mica streak lineation and the intersection with the foliation (trace marked in (a)).

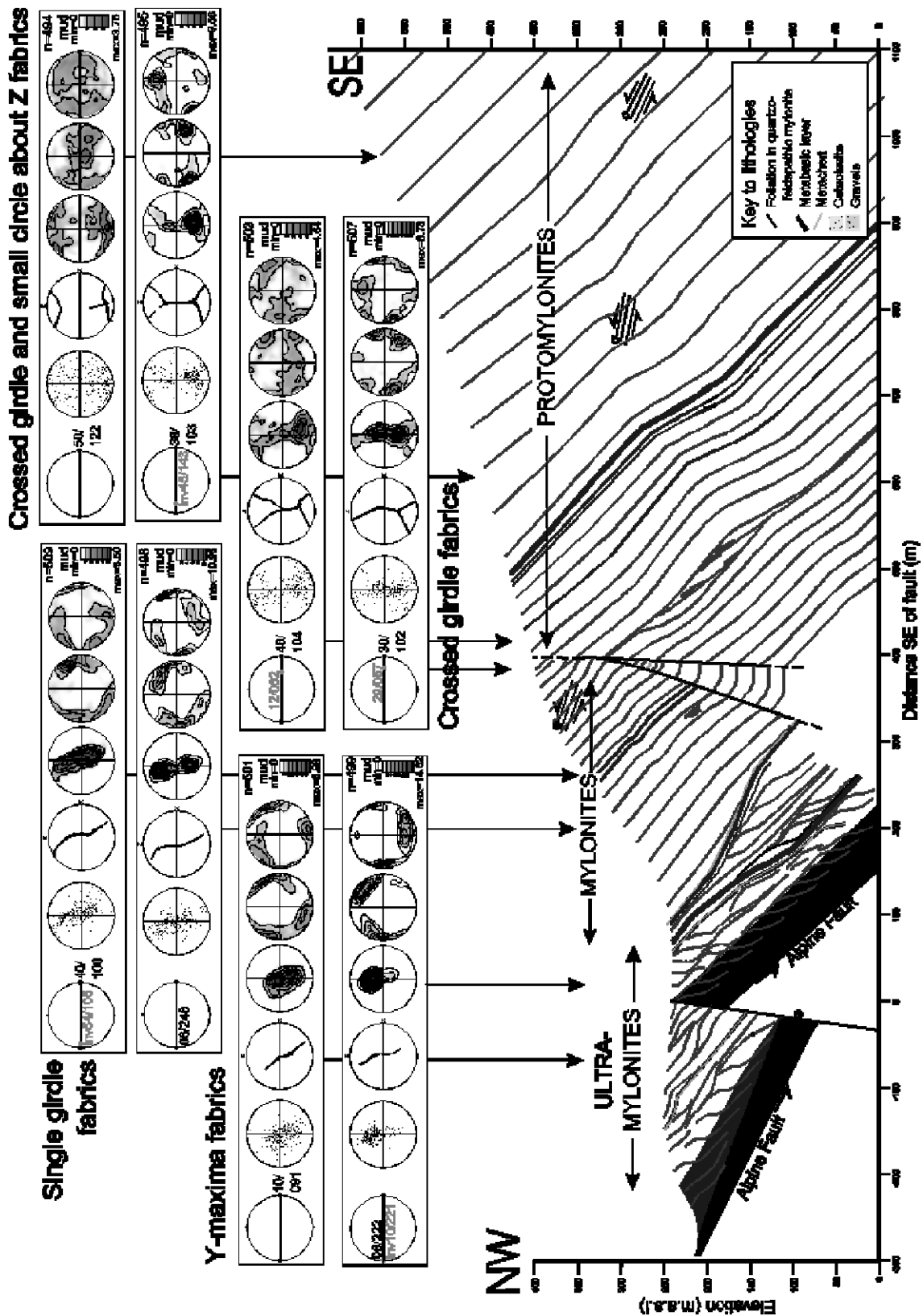


Figure E.12. Cross section of Gaunt Creek mylonite zone (Toy 2008), with quartz CPOs. (within boxes, from left to right, are; kinematic reference frame and lineation information, lower hemisphere point plot of 500 c-axes, fabric skeleton constructed from contoured c-axis plot, contoured lower hemisphere equal area plot of the 500 c-axes, contoured upper and lower hemisphere plots of a-axes Stereonets are lower hemisphere Schmidt projections. The c-axis plot view is up-foliation and towards the NW. mud = multiples of uniform density.

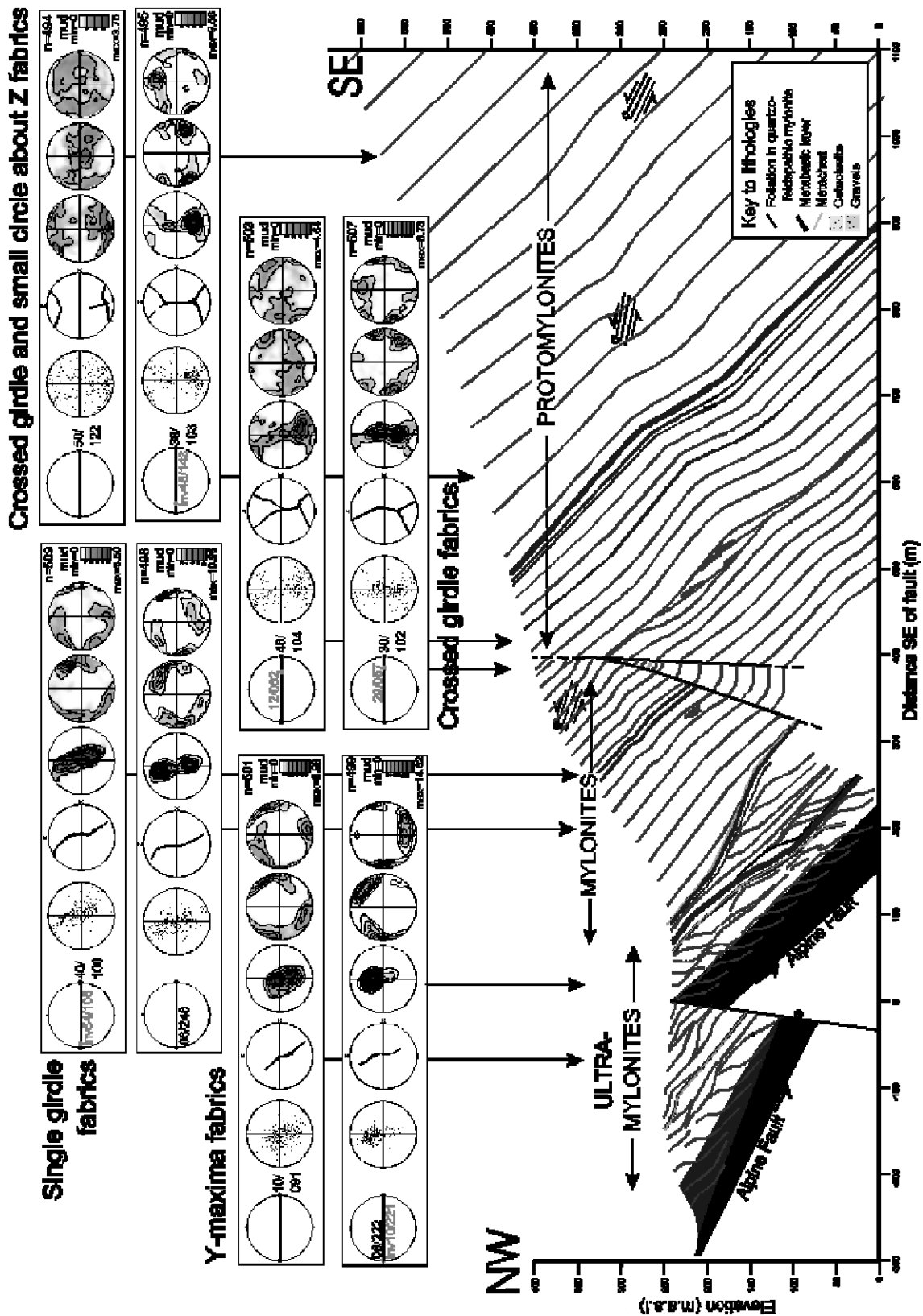


Figure E.12. Cross section of Gaunt Creek mylonite zone (Toy 2008), with quartz CPOs. (within boxes, from left to right, are; kinematic reference frame and lineation information, lower hemisphere point plot of 500 c-axes, fabric skeleton constructed from contoured c-axis plot, contoured lower hemisphere equal area plot of the 500 c-axes, contoured upper and lower hemisphere plots of a-axes Stereonets are lower hemisphere Schmidt projections. The c-axis plot view is up-foliation and towards the NW. mud = multiples of uniform density.

STOP I: WAIHO VALLEY / FRANZ JOSEF GLACIER

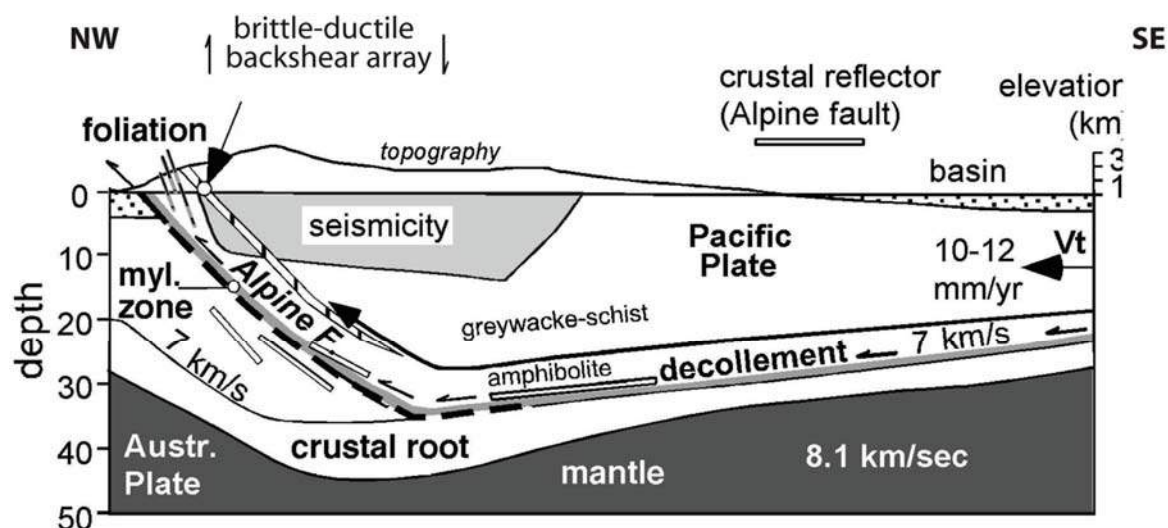
T. Little, R. Norris, A. Cooper

Drive to the Franz Josef Glacier trailhead and park. Follow walking track towards the glacier terminus (note that in places this track detours to the right up the valley wall to avoid the Waiho River).

WAIHO VALLEY SCHISTS – OVERVIEW

The schists of the Waiho Valley below the terminus of the Franz Josef Glacier occur in the hangingwall of the Alpine Fault (Figure I.1). The car park is near the oligoclase (albite-out) isograd, about 4 km east of the recent fault trace. The garnet isograd lies some distance east of the glacier terminus, so that the section to be examined lies within the garnet zone (Figure I.2).

The amphibolite facies schists are mostly pelitic or psammitic in composition, but locally include bands of other protoliths, such as metachert and mafic metavolcanic rocks. Zones of folding with well-developed SW-plunging fold hinges and rodding lineation are typical of the schists outside of the mylonite zone of the fault. During the late Cenozoic transpression, these late Mesozoic ("Alpine") fabrics were constructively reinforced (further "flattened" and tightened), together with some renewed mineral growth to yield the strong, steeply SE-dipping foliation that is exposed near the glacier terminus today. Finally, the rocks were exhumed in the hangingwall of the Alpine Fault (Little et al. 2002a; see detailed discussion below). At this time, ductile deformation became strongly localized into the Alpine mylonite zone with "far-field" shearing extending several kilometres up-section from that zone (Figure I.8).



Geophysical interpretation of the deep crustal structure along a NW-SE cross-section through the central Southern Alps [after Kleffman et al., 1998; Leitner et al., 2001; Stern et al., 2001], also showing selected geological features in Alpine fault's hanging wall [from Little et al., 2002a]. Local convergent plate velocity (10–12 mm yr from DeMets et al. [1990, 1994] and Walcott [1998]. Figure from Little, 2004.

Figure E.13.

Holm et al. (1989) recognized a sequence of structures that post-date these folds and foliation, and which represent sequential development during progressive exhumation of the schist in the hangingwall of the Alpine Fault (Figure I.5). Fluid inclusion studies of quartz

deposited in veins associated with these structures (ductilely deformed cross-cutting veins, internal boudinage of the foliation, semi-ductile shears, and vertical and horizontal extension fractures) allow a pressure-temperature-time plot to be constructed for the uplift and exhumation of these rocks (Figure I.12). This shows slow cooling from depths >20 km and $T > 500^{\circ}\text{C}$ until the brittle-ductile transition at about 350°C and 6-8 km, after which the rocks cool rapidly on a high thermal gradient to the surface. Unpublished O-isotope data from Wickham and Norris (unpublished data) and H-isotope data from Jenkin et al. (1994) allow constraints on fluid-rock interaction during uplift (Figure I.13).

Brittle faults are evident in the valley walls (Figure I.4). These strike roughly E-W and have shear sense indicators showing a dextral shear sense, compatible with them being "riedel" shears relative to the Alpine Fault. Some show an overprint of a normal displacement late in their history (Hanson et al. 1990).

Very young (post last glacial coverage) fractures on glacially scoured surfaces of roches moutonee in the valley indicate a stress orientation similar to that inferred from geodetic data (Norris and Cooper 1986) and may represent stress relief fracturing following retreat of the ice load. Since 1987, however, the glacier has advanced back over these outcrops and they may or may not be clear to examine on this trip!

More detailed description and discussion are presented below.

We will follow the sign posted walking track down to the river flats, and proceed up stream to the current terminus of the Glacier, which has retreated several hundred meters in the past five years. The round-trip back to the vehicles will take us about two hours.

MYLONITIC VS. NON-MYLONITIC ALPINE SCHIST NEAR FRANZ JOSEF GLACIER

The parking lot for the Franz Josef Glacier walk is located ~4 km to the SE of the trace of the Alpine Fault, on the west bank of the (rapidly aggrading) Waiho River (Figure I.2).

Simple Bedrock Geological Map of Franz Josef Glacier region

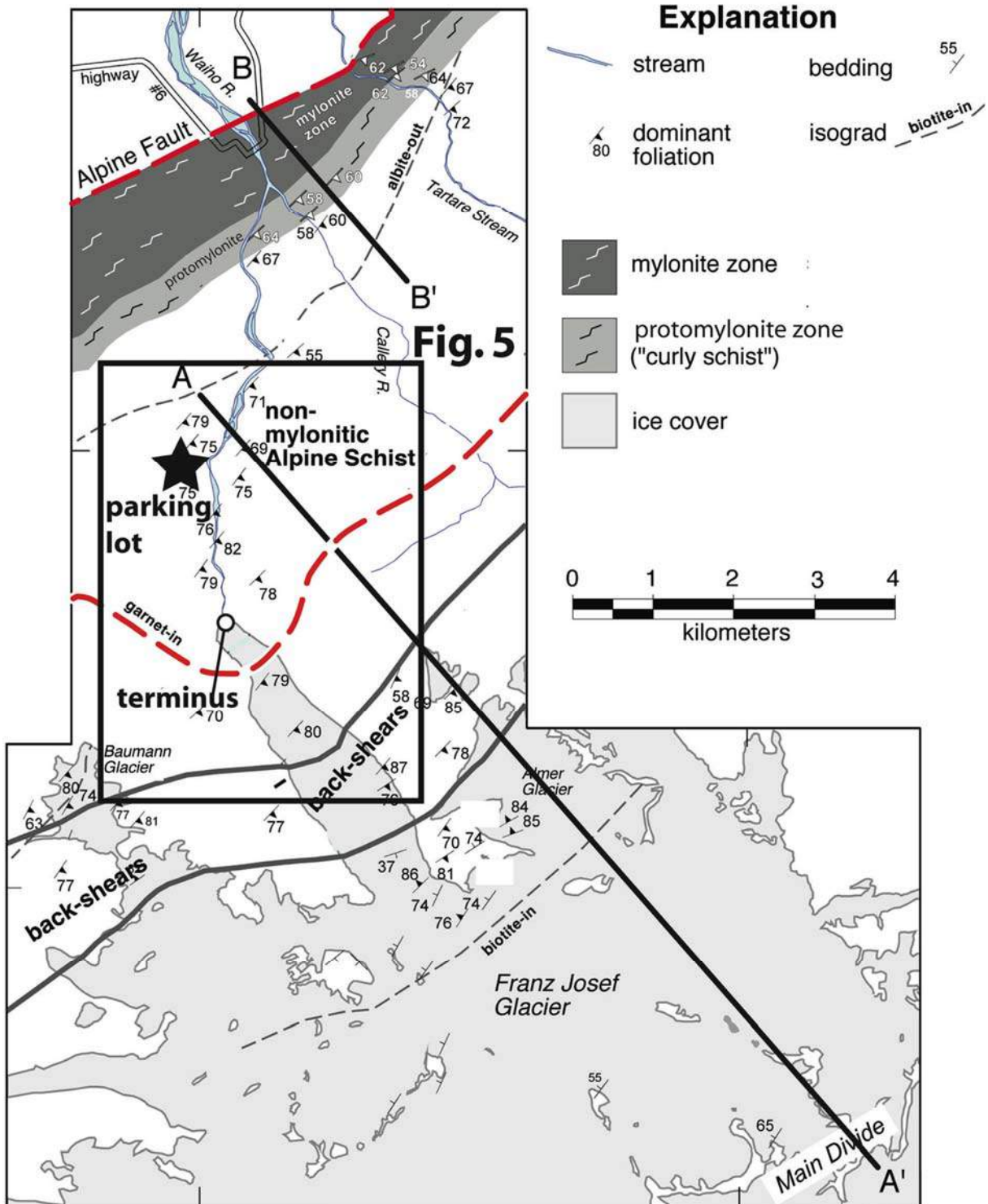


Figure E.14.

The purpose of this stop is to examine superb (glacially scoured) outcrops the highest-grade, non-mylonitic part of the Alpine Schist in the Alpine Fault's hangingwall. These schists are located structurally above the Alpine mylonite zone. The rocks at this stop can be considered to have been the "starting" rock type for the adjacent mylonite zone rocks to the NW that were derived from them by ductile shearing. The contact between late Cenozoic mylonitic zone, and the (in-part) older non-mylonitic part of the Alpine schist is both concordant and

gradational, involving a progressive increase in shearing related strain intensity towards the Alpine Fault (e.g. Sibson et al. 1981; Holm et al. 1989; Little et al. 2002a; Norris and Cooper 2003). The outer protomylonitic ("curly schist") part of the Alpine mylonite zone is transitional, preserving many fabric elements (garnet porphyroblasts, remnant quartz rodding and intersection lineations, quartz veins, metachert bands, mafic lenses) that have been "inherited" into that pervasively shear-banded protomylonite from its non-mylonitic Alpine Schist precursor. The protomylonites ("Curly Schist") and their shear bands are well exposed in Tartare Stream near Franz Josef village (these are visited in Stop H in this guide).

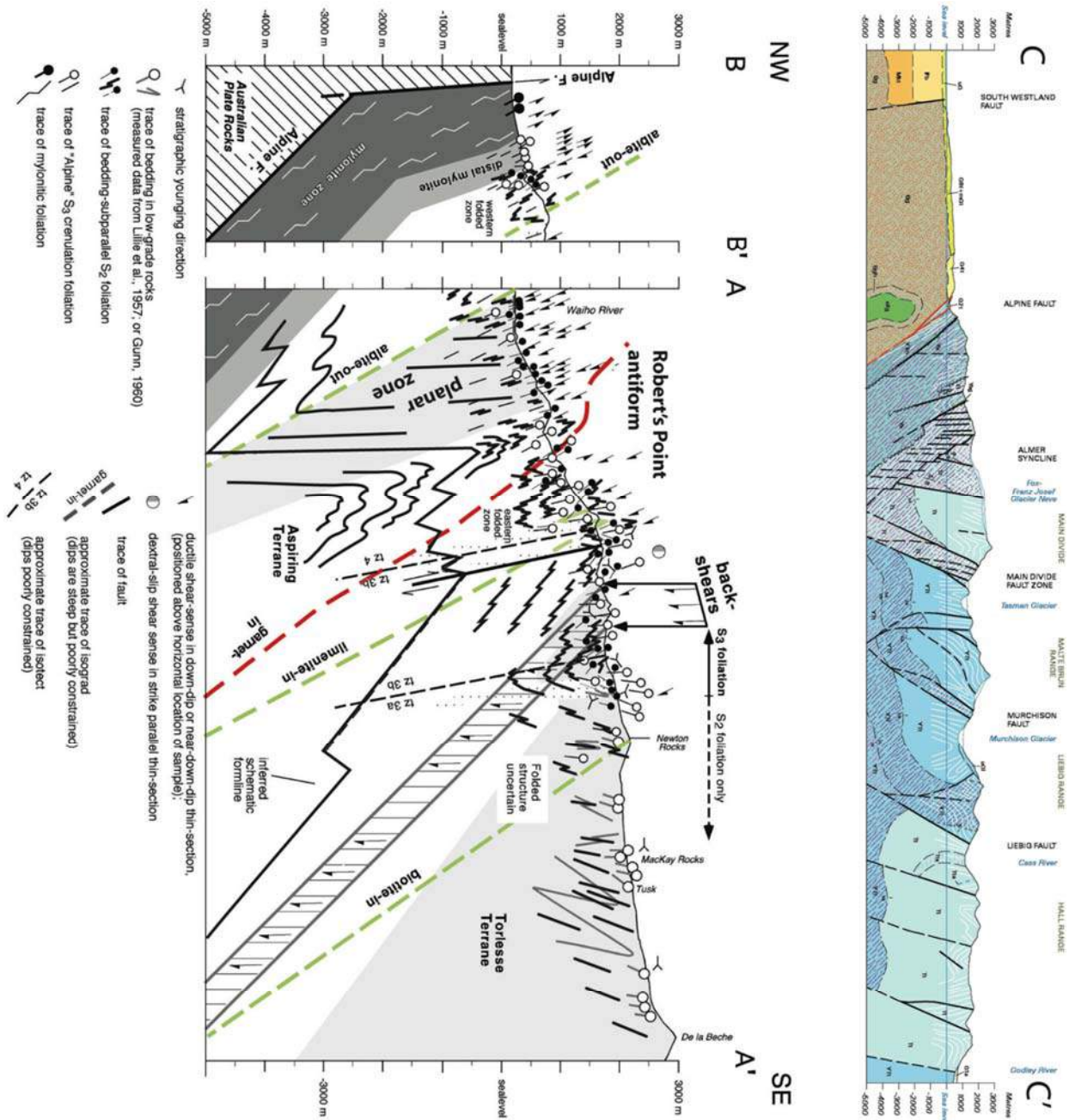
ALPINE SCHIST ROCK TYPES (PROTOLITHS)

The rocks exposed below the glacier are dominated by dark-colored semi-pelitic and quartzofeldspathic lithologies derived from argillite and greywacke sandstone (e.g. 58-73% SiO₂; Grapes and Watanabe 1992, 1994). Less common are decimeter to meter-thick interlayers of green-colored mafic rock (now amphibolite or chlorite-amphibole-rich schist) and light-colored metachert bands (most common near the glacier toe). This oceanic assemblage is more representative of the Aspiring Terrane (Norris and Crow 1987; Grapes et al. 1998) than of the sandstone-dominated Torlesse Terrane, which dominates exposures farther up the Glacier in the lower grade, structurally higher parts of the crustal section (Figure I.3). Younger igneous rocks (such as pegmatites) are absent at Franz Josef Glacier. The depositional age of the rocks forming the schist, based on the fossil content of its less metamorphosed equivalents elsewhere in New Zealand, is likely to be Permian to Early Cretaceous.

THERMOCHRONOLOGY AND REGIONAL METAMORPHISM

The Barrovian metamorphic sequence preserved in the Pacific Plate rocks (e.g. Grapes 1995) has been tilted to the SE in the hangingwall of the Alpine Fault so that lower temperature mineral isograds crop out at increasing distance southeastward from the Alpine fault (Figure I.1, Figure I.2, Figure I.3, Figure I.4). Near the glacier toe, most of the rocks are garnet-muscovite-biotite-plagioclase-quartz schists. Most also contain minor chlorite, ilmenite, epidote and graphite. The rocks are not aluminous enough to contain aluminosilicate polymorphs, but kyanite has locally been reported in rocks of appropriate composition near Haast (Cooper 1980). Kennedy (2005) mapped the position of the garnet-in isograd across the bottom and flanks of the lower Waiho Valley to assess its 3-D shape (Figure I.4). A typical garnet near this isograd has a composition of almandine₅₀grossular₂₈spessartine₂₀pyrope with little zoning from core to rim. On the basis of an examination of 575 samples, this boundary was determined to dip moderately (~30°) SE, subparallel to the Alpine Fault and to the mean dip of the S2 (early) foliation in the rocks (Kennedy 2005). The isograd has been deformed by the "Alpine folds" (in particular the Robert's Point antiform), but was less appressed during that folding than was S2. This relationship accords with abundant microstructural evidence for the synchronicity of the main Alpine Schist metamorphism with "Alpine" folding throughout the Southern Alps (Grindley 1963; Findlay 1987; Little et al. 2002a). The "Alpine" deformation produced the NNE-striking, and steeply SE-dipping Alpine foliation ("S3"). The age of the regional metamorphism has been difficult to determine, in large part because of the veil of young cooling "resetting" the spectrum of thermochronometric systems in these rapidly exhumed rocks (Batt et al. 2000; Little et al. 2005). Near Franz Josef Glacier, ⁴⁰Ar/³⁹Ar ages on hornblende are 3-5 Ma, K/Ar and ⁴⁰Ar/³⁹Ar ages on muscovite <3 Ma, biotite, <2 Ma, and fission-track on zircon <1 Ma

(Tippert and Kamp 1993; Chamberlain et al. 1995; Batt et al. 2000; Little et al. 2005). Vry et al. (2004) dated the high-temperature (Barrovian) regional metamorphism at several localities in the central and northern part of the Alpine Schist as late Cretaceous (~86 Ma) using the Lt-Hf and Sm-Nd techniques on garnet; whereas Mortimer and Cooper (1994) obtained ages farther south near Haast of ~71-100 Ma using U-Pb on monazite and by means a Sm-Nd whole-rock isochron. Some mineral growth (especially renewed growth of biotite, and in some mylonitic rocks, also garnet) probably continued into the late Cenozoic (Little et al. 2002a; Vry et al. 2004).



Cross-Sections A-A' and B-B' are from Little et al., 2002a). See previous map for location. The smaller-scale section C-C' is from Cox & Barrell (2007), and is located ~10 km to the west of Franz Josef Glacier.

Figure E.15.

SIGNIFICANCE AND AGE OF THE LAMINATED FOLIATION AT FRANZ JOSEF GLACIER

A conspicuous feature of the Alpine Schists at Franz Josef Glacier is the planar and strongly laminated (and segregated) nature of their dominant foliation (Figure 1.5a). This is a remarkable attribute given the abundance of folds and mm-cm scale crenulations ("Alpine" or F3 folds, typically SW plunging) that occur widely throughout in the Alpine Schist. At Franz Josef Glacier, the foliation typically strikes ~040 (about 10-15° anticlockwise of the Alpine Fault's strike) and dips 70-80° SE (Figure 1.2, Figure 1.8, a and b). Such planar foliation zones, including the one exposed below the terminus of Franz Josef Glacier, are generally up to several kilometers wide, bounded on both sides by folded domains (Figure 1.3, Figure 1.4). There have been two interpretations for the origin of these zones of planar fabric, both of which agree that the planar fabrics represent zones of high strain. One view (e.g. Findlay 1987; Holm et al. 1989) holds that the planar foliation formed during the syn-metamorphic "Alpine deformation" as a result of the almost complete transposition of the older S2 foliation during that last phase of ductile deformation. S2 is a regionally widespread fabric that is typically strongly segregated, and subparallel to relict bedding and compositional layering. It is often gently dipping, on average, and is the form surface for the abundant mm-km-scale "Alpine" folds in the Alpine Schist. These workers attributed this high-strain to dextral wrenching or transpression during early phases of Pacific-Australia plate motion (probably in the Miocene).

An alternate interpretation is that the finely laminated and strongly segregated foliation exposed in the planar zones records high-strains that were inherited from the older (Jurassic Otago Schist age?) deformation. In this view, this foliation (S2) has been locally steepened on the limbs of km-scale "Alpine" (F3) folds to form the steeply dipping planar fabric zones like the one near Franz Josef Glacier. At the glacier, the planar zone occupies the inverted NW limb of the Robert's Point (F3) antiform (Figure 1.3, Figure 1.4), and sparse parasitic F3 folds (verging SE towards the Robert's Point antiform) are not uncommon (Figure 1.5e). In the planar fabric zones, ductile deformation mostly caused layer-parallel stretching and "amplification" of the folded S2 fabric rather than its prolonged shortening or folding to form a new, cross-cutting foliation (S3). The late stage overprint of layer-parallel stretching, some of it probably late Cenozoic in age, accomplished a constructive reinforcement of the S2 foliation, and contributed to various types of boudinage structures seen near the glacier terminus (Figure 1.5, b, c and d). Quartz veins oblique to the foliation were (depending on their attitude) either shortened and buckle folded (Figure 1.5f) or stretched and boudinaged (Figure 1.5c).

Outside of the planar zones, the syn-metamorphic "Alpine" foliation ("S3") is a crenulation fabric that typically dips steeply SE (Figure 1.8). Closer to the Main Divide, it is typically near-vertical (dipping either way). This foliation is axial planar to abundant mm to km-scale folds of the layered S2 fabric (Figure 1.4, Figure 1.5g). The hinge-lines of these structures and related intersection lineations (L23) commonly plunge SW (Figure 1.8c).

The above-cited dating results on Alpine Schist garnet suggest that development of the S3 fabric initiated in the late Cretaceous. During the Cenozoic this foliation was further deformed (reinforced, strengthened), and that the "Alpine" folds were tightened, as a result of the onset of Pacific-Australia plate motion, causing a later imprint of transpressional deformation. Coincidentally or otherwise, this last increment of ductile deformation imposed a direction of maximum shortening that was approximately perpendicular to the mean

foliation attitude inherited from the earlier (D3) deformation. Reinforcement (with some new mineral growth, especially of biotite) continued until the rocks were exhumed by uplift and erosion along the Alpine Fault in the late Cenozoic (Little et al. 2002a). These authors infer that this final Cenozoic increment of S3 strengthening in the non-mylonitic Alpine Schist (“D3b”) was coeval with mylonitic shearing closer to the Alpine fault. This increment has not been dated by geochronologic techniques.

LINEATIONS, MICROSTRUCTURES AND SHEAR-SENSE IN THE NON-MYLONITIC SCHIST

The dominant lineation in the Alpine Schist in the planar zone at Franz Josef Glacier is a quartz rodding lineation that plunges moderately to the SW (Figure I.8c). The lineation is also defined by elongate (mm-scale) biotite porphyroblasts that have a statistical linear alignment in the plane of the foliation (Palmer 2000). Like the foliation on which it occurs, this lineation is a composite (hybrid) fabric element. Inherited from the high-strain S2 fabric, it was overprinted during the subsequent “Alpine” ductile deformation (including its final, late Cenozoic increment, D3b). Foliation surfaces at Franz Josef Glacier are typically striped by golden-coloured biotite gash veins that are arranged approximately perpendicular to the dominant lineation (Figure I.5h). Similar to “flame foliations” described by Maeder et al. (2007), these (internally deformed) gash veins reflect foliation-orthogonal shortening and SW-plunging finite extension during a late increment of pervasive biotite neocrystallisation and grain growth in the Alpine Schist. Little et al. (2002a, 2002b) ascribe much of this “biotite flooding” to late Cenozoic deformation and fluid flow (an inference that has not yet been demonstrated by geochronology).

Spectacular microboudinage, cleavage tiling, and (variable) domino-like rotation of elongate biotite porphyroblasts are conspicuous microstructural features in the non-mylonitic Alpine Schist (Figure I.6, Figure I.7). These and a host of other microstructures reveal a consistent top-down-to-the-SE (+dextral) sense of shearing throughout the garnet-zone part of the non-mylonitic Alpine Schist, not only at Franz Josef Glacier, but also at Whataroa River (Holcombe and Little 2001; Little et al. 2002b, Little et al. 2007). Holcombe and Little (2001) used the variable pattern of rotation of elongate biotite grains relative to the main foliation to document a style of ductile flow involving both a component of top-down-to-the-SE shearing (bulk shear strain, γ , of ~ 0.6), and a “pure shear” component of foliation-orthogonal thinning (Figure I.6, Figure I.7).

Higher up in the structural section at Franz Josef Glacier (in the biotite-zone), the same sense of shear is macroscopically expressed by offsets of marker veins across a thinly (< 1 m) and regularly spaced, serial array of discrete faults. These brittle-ductile “backshears” strike sub-parallel to the Alpine Fault dip steeply, formed at temperatures of $\sim 450^\circ\text{C}$ and depths of > 20 km, and were conduits for upward flow of metamorphic fluids from depth (Wightman et al. 2006; Wightman and Little 2007) (Figure I.1, Figure I.3, Figure I.4). The backshears are the youngest ductile structures in the Alpine Schist, cross-cut all other fabric elements in the hangingwall of the Alpine Fault, and (like the shearing in the garnet-zone rocks) are ascribed to the final (late Cenozoic, “D3b”) phase of ductile deformation.

Geologic Map of lower Franz Josef Glacier area (from T. Little unpub. data, GIS database)

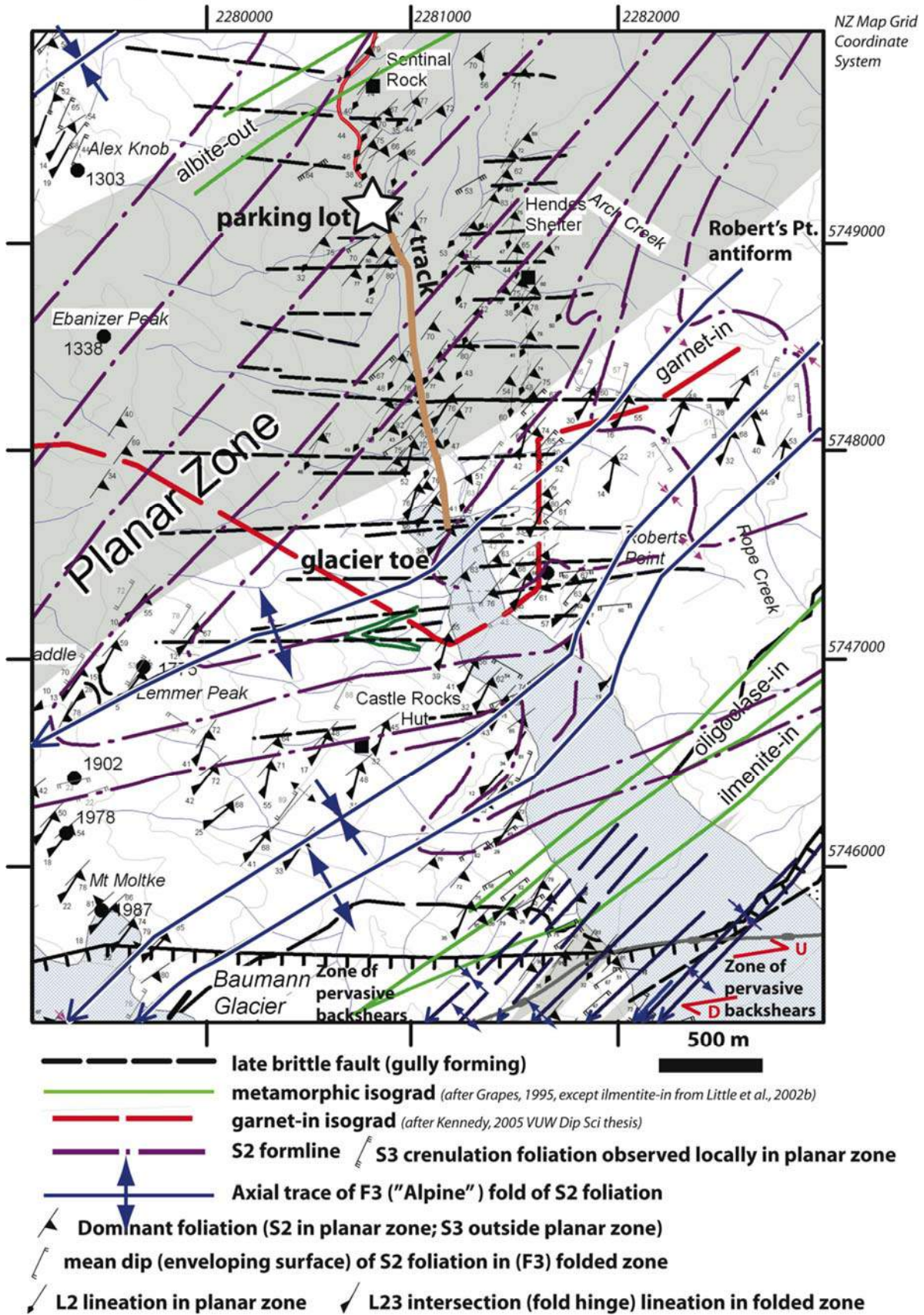


Figure E.16.

“SOFT FOOTPRINT” OF LATE CENOZOIC STRAIN IN THE ALPINE SCHIST AND DEFORMATION SUMMARY

Holm et al. (1989) used estimates of linear shortening of buckled quartz veins (e.g. Figure I.5f) to estimate a foliation-orthogonal shortening strain of ~50-75% in the Alpine Schist near Franz Josef Glacier. They ascribed this (minimum) shortening strain to late Cenozoic deformation. Little et al. (2002b) used outcrop data, plus several types of microstructural strain gauges to assess magnitudes of shortening perpendicular to the foliation (and also as extension parallel to it). They measured a value of total foliation-orthogonal shortening of buckled quartz veins of 75% that was similar to Holm et al. (1989) value, but— by contrast— inferred that much of this deformation was probably pre-late Cenozoic in age. Shortening since Cretaceous growth of garnet porphyroblasts was shown by Little et al. (2002b) to be ~50%, whereas shortening since growth of (commonly later-stage) biotite porphyroblasts and gash veins was shown to be ~30-40%. This last increment of deformation, they attributed to the late Cenozoic. Both studies, using different types of data, inferred a finite strain that was strongly oblate (pancake-shaped), a deformational attribute that is expectable in ductile transpression zones.

The “soft footprint” (~40% shortening), oblate shape, and SW-pitching extension direction of the late Cenozoic deformational imprint and strain affecting the hangingwall rocks of the Alpine Fault was modeled kinematically by Little (2004). Most of this deformation he attributed to up-ramping (and backshearing) of the Pacific Plate rocks as they encountered the relatively unyielding SE- dipping footwall ramp of the Alpine Fault. This pulse of deformation was inferred to be a transient phenomenon that was associated with temporarily high strain-rates (and high fluid pressures), and that caused deep embrittlement into the lower crust (Wightman et al. 2006; Wightman and Little, 2007). The up-ramping deformation accomplished the observed SE-tilting of the crustal section against the Alpine Fault and caused incoming vertical foliations to be tilted to a steep SE dip (Figure I.9). Because plate boundary deformation is strongly focused onto on a single oblique-slip structure (the Alpine Fault), oblique convergence in the Southern Alps is accommodated chiefly by translation and erosion. Consequently, internal deformation of the Alpine Schist to the east of that rapidly-slipping plate boundary fault has been comparatively modest, and older fabrics are preserved beneath the veil of younger deformational overprints (Little et al. 2007).

The cartoon of Figure I.10 illustrates thermochronological evidence for a “blister-like” zone of enhanced rates of uplift and exhumation of Pacific Plate near Franz Josef Glacier, and some inferred geodynamic implications of this relationship.

Ductile Structures, Garnet-Zone Alpine Schist, Franz Josef Glacier

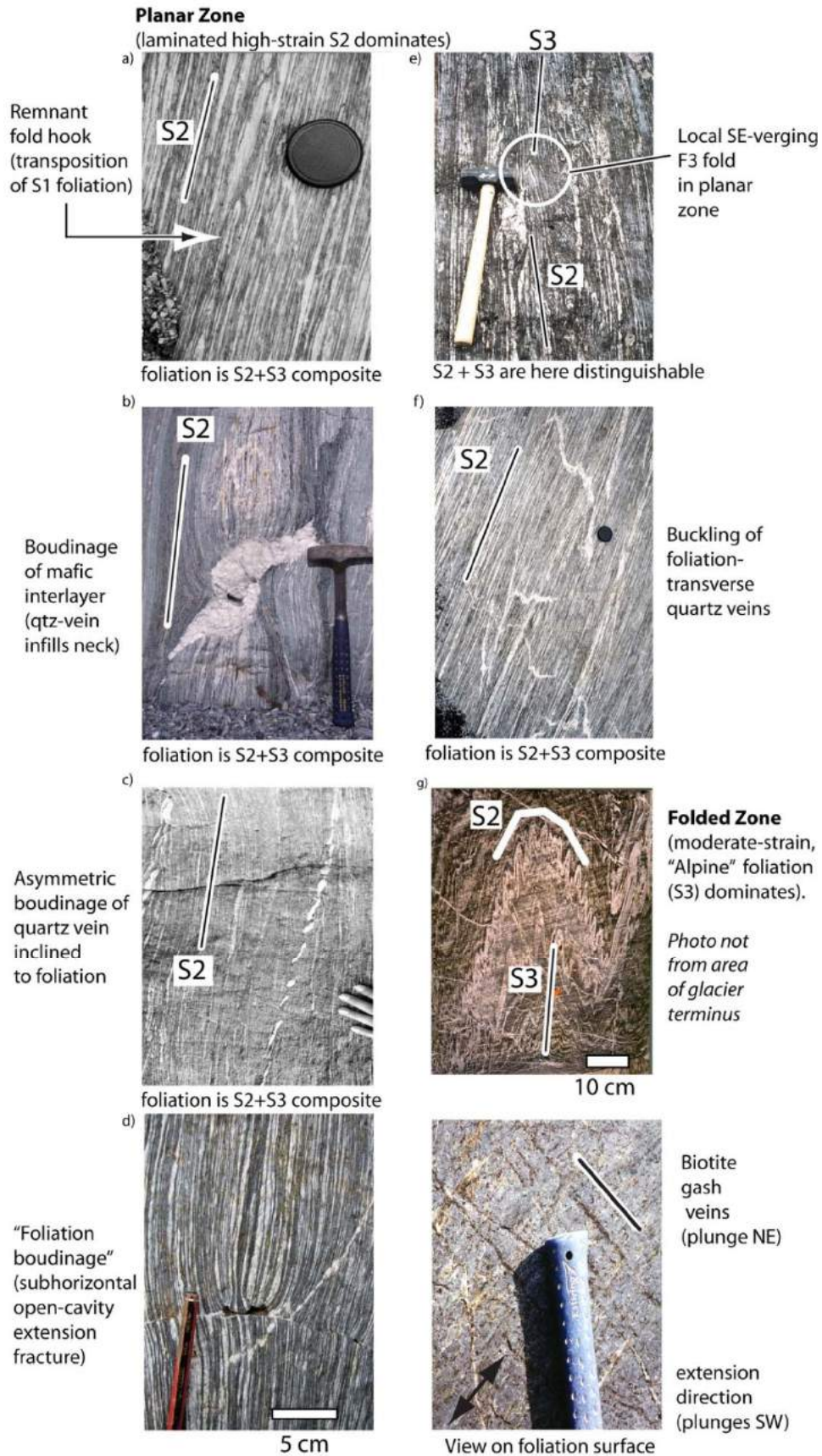
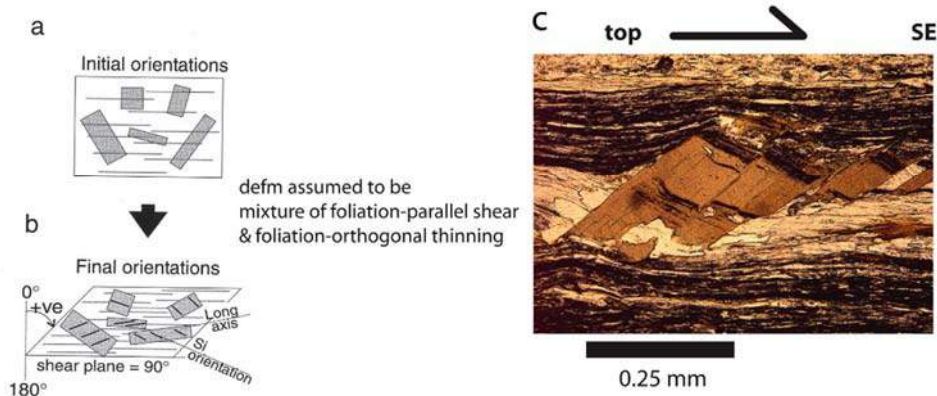


Figure E.17.

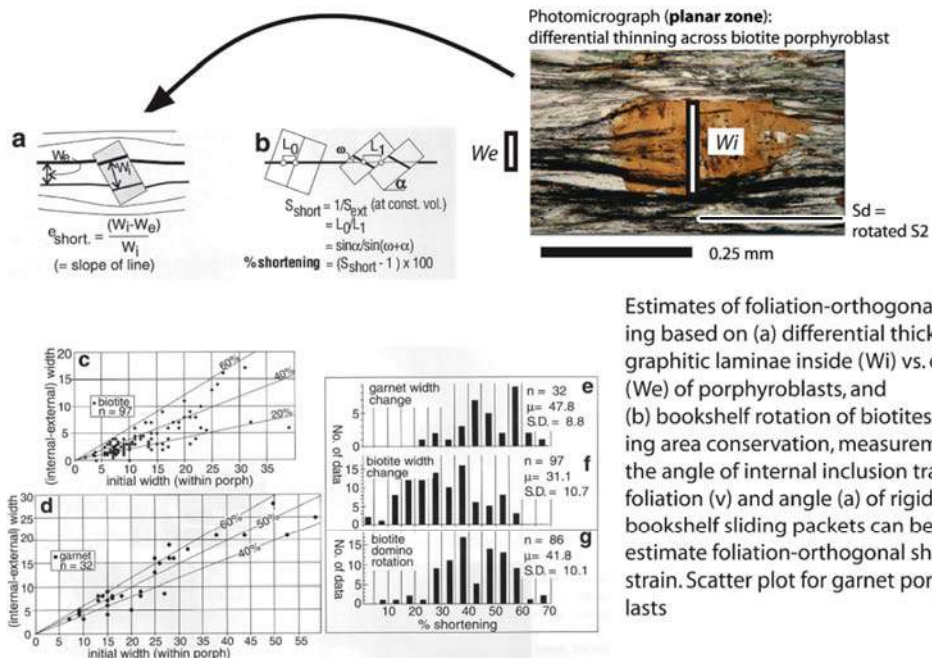
“Rotated” biotite porphyroblasts in garnet-zone Alpine Schist, Franz Josef Glacier (from Holcombe & Little, 2001)



a, b, Cartoons illustrating the concept of using the variably rotated (relative to external foliation) biotite porphyroblasts in Alpine schist to measure the sense of shear and degree of foliation-orthogonal “flattening” strain (mean “kinematic vorticity number” of the flow; i.e., “ratio” of simple shear to pure shear). Note that the foliation at Franz Josef Glacier is not horizontal, but dips steeply SE. **c)** example photomicrograph from Franz Josef Glacier showing domino-style rotation of biotite porphyroblast relative to external foliation. Most of the biotite laths are rotated in a top-to-the-SE shear sense that is antithetic to Alpine Fault dip-slip. Little et al. (2002b) additionally used these domino structures to calculate post-biotite finite strains in much the same way that stratal dips are used to estimate extensional strains in normal faulted tilt domains at a crustal scale (see Figs. 8b, 8g, below).

Figure E.18.

Microstructural estimates of foliation-orthogonal shortening relative to growth of garnet and biotite (From Little et al., 2002b)

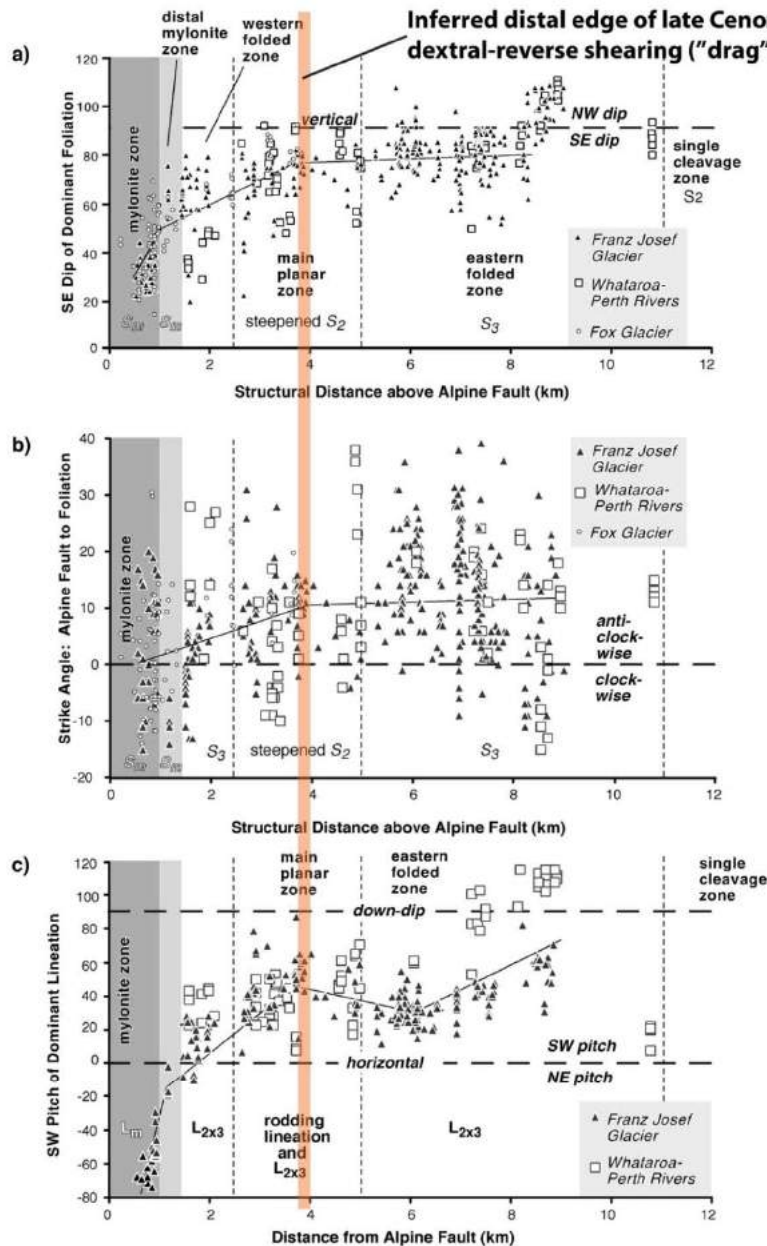


Estimates of foliation-orthogonal shortening based on (a) differential thickness of graphitic laminae inside (W_i) vs. outside (W_e) of porphyroblasts, and (b) bookshelf rotation of biotites. Assuming area conservation, measurements of the angle of internal inclusion trails to foliation (ν) and angle (α) of rigid bookshelf sliding packets can be used to estimate foliation-orthogonal shortening strain. Scatter plot for garnet porphyroblasts

(c) graphs the internal thicknesses of graphitic marker laminae (W_i) in biotite against their external thickness (W_e). Reference slopes for 40, 50, and 60% shortening strains are shown as dashed lines. Scatter plot (d) presents similar data for garnet porphyroblasts. Histogram (e) plots frequency against individual strain estimates based on changing lamination widths across garnet grains. Histogram (f) plots similar data for biotite grains. Histogram (g) plots frequency against individual shortening estimates based on bookshelf rotation of biotites.

Figure E.19.

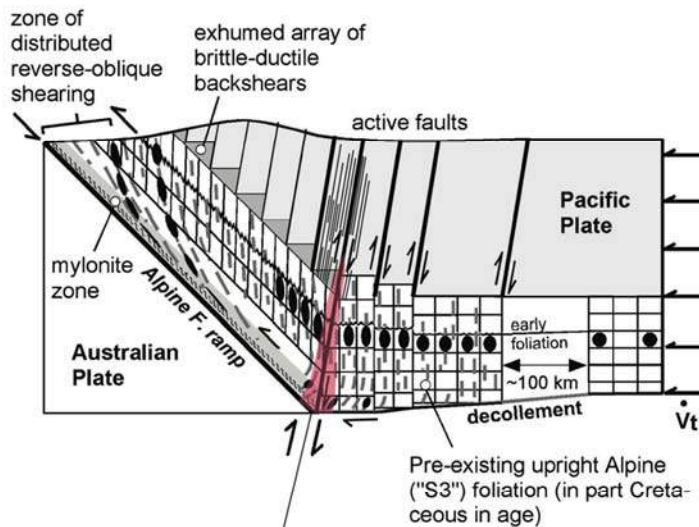
Changing Fabric Attitudes with Structural Distance from the Alpine Fault



Scatter plots showing changing attitude of foliations and lineations in the Alpine Schist as a function of structural distance orthogonal to the (mean) Alpine Fault. Note apparent kinks in all data sets at ~4 km from the Alpine Fault, interpreted as the far-field onset of late Cenozoic dextral-reverse shear ("drag") related to the Alpine fault; (a) dip angle of the dominant foliation (S₃ in folded zones, S₂ in planar zones, mylonitic foliation (S_m) in mylonite and distal mylonite zones); (b) horizontal angle between strike of dominant foliation and strike of Alpine Fault. Fine lines show inferred mean trends; (c) shows variation in type of dominant lineation (L_{2x3} intersection in folded zones, L₂ rodding lineation in planar zone, L_m stretching lineation in mylonite zones) and its pitch relative to local foliation strike (SW pitches are plotted as positive). From Little et al., 2002a, 2002b.

Figure E.20

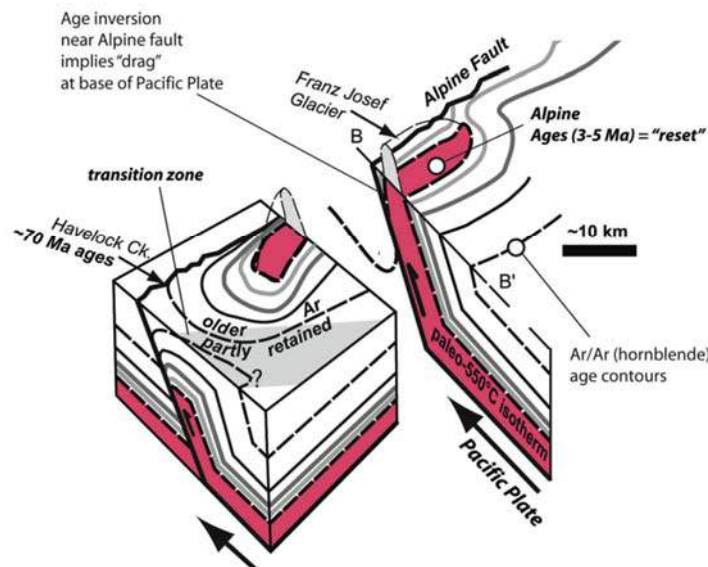
Cartoon of late Cenozoic ductile strain accumulation (overprint) in Alpine Schist related to oblique-slip up-ramping of Pacific Plate
 (after Little, 2004; Wightman & Little, 2007)



Zone of transient late Cenozoic dextral-oblique back-shearing causing deep embrittlement into lower crust. Ductile overprint in nonmylonitic rocks tilts foliation to steep SE dip & imparts late-incremental SW-pitching stretch. In garnet-zone rocks, this overprint is associated with a distributed top-down-to-the-SE (back-) shearing, whereas in the structurally higher, exhumed array of brittle-ductile backshears, this deformation is much more discrete (slip on systematically spaced faults).

Figure E.21.

"Blister" of reset hornblende Ar/Ar ages near Franz Josef Glacier
 (from Little et al., 2005)



- Implies complete exhumation through argon partial retention zone for hornblende, but only in Glaciers area
- Exhumational steady-state has not been achieved to North or South
- Paleo-isotherm corresponding to "closure temperature" for hornblende (~550°C) was advected westward into the orogen & resided in lower crust, therefore was probably little perturbed by orogenic deformation.
- For original (pre-uplift) geothermal gradient of ~20°C/km, this implies a time-integrated vertical exhumation-rate of ~6-9 mm/yr near the central Alpine Fault (slower rates to North and South)
- There has been >40-45 km of finite dip-slip on the central Alpine Fault (assuming a 40-50° dip)

Figure E.22.

ISOTOPIC EVOLUTION OF FLUIDS DURING EXHUMATION OF SCHIST IN THE HANGINGWALL OF THE ALPINE FAULT

In the Alpine Schists 2-5 km east of the Alpine Fault, a sequence of structural features represent deformation during uplift and exhumation in the hangingwall of the fault (Holm et al. 1989) (Figure I.11). Quartz-carbonate veins with biotite-rich selvages cross-cut the Alpine foliation (Figure I.14b), but are themselves deformed. Holm et al. (1989) calculated that a 50% flattening strain had affected the rock since the formation of the veins. Fluid inclusions in quartz indicate a depth of formation of 15-20 km assuming a temperature of c. 450°C. Foliation boudinage and localised ductile shear zones represent strain localisation and brittle-ductile behaviour and overprint the earlier veins (Figure I.14c, d). Fluid inclusions in quartz precipitated in the boudin necks indicate a temperature of c. 300-350°C and a depth of 6-8 km. Later sub-horizontal extension fractures contain euhedral quartz, calcite and chlorite (Figure I.14a, e). Fluid inclusions indicate temperatures of c. 250°C at depths of 2-3 km (Holm et al. 1989).

The uplift path of the hangingwall rocks based on estimates of PT conditions of formation of the three types structures from fluid inclusion studies is illustrated in Figure I.11 (after Holm et al. 1989).

The late extension veins occur in both sub-horizontal and subvertical orientations. Their line of intersection is sub-parallel to estimates of the σ_1 direction. The two orientations appear to be coeval, suggesting repeated interchange of σ_2 and σ_3 in the upper part of the seismogenic crust. This may occur during the stress build-up and release of an earthquake cycle, and be an effective means of allowing penetration of meteoric fluids into the rocks and their subsequent pressurization.

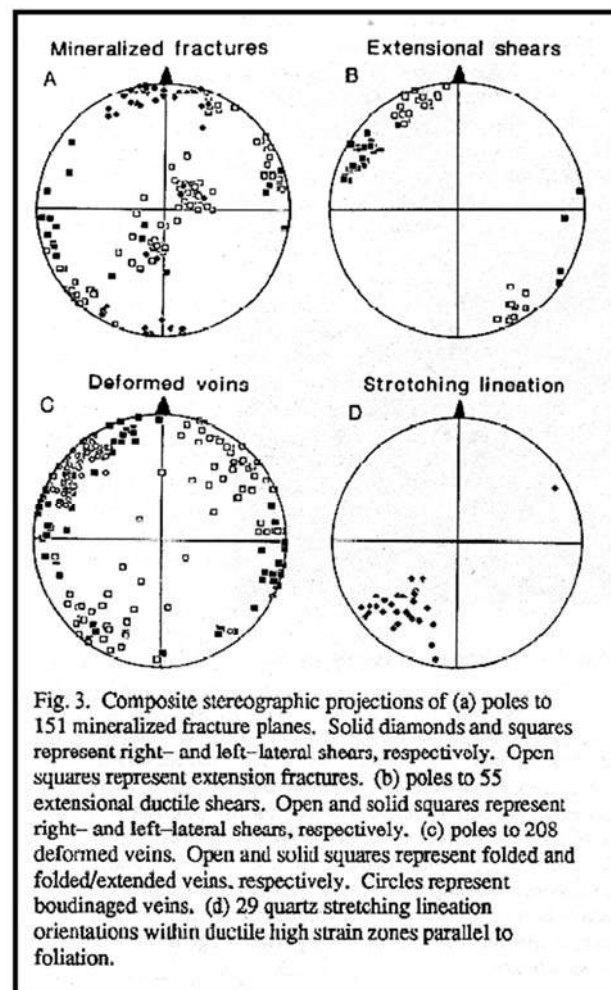


Figure E.23. P-T conditions along an uplift path in Alpine Schist at Franz Josef. After Holm et al. (1989)

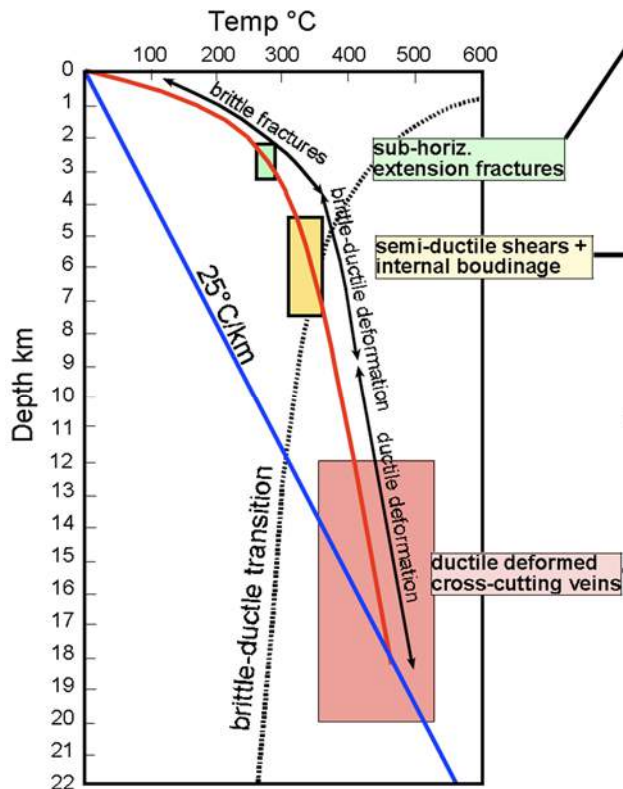


Figure E.24. P-T conditions along an uplift path in Alpine Schist at Franz Josef. After Holm et al. (1989)

Oxygen isotope measurements (n=39) on quartz from the country rock schist, from the early deformed veins, the boudin necks and the sub-horizontal extension fractures all lie within a range of $^{18}\text{O} = 10-14.3\text{‰}$. The country rock quartz has a mean = 12.5‰ , s.d.= 1.35‰ , the early vein quartz mean = 12.8‰ , s.d.= 1.6‰ , the quartz in the boudin necks mean = 13.5‰ , s.d. = 1.0‰ , and quartz in the late sub-horizontal fractures mean = 12.8‰ , s.d.= 0.4‰ . The mean values are all compatible with buffering of the coexisting fluid by the country rock isotopic composition. The standard deviation of the early veins is comparable to that of the country rock, suggesting local equilibrium compatible with derivation of the silica by solution in the wall rock. This is also supported by measurements of two samples of veins and their adjacent wall rocks. The boudin neck quartz has a smaller standard deviation, representing a

smaller spread of values possibly due to fluid equilibration with country rock over a larger volume than the immediate wall-rocks. The late sub-horizontal veins have the lowest standard deviation indicating the fluid equilibrated with average country rock. Calculated fluid compositions in equilibrium with quartz from the various sites indicate a progressive reduction in ^{18}O from the early veins through to the late extension fractures. This is likely to be due to equilibration of the fluid at progressively lower temperatures with the host schist. (Jenkin et al. 1994) report similar ^{18}O values from the late quartz veins but light values of D indicating a substantial component of meteoric fluid. The lack of a shift to lighter values of ^{18}O in the vein quartz indicates a fluid largely equilibrated with country rock oxygen but retaining the hydrogen isotopic signature of a parent meteoric fluid. The reduction in standard deviation of ^{18}O values may reflect increasing quantities of circulating meteoric fluid through a fracture porosity at and above the brittle-ductile transition. The total fluid-rock ratio must however have remained small for the oxygen isotopes to have equilibrated.

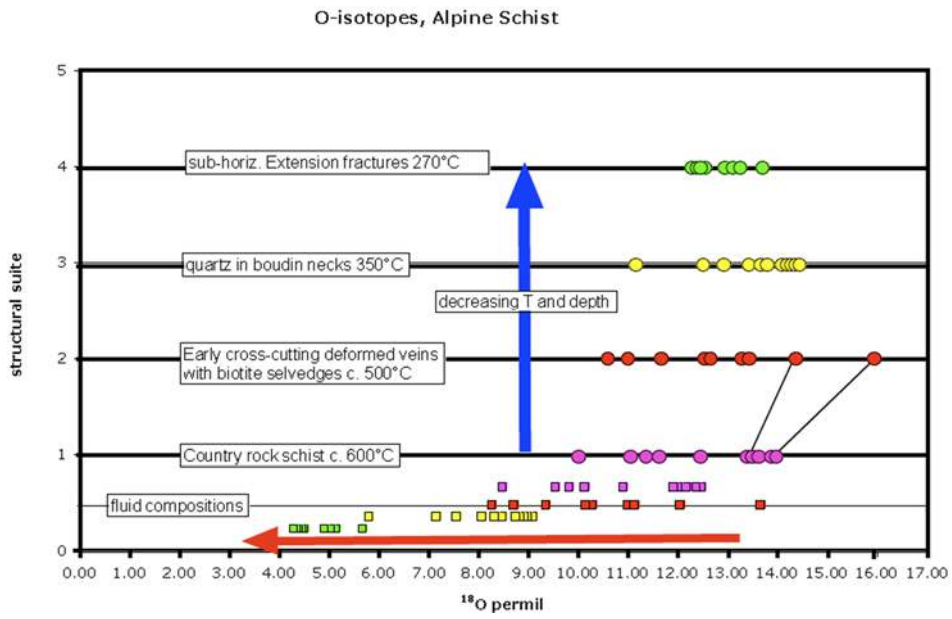
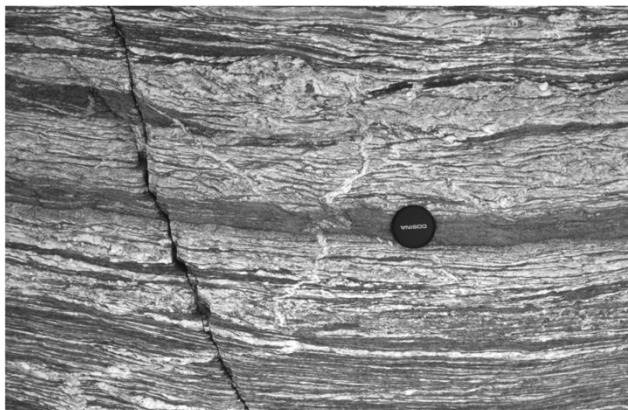


Figure E.25.
Summary of oxygen isotope measurements from veins in Alpine Schist at Franz Josef



A: Euhedral quartz and calcite crystals on surface of sub-horizontal fracture



B: Buckled cross-cutting quartz-carbonate vein. Note dark biotite-rich selvage



C: Semi-ductile shears and internal boudinage



D: Cross-cutting, ductilely deformed veins.



E: Sub-horizontal extension fracture

Figure E.26. Quartz and carbonate veins in outcrop at Franz Josef

STOP J: DOUGHBOY CREEK

In its lower reaches, near the road, Doughboy Creek flows through thick gravel terraces, and the hard rock sequence is not exposed. However, approximately 1.5 km upstream, a large slip exposes quartzofeldspathic mylonite containing abundant deformed pegmatite veins. The undeformed protolith of these veins occurs on the crest of the Mataketake Range, some 10 km to the SE of this location. The pegmatites were deformed within the fault zone, developing extensively recrystallised quartz, feldspar, and muscovite fish that are visible in many hand specimens, such as the blocks that have washed down Doughboy Creek. The decrease in mean thickness of pegmatites between the schists of the Mataketake Range and the protomylonites at Doughboy Creek indicate shear strains of between 10 and 15 (Norris & Cooper 2003). This analysis is further discussed in description of Stop 15.

N.B. The prominent granite and pegmatite boulders forming the stop banks at the Paringa River, and the sea wall at nearby Bruce Bay are from the Tuhua Group of late Paleozoic age and are quarried at a site behind the Paringa Post Office.

STOP K: HAAST RIVER BRIDGE OR VISITOR'S CENTRE

From the Haast River bridge there are excellent views of the Alpine Fault scarp. The Alpine Fault is the major structure of the South Island and represents the boundary between the Pacific and Australian plates. In Westland the fault separates Haast Schist to the east from Tasman Metamorphic Belt rocks to the west.

At the present day the Alpine Fault is active and has an oblique-slip character - recent terraces and their associated channels, rivers and streams attest to both lateral and vertical movement. The total dextral slip on the fault is constrained by the 460-480 km lateral displacement of the Dun Mountain Ophiolite Belt (Wellman 1955), while the restricted outcrop of high-grade kyanite-bearing, amphibolite facies schists adjacent to the fault requires appreciable vertical uplift, which may be as high as 25 km (Cooper 1980).

Although the extent of these displacements is reasonably well established, the timing of the dextral shear was for a long time the subject of controversial debate. Wellman (1964) proposed that the plate boundary and the Alpine Fault are entirely of Neogene age, a view supported by sea-floor spreading results (e.g. Molnar et al. 1975) and by the sedimentary history of southern New Zealand (Carter and Norris 1976). Suggate (1963) however, proposed that part of the transcurrent movement took place during the Rangitata Orogeny (Jurassic-Cretaceous) and part in the Kaikoura Orogeny (Miocene-Recent). Other plate tectonic reconstructions (e.g. Weissel et al. 1972) also require a plate boundary through New Zealand from the inception of sea-floor spreading in the late Cretaceous. A critical line of evidence by Suggate is the apparent lateral offset by only ca 130 km of presumed coeval Cretaceous lamprophyre dyke swarms. However, work has shown these dyke swarms to be non-coeval and in fact the southern swarm to be of Neogene age (see discussion for Haast section and Cooper et al. (1987)).

The average rate of plate displacement at Franz Josef is 37.5 mm/y (DeMets et al. 1990, 1994), with a plate vector of 071°. The motion is obliquely convergent on the plate boundary, with components normal to the fault of 10 mm/y, and parallel to the fault of 36

mm/y. Due to a lack of suitable dated marker horizons at the Alpine Fault, the rate of transcurrent movement as determined from geological field evidence is not tightly constrained, but is between 60 and 75% of that predicted. Resurveys of 100 yr old geodetic networks suggest that accumulating elastic strain is distributed over a zone up to 100 km wide east of the Alpine Fault (Walcott 1978), with the total integrated shear strain consistent with the plate tectonic rate. Shear strain rates in the range 0.5 to 0.6 ppm/y with a principal axis of relative contraction at about 110° were reported for networks in the central and northern parts of the Alpine Fault (Walcott 1984, fig. 10). These determinations have been supplemented by results from small aperture networks, centered on the fault, such as the one extending across the fault at Haast River (Wood and Blick 1986, fig. 10). Strain rates at the fault range from 0.4 to 1.4 ppm/y, but with essentially the same azimuth of relative contraction.

Over the last 15 years, high precision GPS measurements have been made across the South Island (e.g. Beavan et al., 2000) that provide a detailed map of strain accumulation. Shear strain reduces exponentially east of the Alpine Fault and is best fitted as representative of elastic strain around an east-dipping fault that is fully locked to depths of 5-10 km (Beavan et al. 1999; Pearson et al. 2000) and creeping aseismically at c. 25 mm/yr below this depth, although some degree of interseismic coupling may persist to as deep as c. 18km (Wallace et al. 2007).

Uplift and strike-slip rates at the Alpine Fault itself have been determined on the basis of displacement of marine and fluvial sedimentary sequences, and offset landforms:

- at Paringa River, 45 km northeast of Haast, localised rates of 10.7 mm/y (Suggate 1968), revised to 13.7 mm/y (Simpson et al. 1994) and a more regional rate of 7 to 8 mm/y (Simpson et al. 1994) have been calculated for the last 16 ka
- at Haast River minimum vertical and horizontal rates of 23.5 mm/y and 2.25 mm/y have been calculated for the last 4 ka (Cooper and Norris 1995).
- at Okuru River, 5 km south of Haast, a vertical rate of 4 mm/y has been determined for the last c. 10 ka (Cooper and Bishop 1979; Norris & Cooper 2001).
- at Hokuri Creek, Lake McKerrow, Hull and Berryman (1986) document uplift rates of 2.2 mm/y and 1.6 mm/yr for marine shells northwest and southeast respectively of the Alpine Fault. Sutherland and Norris (1995) document an uplift rate of 1.4 mm/y at a locality 1 km northwest of the fault in the same region, based on displacement of marine shells.
- Sutherland et al. (2006) have calculated a horizontal rate based on offset moraines and other glacial features of 23.5 ± 2 mm/y determined over a time span of 75 ka.
- Barnes (2009) examined the bathymetric expression of glacial geomorphic features formed in the last 20 ka, offshore Fiordland, to determine strike slip rates of 27.2 (-3.0/+1.8) mm/yr between Milford and Caswell Sounds, increasing southward to 31.4 (-3.5/+2.1) mm/yr between Caswell and Doubtful Sounds.

In contrast to the measured uplift rates, the rate of uplift at Haast at the present day, predicted from plate motions (DeMets et al. 1994), should be as high as 9 mm/y. The discrepancy between rates of vertical motion observed at the Alpine Fault south of Haast

and those predicted can probably be explained by distributed movement within the Haast Schist east of the fault and offshore shortening by underthrusting of the Tasman Sea.

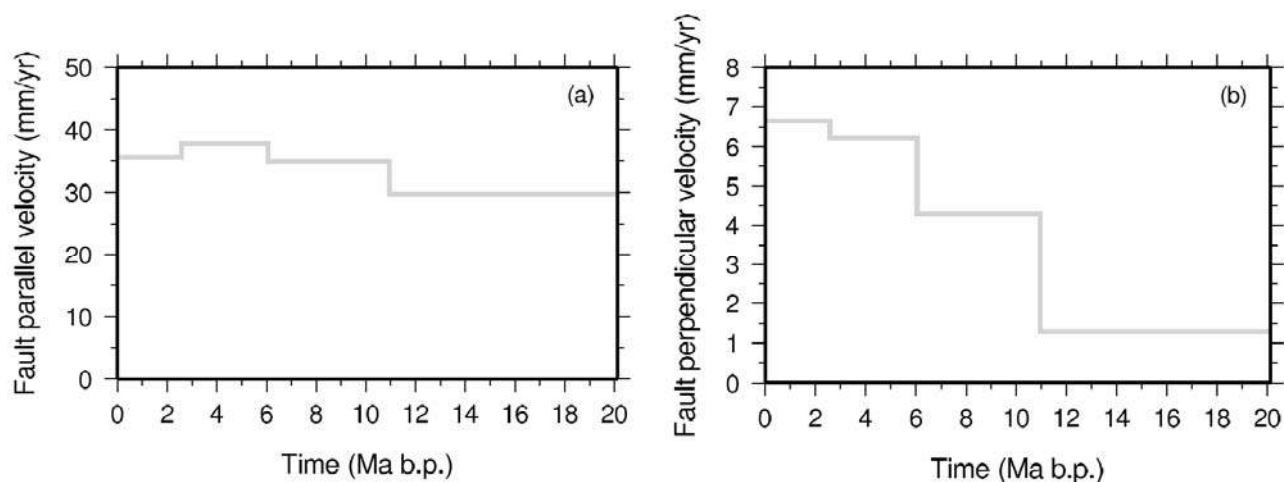


Figure 12: Components of velocity of the Pacific with respect to the Australian Plate (a) parallel to, and (b) perpendicular to the Alpine Fault in its central section, calculated from the plate motion model presented by Cande & Stock (2004).

The most recent plate motion models for the region, from new fits of magnetic anomaly and oceanic fracture zone intersections (fig. 12), indicate that the component of oblique plate motions that results in convergence across the plate boundary has increased relatively steadily over the last 20 million years (Cande & Stock 2004). However, it is likely uplift rates accelerated markedly around 5 Ma, when data from the Waiho-1 petroleum borehole indicate there was a dramatic increase in the sedimentation rate offshore (Sutherland 1996). Accelerating uplift since the Pliocene is also compatible with the sedimentological evidence from West Coast stratigraphic sequences where Alpine Schist detritus is first encountered in gravels only 2 m.y. old (Wellman 1979). The c. 5 Ma age is commonly accepted as the age of initiation of the Alpine Fault as a distinct structure (e.g. Toy et al. 2008).

If the weather is clear, the view southwards from the Haast bridge shows flat-topped steps up to 1.3 km long developed at ca 1450 m a.s.l. on schist ridges east of the Alpine Fault. Lower, less widespread, steps are also present, the most conspicuous being at 960 m a.s.l. Rounded quartz granules, with surface textures indicative of a high energy subaqueous environment, closely similar to textures on present day Haast beach pebbles, have been collected from both high altitude terraces (Cooper and Bishop, 1979). The horizontal steps are interpreted as remnants of uplifted marine platforms which developed on an open-ocean coast as the Southern Alps were rising. Unfortunately the age of these high altitude surfaces is not known and the chances of a direct determination appear slight.

A detailed analysis of contoured topographic maps of the Alpine Front suggest that correlatives of the Okuru platforms occur over the length of the Southern Alps. Furthermore a flight or sequence of terraces, comprising 16 discrete surfaces, can be recognised from the Haast area northeastwards to Hokitika. Field work has established that rounded quartz pebbles occur on most of these surfaces. A similar number of terraces have been

recognised worldwide (e.g. Chappell's work on Huon Peninsula, New Guinea), and are interpreted as having formed during interglacial high level stands, preserved by uplift on tectonically active coastlines. Using the New Guinea stratigraphy of terrace ages (determined from radiometric dates on coral), plots have been constructed of altitude of Westland terraces against inferred age (fig. 11). A straight line relationship implies (a) that a correct correlation has been made with the New Guinea sequence, and (b) that the uplift rate has been constant over the time period during which the terrace flight developed. The slope of the straight line gives the rate of uplift. For the past 140 000 years the uplift rate appears to have been constant at approximately 5.8 mm/y at Haast rising to 7.8 mm/y at Franz Josef (Bull and Cooper, 1986).

Although based on tenuous correlations, the Haast uplift rate based on high altitude terraces is compatible with that determined at nearby Okuru River by Cooper and Bishop (1979). The increase in uplift rate to the northeast predicted by terrace uplift is also compatible with the increased summit elevations that occur northeastwards towards Mt Cook, with the uplift map proposed by Wellman (1979), and with measured dip-slip rates on the Alpine Fault (Norris & Cooper 2001).

The Haast River area appears to mark a change in the character of the fault; to the northeast the trace is segmented, broken into more northerly trending thrusts (with development of thick cataclasites) and more easterly trending strike slip sections, while to the southwest the present day uplift component, southeast of the fault, decreases and the fault is predominantly strike slip in character, but with the trace having a 'normal' (055-058°) trend (Berryman et al. 1992, Cooper and Norris 1995).

From Haast, the road follows the coastal plain as far as Ship Creek, crossing a series of prominent shore-parallel dune ridges and alternating interdune hollows clothed in unmodified lowland rainforest. These coastal progradation plains extend up to 3 km inland and have developed close to the mouths of all the major south Westland rivers (Haast, Okuru, Waiatoto, Arawhata and Awarua). Wells and Goff (2007) mapped the dune sequences at five river mouth sites and dated the time of progradation and dune building using the ages of colonizing conifer trees. On the basis of 960 tree ages, they showed that dune formation has taken place in distinct and synchronous episodes, separated by long periods without lasting progradation. Six regional episodes are evident since A.D. 1200. The oldest trees on each dune set indicates dune deposition was complete as early as the decades of A.D. 1830, 1720, 1620, 1500, 1430 and 1280, each episode differing by no more than 20-53 years regionally, and therefore inferred to represent the regional response to the same causal mechanism. Wells and Goff (2007) interpret each dune system as reflecting rapid fluvial transport of large post-seismic sediment pulses from mountain catchments to the coast. The formation of each dune therefore relates to major Alpine Fault earthquakes. Four of the six regional dune-building episodes can be correlated to previously identified earthquakes on the Alpine Fault at A.D. 1826, 1717 and ca 1615. Another earthquake at ca A.D. 1460 has been resolved into two possibly separate events at A.D. 1500 and 1430, while the timing of the A.D. 1220 earthquake has been bracketed between A.D. 1280 and 1230.

From Ship Creek, the road climbs over two well-developed Quaternary terraces, the Sardine terraces of Nathan (1975); the lower terrace (Sardine 1) is underlain by river gravels resting on lake silts whereas the Sardine 2 terrace is underlain by marine sediments deposited during an interglacial highstand of sea-level. Both terraces are older than 40,000 y. B.P.

The road winds through spectacular cuttings within highly deformed late Cretaceous-Cenozoic strata and Paleozoic Greenland group.

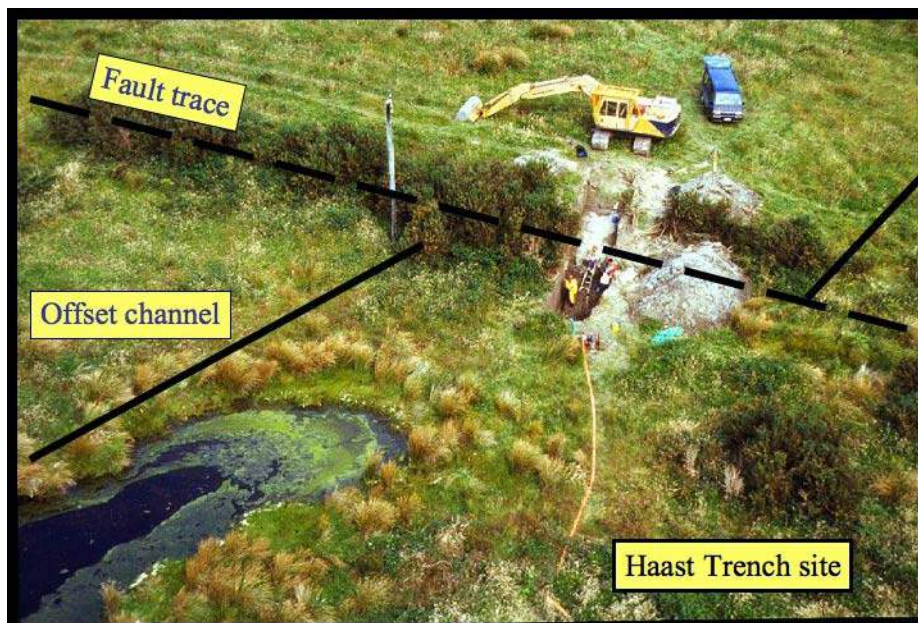
STOP N: SNAPSHOT BLUFF - ALPINE FAULT TRACE

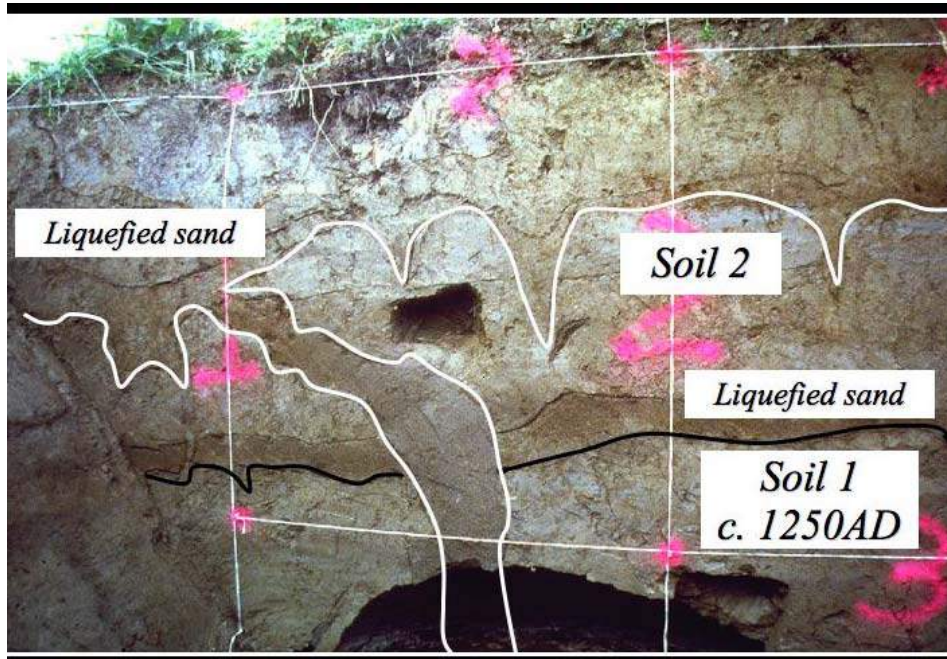
A Recent trace of the Alpine Fault is visible crossing the paddock next to the road (SH6). Vertical displacement of a terrace and lateral displacement of the terrace riser may be seen (fig. 8). The terrace is displaced vertically by 1.5 m, south side up, and its riser by 16m of right slip (authors' unpublished data). It is thought likely that the displacement of the terrace may represent the last two events on the Alpine Fault within the last 800 yr.

On the north bank of the Haast River, the Alpine Fault trace is marked by a 5 to 10 m high scarp, displacing a terrace composed of fluvial sediments radiocarbon dated at between 7300 and 4000 y B.P. A creek channel, deeply incised into the terrace is offset dextrally by 94 m at the fault scarp. Horizontal and vertical offsets of the terrace have occurred at minimum rates of 23.5 mm/y and 2.25 mm/y respectively, for the past 4000 years (Cooper and Norris 1995).

During late summer 1998, a joint IGNS-OU Geology Department team excavated four trenches across the Alpine Fault in south Westland. Two trenches were dug at the Haast River site, and two at Okuru River, to the south. The examination and detailed logging of the trench walls show that there have been three recent earthquake events on the fault trace, each resulting in a lateral offset of approximately 8 m. ¹⁴C dating of seeds in fossil soils gave somewhat ambiguous results, due to sedimentary reworking, but the three events have been tentatively identified at immediately prior to 850 ± 50 yr B.P. (equivalent to an age in calendric years of 1100-1200 AD), later than 400 ± 120 yr B.P. (equivalent to 1420-1630 AD) and later than 262 ± 56 yr B.P. (equivalent to 1640-1670 AD).

Figure 8 (a) Alpine Fault trace at Haast and site of one of the trenches (b) Trench wall showing liquefied sand F and buried soils from last two earthquake ruptures





HAAST – HAWEA: PREAMBLE

The Paleozoic-Mesozoic Rangitata Orogen may be divided broadly into two major assemblages of tectonostratigraphic terranes, the Hokonui Assemblage in the west and the Alpine Assemblage in the east. Each assemblage contains a number of terranes which may or may not have had original stratigraphic relationships with each other. The Hokonui Assemblage consists mainly of fragments of Permian-Jurassic volcanic arcs and arc-related sedimentary basins (Brook Street, Murihiku, Mitai/Dun Mountain terranes). It is generally weakly metamorphosed and only moderately deformed. The Alpine Assemblage is made up mainly of extremely thick sequences of greywacke and argillite with minor basic volcanics and cherts (Caples, Aspiring, Torlesse terranes). It is complexly deformed and metamorphosed up to amphibolite facies. The highest grade rocks crop out adjacent to the Alpine Fault where they have been exposed by recent uplift, but a broad axis of uplift extended through Otago during the late Mesozoic, exposing greenschist and epidote-amphibolite facies rocks as far east as Dunedin. The part of the Alpine Assemblage exhibiting a metamorphic texture (i.e. cleavage or schistosity) is known as the Haast Schist, which includes the Otago Schists, Alpine Schists and Marlborough Schists.

The Haast Schist appears to be derived from at least three major lithologic associations. The eastern, and by far the largest, volume is derived from an extensive and very thick suite of Permian to Jurassic quartzofeldspathic sandstones and argillites, the Torlesse terrane. The western portion is derived from a ?Permian-Jurassic suite of volcanogenic sandstones and argillites, the Caples terrane. Between the two is the Aspiring terrane, a zone completely within the schist and dominated by pelitic schist, spilitic metavolcanics and cherts.

The first recognition of a systematic metamorphic zonation in the Haast Schist was by F.J. Turner (1933, 1938), who described a sequence of isograds along the Haast River. Rocks below the biotite zone were subdivided by Hutton and Turner (1936) into four textural zones based on the degree of schistosity development. Sub-greenschist facies metamorphic

assemblages characterised by pumpellyite with or without prehnite were later described by Coombs (1960) and referred to the prehnite-pumpellyite and pumpellynite-actinolite facies.

The section exposed along the shores of Lake Hawea and its continuation along the Haast River is mainly within schist of the eastern portion derived from Torlesse quartzofeldspathic sediments. The composition of the original rocks is therefore fairly constant over a wide range of metamorphic and deformational states. The complete section takes us from rocks of pumpellyite-actinolite facies in which sedimentary features are still recognisable, to rocks of the oligoclase zone of the amphibolite facies which are best described as quartzofeldspathic gneisses in which all original features have been obliterated.

THE HAAST RIVER SECTION - GENERAL DESCRIPTION

Along the lower Haast River the road cuts obliquely across the isograd-isotect trend, and from east to west is exposed a progressive metamorphic sequence of chlorite (textural zone IV), biotite, garnet, and oligoclase zones.

At Haast River, the earliest folding phase folds a well-developed quartz-albite lamination, suggesting a correlation with F2 at Lake Hawea (fig. 4). These structures have been refolded by F3 structures which have an almost identical style to F2 structures described for the Lake Hawea section. Thus it would appear as if an extra phase of syn-metamorphic folding appears in the higher grade schists. A similar sequence is described in the Mt

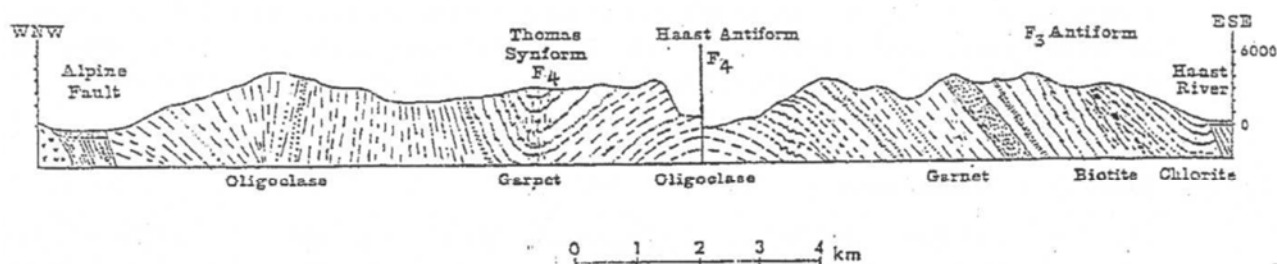


Fig. 4. Structural section along Haast River

Aspiring area by Craw (1985). If we assume progressive non-coaxial deformation of the schist during metamorphism, then it is to be expected that the more highly strained higher-grade schists will exhibit a greater complexity of ductile deformation phases than the lower-grade schists. Detailed mapping of greenschist horizons and the sense of vergence of mesoscopic folds define the hinge zone of a macroscopic antiformal F3 fold opening to the SE in biotite and garnet zone schists of the eastern Haast River area (fig. 4; Cooper 1974). Both biotite and garnet porphyroblasts show random orientation with respect to S2 and S3 surfaces indicating that the metamorphic maximum post-dated both folding phases (Grindley 1963; Cooper 1974).

Further west the dominant foliation is folded by broad, open, subhorizontal macroscopic F4 structures designated the Haast Antiform, Thomas Synform, and Mount Victor Fold Belt (Grindley et al. 1959; Cooper 1974). On a regional scale these structures fold the isograds causing repetition of garnet and oligoclase metamorphic zones (fig. 4). Tightly appressed mesoscopic fold hinges exhibit strained quartz and feldspar and bent flakes of mica on a microscopic scale, attesting to late-metamorphic deformation. Cooper et al. (1987) have suggested that the north-south trending F4 structures, which appear to be associated with

the intrusion of east-west lamprophyre dykes of early Miocene age, formed as en-echelon folds in a dextral strike slip regime along the Alpine Fault at the time of its inception as a through-going transform fault. A post-F4 suite of east-west faults are spatially related to the occurrence of F5 kink or chevron folds. The major structure of this phase, the Burke Fault, is in turn truncated by a NE-striking fault, probably associated with the Moonlight Fault system (White, S.J., 1996, pers. comm.), again with associated kink folds (F6).

Metamorphically the greenschist-epidote amphibolite-amphibolite facies transition has been investigated by Turner (1933), Mason (1962), and Cooper (1971;1972). The epidote-amphibolite facies effectively represents a transitional zone in which albite and actinolite characteristic of lower grades coexist with, but suffer progressive depletion to, oligoclase and hornblende, typical phases of the amphibolite facies. Oligoclase zone gneisses with, further north, concordant partial melt granite-pegmatite sheets (Wellman 1955; Wallace 1974) are truncated to the west by the Alpine Fault.

K-Ar ages of schist micas from Haast River (Mason 1961; Hurley et al. 1962; Adams and Gabites 1985) range from 8 m.y. or less, adjacent to the fault (oligoclase zone) to around 150 m.y. 25 km further east (chlorite zone) (fig 3), the variation being ascribed to differential uplift along the Alpine Fault, or to frictional heating during the Cenozoic (Sheppard et al. 1975; Scholz et al. 1979). There is evidence for excess radiogenic ^{40}Ar in schist minerals near to the Alpine Fault (Gabites & Adams, 1978; Chamberlain et al. 1995). Ages from schists of central and eastern Otago, sufficiently distant from the Alpine Fault to be unaffected by argon loss or redistribution through uplift, range from 133-141 m.y. (Mason 1961; Hurley et al. 1962; Harper and Landis 1967) to as high as 200 m.y. on the lowest grade rocks (Adams et al. 1985) suggesting a Jurassic age of Rangitata metamorphism. The very young K-Ar ages from specimens close to the Alpine Fault, coupled with results from fission track dating of apatite and zircon in schists (Kamp et al. 1989), indicate uplift of the Alpine Schists occurred only recently. Kamp et al. suggest that uplift was underway by about 7 m.y. at Haast River, and by 5 m.y. in the north, at Arthur's Pass.

STOP O: 18 MILE BLUFF

Oligoclase zone quartzofeldspathic schists and gneisses with sub-horizontal schistosity are exposed in the core of the post-metamorphic (F4) Haast Antiform. Views to the southwest up the valley of Gap Creek look practically along the axis of the structure, while schistosity traces on the ridge to the west pick out the complementary Thomas Synform. These large folds fold the isograds but predate the lamprophyre dykes; to the north, near Moeraki River, the folds intersect obliquely the trace of the Alpine Fault.

To the south, folds of the Haast Antiform-Thomas Synform generation have been mapped through the Matukituki River area (Craw 1985), where they are associated with the Moonlight Fault. At Bobs Cove, Lake Wakatipu, Turnbull et al. (1975) describe Oligocene limestones (preserved along the trace of the Moonlight Fault) which are folded by structures having an identical style and orientation to Haast Antiform-type folds further north. The post metamorphic folds at Haast River are interpreted to be post Oligocene, but are cut by lamprophyre intrusions of late Oligocene-early Miocene age. The structural and geometric relationships and chronological development of the Haast folds and associated faults and fractures in south Westland-northwest Otago has been compared to the structures generated during laboratory clay-model simulation of right lateral wrench regimes (Cooper et

al. 1987). They interpreted the folds, Riedel shears, tension fractures and dykes of western Otago as forming during the initial stages of dextral wrenching that was to result in the propagation of the Alpine Fault plate boundary through western South Island. The age of the lamprophyre dyke swarm constrains the age of formation of the Haast Antiform-type folds, which in turn constrains the inception of the Alpine Fault to early Miocene times. Intrusion of highly alkaline and carbonatitic magmas at this time argues strongly for an early transtensional character to the Alpine Fault.

STOP P: PIVOT CREEK

This tributary of Haast River drains predominantly biotite zone schists and good examples of varied quartzofeldspathic, greenschist and metachert lithologies can be sampled in float. Talc-carbonate-chlorite-quartz rocks, representing metamorphosed ultramafites, outcrop upstream in the hinge zone of a macroscopic antiformal F3 fold.

Pivot Creek also contains abundant float of ocellar lamprophyres (occasionally containing cognate hornblende gabbro xenoliths), sodalite- and cancrinite-bearing tinguaites, and trachytes. Dyke contacts with country rock schist show varying degrees of fenitization (Na-metasomatism) with the development of aegirine- and riebeckite-bearing assemblages. Carbonate impregnated and veined float boulders are derived from the vicinity of a norsethite-bearing carbonatite dyke outcropping upstream.

STOP Q: GATES OF HAAST

The schists exposed in the extensive road cuttings are pelitic schists of TZIII, chlorite zone. Several outcrops expose a spectacularly deformed conglomerate, with prominent light green, probably tuffaceous, clasts. Strain analysis indicates a constant volume strain ellipsoid of 3.6:1.3:0.21 (i.e. almost 80% shortening normal to the foliation (Norris & Bishop 1990)).

THE LAKE HAWEA SECTION - GENERAL DESCRIPTION

The shores of Lake Hawea, in particular the West Arm, expose a magnificent section within the Haast Schist, extending from textural zone IIB, pumpellyite-actinolite facies, to textural zone IV, greenschist facies (fig. 1). The main lithology is interbedded psammite and pelite, probably representing metamorphosed flysch. Graded bedding is recognisable at the lower grade (eastern) end of the section. Thick units of laminated pelite and pelitic conglomerate also occur, together with rare thin units of greenschist. The metamorphic mineral assemblage is in general quartz-albite-muscovite-chlorite-titanite with pumpellyite at the eastern end, epidote/clinozoisite at the western end and sporadic stilpnomelane and actinolite.

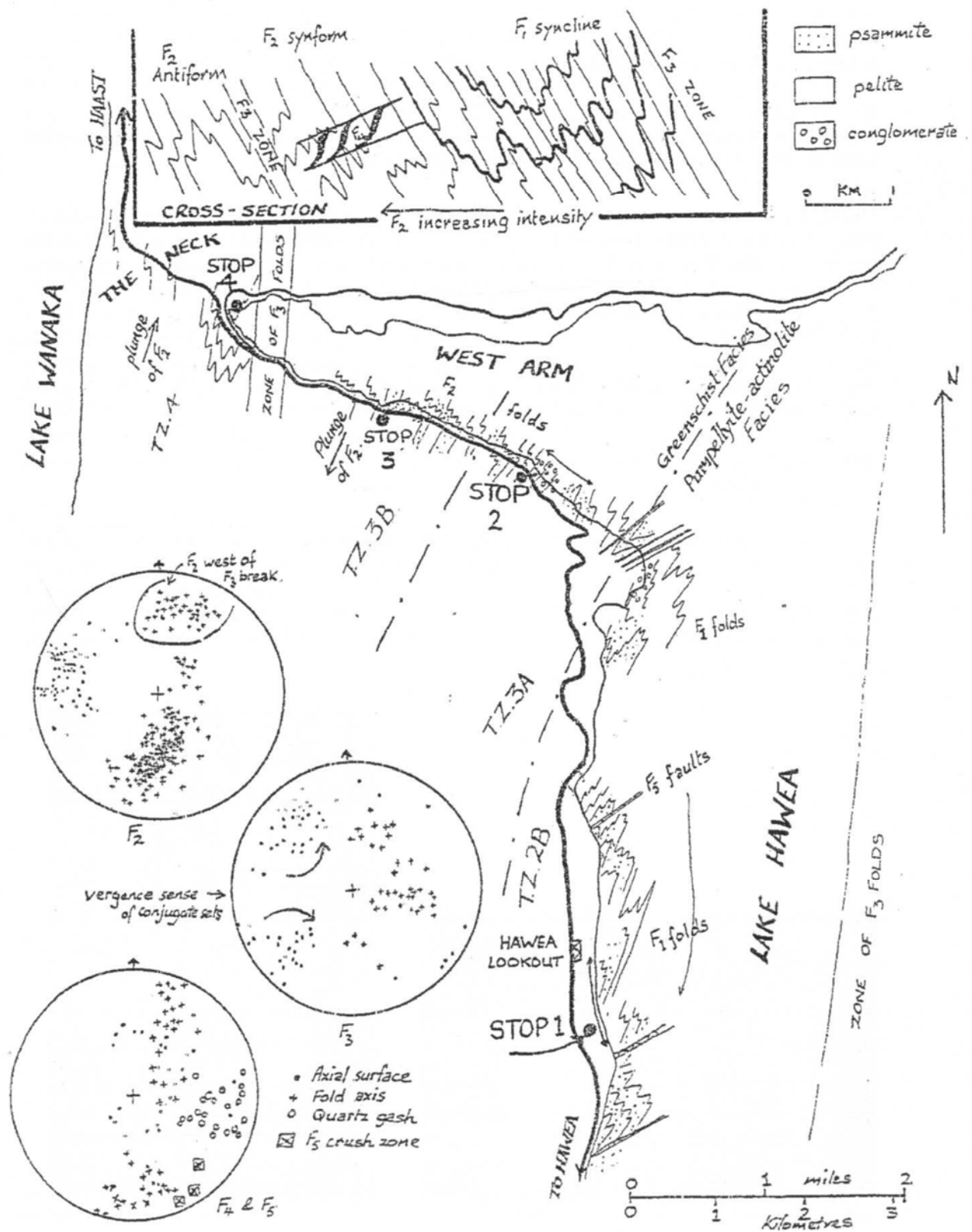


Fig. 1. Structural and metamorphic geology of Lake Hawea

Two generations of early to syn-metamorphic structures and three generations of late to post metamorphic structures have been recognised. The earliest structures recognised are steeply plunging folds in bedding with a well-developed axial-surface cleavage (fig. 2b). They are most clearly seen in the lower grade rocks along the west side of the lake, where fold vergence and graded bedding indicate their being part of the upper limb of a southward facing syncline with an amplitude of about 20 km. This structure is similar to steeply plunging folds described in greywackes further east by Spörli and Lillie (1974) and Ward and Spörli (1979). Accompanying the folds are thick quartz veins and pods developed parallel to the axial surface. Several other vein orientations were produced at the same time. With increasing metamorphic grade westward, metamorphic lamination is developed parallel to the cleavage by pressure solution and recrystallisation. The nature of this lamination is dependent on both the fine and gross lithological characters of the original rock. Deformed conglomerate horizons indicate increasing total strain westward, with constant volume strain ellipsoids for the pebbles of 2.6:1.35:0.3 near the top of TZIIB and 4:1:0.25 within TZIIIA (i.e. 75% shortening perpendicular to cleavage (Norris and Bishop 1990)).

The second generation of structures develop with increasing intensity westwards, from occasional buckles and kinkfolds with patchy development of crenulation cleavage, to an intense, differentiated, crenulation cleavage (fig. 2e) with bedding, early cleavage and early quartz veins (fig. 2d) all tightly folded. Refolded early folds are occasionally recognisable. The form of the later mesoscopic folds is largely governed by the buckling of the early quartz veins and pods which impart a gross mechanical heterogeneity to the rock (fig. 2c). The quartz pods become much thinner in the textural zone IV schists, probably due to greater flattening during deformation. Pressure solution was important in developing the differentiated cleavage and the attenuated folds; quartz veining parallel to the cleavage increases in importance towards higher grade.

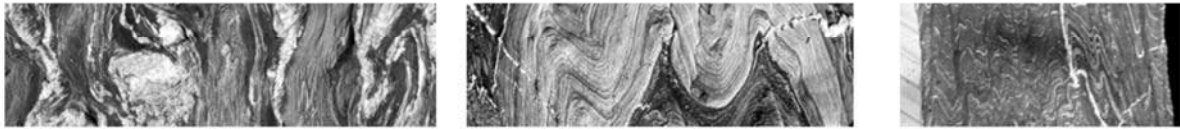
The second generation folds plunge southwards over most of the section but change to northward plunging across a narrow zone of folding and dislocation which trends north-south across the western end of the West Arm. The deformation related to this zone is referred to the third generation of structures; a similar north-south trending zone of deformation is found on the east side of Lake Hawea. Conjugate reclined folds on various scales characterise this generation (fig. 2f); crenulation cleavage is locally developed (fig. 2g) and quartz veining is common. The fourth generation is widespread throughout the area and is mainly represented by shallow dipping conjugate kinkbands (fig. 2i) and zones of en echelon sigmoidal quartz gashes (fig. 2j). Stress analysis for the third and fourth generations indicates a change from subhorizontal compression to subhorizontal extension, assuming no large change in attitude of the foliation (which is a fairly dubious assumption!). On the north side of the Neck, lamprophyre dykes (fig. 2h) dated regionally at 23-28 Ma (Adams and Cooper 1996) postdate kink folds of this folding phase.

The fifth generation of structures consists of northeast- and southeast-trending fault zones containing contorted schists and welded breccia, often impregnated with Fe-rich carbonate. These structures are definitely Cenozoic as, elsewhere, they are associated with and cross lamprophyre dykes of known early Miocene age. Occasional low-angle eastward dipping thrust planes have been recorded; while they definitely post-date F3 (Dingleburn) structures, their relationship with later generations and their regional significance is unknown.

Table 1: Textural zones in the Haast Schist (Turnbull et al., 2001).

Table 3 Revised definitions and features of psammitic and pelitic schist protoliths at different textural grades, as presented in this paper.

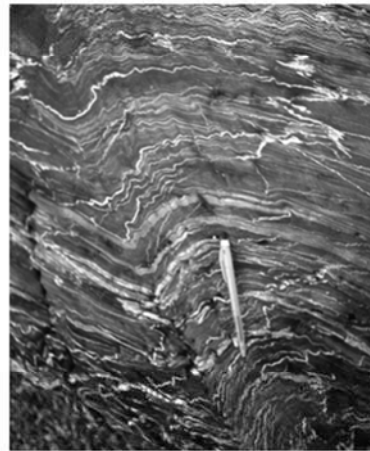
Textural zone	Metamorphic white mica thickness, length, habit	Hand specimen foliation features	Hand specimen quartz vein/segregation features	Thin section textures	Special Otago Schist features	Applicable rock names
I	<5 µm thick/<75 µm long. Naked eye and hand lens reveal only coarse detrital micas	None, or only a spaced fracture cleavage	Local veins	Detrital textures only; no preferred orientation of metamorphic mica	–	Sandstone, mudstone, greywacke, argillite
IIA	<5 µm thick, <75 µm long. Pelites have a matt black colour and can be slaty. Naked eye and hand lens reveal only coarse detrital micas	Weak-mod, anastomosing, penetrative, stronger in fine-grained rocks. Bedding still dominates over cleavage. Hand samples break into wedge-shaped blocks	Local veins	Detrital quartz grains have undulose extinction. Weak preferred orientation of metamorphic micas	–	Foliated greywacke, semi-schist, slate
IIB	5–15 µm thick, <75 µm long. Individual micas not visible through a hand lens. Pelites black but with distinct sheen, psammites grey	Strong, penetrative. Cleavage dominates over bedding which is transposed. Psammitic-pelitic contrasts still easily resolved through colour differences. Hand specimens break into parallel-sided slabs	Appearance of flattened detrital grains may be enhanced but there is no foliation-parallel segregation. Veins locally common but these cut foliation at an angle	Detrital quartz grains still recognisable but mainly composed of subgrains. Strong preferred orientation of mica in anastomosing folia	F2 folds may develop and veins may be locally important. Pumpellyite-out isograd is within TZIIIB	Psammitic or pelitic semi-schist, phyllite, slate
III	15–25 µm thick, 75–125 µm long (very fine sand size). Individual mica grains visible through hand lens, both pelites and psammites are silvery grey	Strong and penetrative but undulating on mm scale, less perfect than IIB. Where seen, psammitic-pelitic contacts are still sharp at mm scale	Distributed foliation-parallel quartz lenses <1 mm thick, throughout rock. Different generations of mm-cm thick veins ubiquitous	Detrital quartz and mica unrecognisable; quartz and mica in rock are approximately equigranular and form sub-mm segregations	Maximum textural grade of volcanoclastic Caples psammites. F2 folds can start to dominate. Garnet-biotite isograd is within TZIII	Quartzofeldspathic schist, greyschist
IV	25–50 µm thick, 125–500 µm long (fine-medium sand size). Individual mica grains clearly visible to naked eye	Strong and penetrative, undulating on mm-cm scale. Psammitic-pelitic contacts blurred at mm scale, but resolvable at cm scale	Essential and widespread quartz veins/segregations >1 mm thick, mainly polydeformed quartz veins	Adjacent quartz and mica grains merge into segregations and folia of variable thickness and length	Main foliation is S2	Quartzofeldspathic schist, greyschist, gneiss



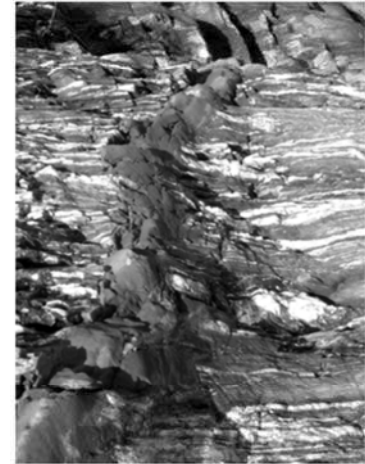
(c) F2 folds in D1 quartz veins and S1. (d) F2 folds in psammites and pelites (e) Differentiated S2 crenulation cleavage



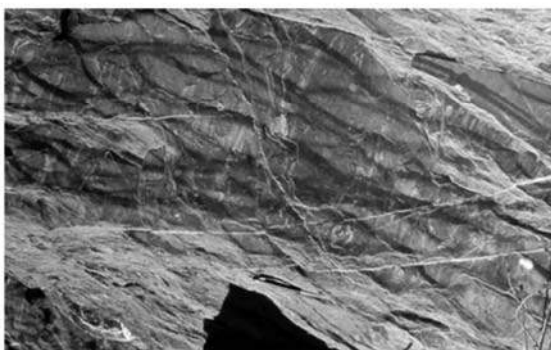
(f) conjugate F3 folds



(g) F3 folds with axial plane S3



(h) crosscutting lamprophyre dyke



(i) F4 kink folds



(j) F4 folds with quartz gashes

STOP R: THE NECK

Textural zone IV, greenschist facies. F2 and L2 are here northward plunging, whereas to the east along the lower grade part of the section they plunge south. A zone of F3 folding and associated faulting crosses the section immediately east of these outcrops and the change in plunge takes place across this zone. Minor kinks and fractures of the F3 generation may be seen in these outcrops.

Note the highly attenuated F2 folds and the very flattened quartz lodes that were so prominent at lower grades. The F2 folds here show sinistral vergence, which coupled with the northward plunge, indicates that they lie on the west limb of a macroscopic F2 synform, whereas the rocks to the east lie within the east limb of the synform.

The road climbs over the narrow neck separating Lakes Hawea and Wanaka. A spectacular view of Lake Wanaka is obtained from a vantage point on the west side of the neck. The road follows the eastern shore of Lake Wanaka to the head of the lake at Makarora. Here the Makarora River flows south from the Main Divide into the head of the lake, forming an extensive delta. A short distance past Makarora the road enters the Mount Aspiring National Park and begins its climb to the Haast Pass. Beech forest forms an extensive cover on the lower slopes of the mountains, while snowy peaks of the Main Divide including Mt Brewster (2423 m - 7950 ft) are visible, if the weather permits. From the pass summit the road winds down the valley of the Haast River through the narrow gorge known as the Gates of Haast, and on to Pleasant Flat where panoramic views of the Southern Alps are obtained, looking up the valleys of the Landsborough and Clark Rivers to Mt Hooker (2652 m - 8700 ft). The lushness of the vegetation reflects the dramatic increase in rainfall that takes place across the Main Divide (e.g. 305 mm - 12 inches/year) at Alexandra and in excess of (6350 mm 250 inches/year) at Haast River.

All the way from Lake Hawea the road has been heading in a fairly constant northerly direction, parallel to the isograds and isotects in the schist. Hence, although a long way from the last stop, the rock type and metamorphic grade are essentially the same.

STOP S: LAKE HAWEA SHORES

Hawea Foreshore

Exposure of textural zone IIB psammities, pelites and metatuff. Psammities are cleaved but generally lack the segregation lamellae present in the pelites, although a coarse lamination is locally developed parallel to cleavage by pressure solution. This results in dark mica-rich seams dividing the rock into thin lenses or microlithons parallel to cleavage. Microscopically, they retain traces of the original clastic texture in a thoroughly recrystallised matrix. Occasional colourless pumpellyite without prehnite indicates the rocks belong to the pumpellyite-actinolite facies. Graded bedding is occasionally preserved in the interbedded psammite/pelite units.

Bedding (S₀) is the form surface of tight to isoclinal folds (wavelength ca 1 metre) with sporadic quartz lodes developed parallel to the axial surfaces (S₁). The lodes contain additional albite and calcite and typically have a chlorite selvage adjacent to the enclosing schist. The folds (F₁) generally show sinistral vergence and occasional graded bedding indicates that they face southwest. This suggests that the rocks are part of the eastern limb of a southwest facing F₁ syncline.

Thin early quartz veins are occasionally found folded and transposed by F1. More commonly however, folded quartz veins are discordant to F1 folds, suggesting emplacement after the initiation of F1 folds and folding during a later stage of deformation during which tightening up of the F1 structures took place.

Bedding and S1 are occasionally folded into tight chevron or kink style folds with steep axial surfaces and steeply plunging hinges. Locally they develop an axial plane crenulation cleavage. Regionally folds of this style and orientation are common in north striking belts paralleled to faults. They are post-metamorphic in age and represent the third phase of deformation recognised in the Lake Hawea area. 2-3 cm quartz gashes, often in an echelon arrays are associated with shallow dipping kinkbands that represent the fourth generation of structures (F4). Folds of this generation are widespread throughout the Hawea section. A third post-metamorphic generation of structures consists of northeast trending faults with associated locally developed folds. The fault planes are impregnated with ankeritic carbonate and commonly have well indurated breccias developed on them. These faults may be related to the Otago block fault system.

West arm of Lake Hawea - east end

The section comprises units of pelitic and interbedded pelitic and psammitic schist, together with units of conglomerate and rare, very thin greenschist horizons (metatuff?). The section is just upgrade from the zone IIIA isograd and from the greenschist facies isograd, so that clinozoisite has largely replaced pumpellyite. The greenschists are rich in actinolite. Thick irregular quartz lodes parallel to S1 are common, and lamination is developed in all psammities although it is very variable in intensity; some thin units of intensely laminated schist may be seen. The conglomerates range from granule to cobble conglomerates, although the clasts are so strongly deformed that generally only the larger ones are recognisable. A prominent band of cobble conglomerate (see section) is folded into an F1 fold. Well over 60% of clasts are of intrabasinal psammite and pelite, while the exotic clasts include tonalite, adamellite and epidosite. K-feldspar in these clasts is largely replaced by chessboard albite+stilpnomelane and biotite by chlorite, but much of the original igneous texture is preserved. Prominent pressure shadow tails of quartz and albite are developed on the clast margin parallel to the foliation. Measurements of clasts suggest a strain ellipsoid shape of 4:1:0.25 (75% flattening perpendicular to foliation), with the long axis parallel to the F1 fold axis (Norris and Bishop 1990). This estimate of flattening undoubtedly represents a minimum value, due to the difficulty of measuring the most deformed clasts.

F1 folds in bedding are easily recognised at the east end of the section - they are very appressed and transposition along their axial surfaces is locally strongly developed. F2 folds, with moderately steeply southward plunging axes, occur sporadically, particularly in the D1 quartz lodes. A crenulation cleavage is developed locally around the folded lodes. F2 folds and S2 cleavage increase in intensity towards the west end of the section. F4 kink folds and associated quartz gashes and veins are abundant - they usually dip shallowly westward, with some en echelon gashes dipping more steeply. The road outcrop opposite the passing bay show intense development of F4 kink bands to the extent that a crude crenulation cleavage is developed.

Many generations of veins containing quartz and other silicates may be seen – these apparently formed during all stages of the metamorphic and structural history. Their

presence attests to the ease of transfer of material in solution – plentiful fluid inclusions in the vein material indicate the former presence of a fluid phase

West Arm, Lake Hawea – west end

The party will work its way down to the first exposures on the lakeshore about 100m to the east (provided the lake level is not too high - otherwise we will examine the road cuttings). For the next 200-300 m eastward there are extensive exposures of interbanded psammities and pelites showing intensive folding by the D2 generation of structures. The rocks are in textural zone IIIB, greenschist facies, chlorite zone. Note the folding of S1 segregation laminae and the development of an S2 crenulation cleavage. The folds in general have formed by a buckling process and psammities and pelites form class 1C and 3 styles respectively (as defined by Ramsay 1967). The folds show thickened hinges and thinned limbs, sometimes to the extreme; the process is helped by pressure solution along the axial surface cleavage which locally leads to a differentiated crenulation cleavage.

The D1 quartz lodes represent heterogeneities in the rocks during D2 folding - folds in psammite bands often show intense distortion in the neighbourhood of a buckled quartz lode. The D2 deformation appears to have been strongly non-co-axial, at least locally, as F2 folds with S1 as form surface have been refolded by identical folds of ostensibly the same generation. In the more pelitic lithologies, the quartz lodes largely controlled the development of minor structures. Boudinage and the development of quartz rodding may also be seen. Refolded F1 folds are occasionally recognisable within this section. As along most of the West Arm section, the F2 folds show sinistral vergence.

REFERENCES

- Adams, C. J. and Nathan, S. 1978. Cretaceous chronology of the lower Buller Valley, South Island, New Zealand. *New Zealand Journal of Geology and Geophysics* 21, 455-462.
- Barth, N.C., Toy, V.G., Langridge, R., Norris, R.J. 2012. Scale dependence of oblique plate boundary partitioning: new insights from LiDAR, central Alpine Fault Zone, New Zealand. *Lithosphere* 4(X), 1-14. doi: 10.1130/L201.1
- Batt, G. E., Braun, J., Kohn, B. P. and McDougall, I. 2000. Thermochronological analysis of the dynamics of the Southern Alps, New Zealand. *Geological Society of America Bulletin* 112(2), 250-266.
- Berryman, J. R. 1975. Earth Deformation Studies Reconnaissance of the Alpine Fault. In: *New Zealand Geological Survey, Earth Deformation Section E.D.S. 30a & 30b*. Department of Scientific and Industrial Research, Lower Hutt. Berryman, K., Almond, P., Villamor, P., Read, S., Tonkin, P., Alloway, B. 2009. Alpine Fault ruptures shape the geomorphology of Westland, New Zealand: data from the Whataroa Catchment. 7th International Conference on Geomorphology, Melbourne, Australia.
- Berryman, K. R.; Almond, P.; Tonkin, P.; Read, S. A. L.; Cullen, L.; Duncan, R.; Stewart, G.; Alloway, B. V.; Barrell, D. J. A.; McSaveney, M. J. 2001 Alpine Fault rupture and landscape evolution in Westland, New Zealand. p. 28 In: Litchfield, N.J. (comp.) *Ten years of paleoseismology in the ILP : progress and prospects : 17-21 December 2001, Kaikoura, New Zealand : programme and abstracts*. Lower Hutt: Institute of Geological & Nuclear Sciences Limited. Institute of Geological & Nuclear Sciences information series 50.
- Berryman, K.R.; Wilson, K.J.; Cochran, U.A.; Biasi, G. 2009 Progress towards deciphering a c. 7kyr record of surface ruptures on the Alpine Fault. p. 21 In: Barrell, D.J.A.; Tulloch, A.J. (eds) *Geological Society of New Zealand & New Zealand Geophysical Society Joint Annual Conference, Oamaru, 23-27 November 2009: programme and abstracts*. Geological Society of New Zealand miscellaneous publication 128A.
- Billia, M., Timms, N., Toy, V., Hart, R., Prior D. 2013. Grain boundary dissolution porosity in quartzofeldspathic ultramylonites: Implications for permeability enhancement and weakening of mid-crustal shear zones. *Journal of Structural Geology* 53, 2-14. doi: 10.1016/j.jsg.2013.05.004
- Boulton, C.J., Toy, V.G. 2008. Shallow coseismic rocks of the Alpine Fault zone. Abstract and Poster. *Geosciences '09*. Te Papa, Wellington.
- Boulton, C., Moore, D.E., Lockner, D.A., Toy, V.G., Townend, J., Sutherland, R., 2014. Frictional properties of exhumed fault gouges in DFDP-1 cores, Alpine Fault, New Zealand. *Geophysical Research Letters*, doi: 10.1002/2013GL058236 .
- Boulton, C.J., Carpenter, B.M., Toy, V.G., Marone, C. 2012. Physical properties of surface-outcrop cataclastic fault rocks, Alpine Fault, New Zealand. *Geochemistry, Geophysics, Geosystems* 13, Q01018. doi:10.1029/2011GC003872.
- Carpenter, B.M. Kitajima, H., Sutherland, R., Townend, J., Toy, V.G., Saffer, D. 2014. Hydraulic and acoustic properties of the active Alpine Fault, New Zealand: Laboratory measurements on DFDP-1 drill core. *Earth and Planetary Science Letters* 390, 45-51. Chamberlain, C. P., Zeitler, P. F. and Cooper, A. F. 1995. Geochronologic constraints of the uplift and metamorphism along the Alpine Fault, South Island, New Zealand. *New Zealand Journal of Geology and Geophysics* 38, 515-523.

- Cooper, A. F. 1980. Retrograde alteration of chromian kyanite in metachert and amphibolite whiteschist from the Southern Alps, New Zealand, with implications for uplift on the Alpine Fault. *Contributions to Mineralogy and Petrology* 75, 153-164.
- Cooper, A. F. and Norris, R. J. 1994. Anatomy, structural evolution, and slip rate of a plate-boundary thrust: The Alpine Fault at Gaunt Creek, Westland, New Zealand. *Geological Society of America Bulletin* 106, 627-635.
- Cox, S., and Barrell, D. 2007. Geology of the Aoraki Area, Geological and Nuclear Sciences, Ltd, Lower Hutt, New Zealand: 1,250,000 Geological Map Sheet 15.
- Cox, S.C.; Barrell, D.J.A. (comps) 2007 Geology of the Aoraki area : scale 1:250,000. Lower Hutt: GNS Science. Institute of Geological & Nuclear Sciences 1:250,000 geological map 15 . 71 p. + 1 folded map.
- Craw, D. 1988. Shallow-level metasomatic fluids in a high uplift rate metamorphic belt; Alpine Schist, New Zealand. *Journal of Metamorphic Geology* 6, 1-16.
- Craw, D. 1997. Fluid inclusion evidence for geothermal structure beneath the Southern Alps, New Zealand. *New Zealand Journal of Geology and Geophysics* 40, 43-52.
- Cullen, L.E., Duncan, R.P., Wells, A., Stewart, G.H., 2003. Floodplain and regional scale variation in earthquake effects on forests, Westland, New Zealand: *Journal of the Royal Society of New Zealand* 33: 693–701.
- Cutten H 1985. Reconnaissance of the Alpine Fault and Local Geology of South Westland. K. Berryman and H. Cutten, N.Z. Geological Survey, Earth Deformation Section E.D.S. 85/4. Dept. of Scientific and Industrial Research, New Zealand.
- Findlay, R. H. 1987. Structure and interpretation of the Alpine schists in Copland and Cook River Valleys, South Island, New Zealand. *New Zealand Journal of Geology and Geophysics* 30, 117-138.
- Gillam, B., Little, T.A., Smith, E., Toy, V.G., 2013. Extensional shear band development on the outer margin of the Alpine mylonite zone, Tatara Stream, Southern Alps, New Zealand. *Journal of Structural Geology*, 53, 1-20. doi:10.1016/j.jsg.2013.06.010.
- Grapes, R. H. 1995. Uplift and exhumation of Alpine Schist, Southern Alps, New Zealand: thermobarometric constraints. *New Zealand Journal of Geology and Geophysics* 38, 525-533.
- Grapes, R. H. and Watanabe, T. 1992. Metamorphism and uplift of Alpine Schist in the Franz Josef-Fox Glacier area of the Southern Alps, New Zealand. *Journal of Metamorphic Geology* 10, 171-180.
- Grapes, R. H. and Watanabe, T. 1994. Mineral composition variation in Alpine Schist, Southern Alps, New Zealand; Implications for recrystallization and exhumation. *The Island Arc* 3, 163-181.
- Grapes, R., Little, T. A. and Vry, J. K. 1998. Aspiring lithological association extended through Alpine Schist, Marlborough Schist and Wellington greywacke. *Geological Society of New Zealand Miscellaneous Publication* 101A, 151.
- Griffiths, G. A., 1979, High sediment yields from major rivers of the Western Southern Alps, New Zealand: *Nature* 282: 61–63.
- Grindley, G. W. 1963. Structure of the Alpine Schists of South Westland, Southern Alps, New Zealand. *New Zealand Journal of Geology and Geophysics* 6, 872-930.

- Hanson, C. R., Norris, R. J. and Cooper, A. F. 1990. Regional fracture patterns east of the Alpine Fault between the Fox and Franz Josef glaciers, Westland, New Zealand. *New Zealand Journal of Geology & Geophysics* 33, 617-622.
- Holcombe, R. J. and Little, T. A. 2001. A sensitive vorticity gauge using rotated porphyroblasts, and its application to rocks adjacent to the Alpine Fault, New Zealand. *Journal of Structural Geology* 23, 979-989.
- Holm, D. K., Norris, R. J. and Craw, D. 1989. Brittle and ductile deformation in a zone of rapid uplift : Central Southern Alps, New Zealand. *Tectonics* 8, 153-168.
- Jenkin, G. R. T., Craw, D. and Fallick, A. E. 1994. Stable isotopic and fluid inclusion evidence for meteoric fluid penetration into an active mountain belt; Alpine Schist, New Zealand. *Journal of Metamorphic Geology* 12, 429-444.
- Ji, S. and Xia, B. 2002. *Rheology of Polyphase Earth Materials*. Montreal: Polytechnic International Press.
- Kennedy, C. 2005. Structure and petrology of the garnet isograd, Franz Josef, Westland, New Zealand, Victoria University.
- Little, T. A. 2004. Transpressive ductile flow and oblique ramping of lower crust in a two-sided orogen: Insight from quartz grain-shape fabrics near the Alpine Fault, New Zealand. *Tectonics* 23, TC2013.
- Little, T. A., Cox, S., Vry, J. K. and Batt, G. 2005. Variations in exhumation level and uplift rate along the oblique-slip Alpine Fault, central Southern Alps, New Zealand. *Geological Society of America Bulletin* 117(5/6), 707-723.
- Little, T. A., Holcombe, R. J. and Ilg, B. R. 2002a. Ductile fabrics in the zone of active oblique convergence near the Alpine Fault, New Zealand: identifying the neotectonic overprint. *Journal of Structural Geology* 24, 193-217.
- Little, T. A., Holcombe, R. J. and Ilg, B. R. 2002b. Kinematics of oblique collision and ramping inferred from microstructures and strain in middle crustal rocks, central Southern Alps, New Zealand. *Journal of Structural Geology* 20, 219-239.
- Little, T. A., Wightman, R. H., Holcombe, R. J. and Hill, M. P. 2007. Transpression models and ductile deformation of the lower crust of the Pacific Plate in the central Southern Alps, a perspective from structural geology. In: *Tectonics of a Continental Transform Plate Boundary: The South Island, New Zealand*: (edited by Davey, F., Okaya, D. and Stern, T.). American Geophysical Union, Washington, D.C., 273-290.
- Maeder, X., Passchier, C. W. and Trouw, R. A. J. 2007. Flame foliation: Evidence for a schistosity formed normal to the extension direction. *Journal of Structural Geology* 29(3), 378-384.
- Mortimer, N. and Cooper, A. F. 1994. U-Pb ages and Sm-Nd ages from the Alpine Schist, New Zealand. *New Zealand Journal of Geology and Geophysics* 47, 21-28.
- Nathan, S., Rattenbury, M. S. and Suggate, R. P. 2002. *Geology of the Greymouth area*. Institute of Geological and Nuclear Sciences.

- Niemeijer, A., Boulton, C., Toy, V.G., Townend, J., Sutherland, R., 2016. Large-displacement Implications for deep rupture propagation. *Journal of Geophysical Research*, doi: 10.1002/2015JB012593, hydrothermal frictional properties of DFDP-1 fault rocks, Alpine Fault, New Zealand:
- Norris, R. J. and Cooper, A. F. 1986. Small-scale fractures, glaciated surfaces, and recent strain adjacent to the Alpine fault, New Zealand. *Geology* 14, 687-690.
- Norris, R. J. and Cooper, A. F. 1995. Origin of small-scale segmentation and transpressional thrusting along the Alpine Fault, New Zealand. *Geological Society of America Bulletin* 107, 231-240.
- Norris, R. J. and Cooper, A. F. 1997. Erosional control on the structural evolution of a transpressional thrust complex on the Alpine Fault, New Zealand. *Journal of Structural Geology* 19(10), 1323-1343.
- Norris, R. J. and Cooper, A. F. 2003. Very high strains recorded in mylonites along the Alpine Fault, New Zealand: implications for the deep structure of plate boundary faults. *Journal of Structural Geology* 20, 2141-2157.
- Norris, R. J. and Cooper, A. F. 2008. The Alpine Fault, New Zealand: Surface geology and field relationships. In Okaya, D., Stern, T. and Davy, F. (eds), *Tectonics of a continental transform plate boundary: the South Island, New Zealand*, American Geophysical Union Monograph, Washington DC., 159-170.
- Norris, R. J. and Craw, D. 1987. Aspiring terrane: an oceanic assemblage from New Zealand and its implications for Mesozoic terrane accretion in the Southwest Pacific. In: *Terrane Accretion in Orogenic Belts 19*. American Geophysical Union, Washington, D.C., 169-177.
- Norris, R.J., Koons, P.O. and Cooper, A.F. 1990. The obliquely-convergent plate boundary in the South Island of New Zealand: implications for ancient collision zones. *Journal of Structural Geology* 12 (5/6). 715-725.
- Norris, R. J., Toy, V. G., 2014. Continental transforms: A view from the Alpine Fault. *Journal of Structural Geology* 64, 3-31. doi: 10.1016/j.jsg.2014.03.003.
- Palmer, E. 2000. Growth and deformation history of Alpine Schist garnets. Franz Josef Glacier, Westland, New Zealand Victoria University.
- Rattenbury, M. S. 1987. Timing of mylonitisation west of the Alpine Fault, central Westland, New Zealand. *New Zealand Journal of Geology and Geophysics* 30, 287-297.
- Rattenbury, M. S. 1991. The Fraser Complex: high-grade metamorphic, igneous and mylonitic rocks of central Westland. *New Zealand Journal of Geology and Geophysics* 34, 23-33.
- Rattenbury, M. S., Cooper, A. F. and Norris, R. J. 1988. Recent Alpine Fault thrusting at Kaka Creek, central Westland, New Zealand (Note). *New Zealand Journal of Geology and Geophysics* 31, 117-120.
- Read, S. E. 1994. Alpine Fault Segmentation and Range Front Structure between Gaunt Creek and Little Man River, near Whataroa, central Westland, New Zealand. Unpublished BSc(Hons) thesis, University of Otago.
- Reed, J. J. 1964. Mylonites, cataclasites, and associated rocks along the Alpine Fault, South Island, New Zealand. *New Zealand Journal of Geology and Geophysics* 7, 645-684.

- Sammis, G.C., Osborne, R.H., Anderson, J.L., Banerdt, M., and White, P. 1986. Self-similar cataclasis in the formation of fault gouge. *Pure and Applied Geophysics*. 124, 53-78.
- Schleicher, A.J., Sutherland, R., Townend, J., Toy, V.G., van der Pluijm, B. 2015,.. Clay mineral formation and fabric development in the DFDP-1B borehole, central Alpine Fault, New Zealand. *New Zealand Journal of Geology & Geophysics* doi: 10.1080/00288306.2014.979841.
- Sibson, R. H., White, S. H. and Atkinson, B. K. 1979. Fault rock distribution and structure within the Alpine Fault zone: a preliminary account. *Royal Society of New Zealand Bulletin* 18, 55-65.
- Sibson, R. H., White, S. H. and Atkinson, B. K. 1981. Structure and distribution of fault rocks in the Alpine Fault Zone, New Zealand. In: *Thrust and Nappe Tectonics 9*. Geological Society, London, 197-210.
- Spray, J. G. 1987. Artificial generation of pseudotachylite using friction welding apparatus: simulation of melting on a fault plane. *Journal of Structural Geology* 9(1), 49-60.
- Stern et al. 2007. Geophysical exploration of the Alpine Fault zone. *Geophysical Monograph* 175: 207-233.
- Stern, T., Kleffmann, S., Okaya, D., Scherwath, M. and Bannister, S. 2001. Low seismic-wave speeds and enhanced fluid pressure beneath the Southern Alps of New Zealand. *Geology* 29(8), 679-682.
- Suggate, R.P., 1990, Late Pliocene and Quaternary glaciations of New Zealand: *Quaternary Science Reviews*, v. 9, p. 175–197,
- Sutherland, R.; Townend, J.; Toy, V.; the DFDP-2 Science Team, 2015: Deep Fault Drilling Project (DFDP), Alpine Fault Boreholes DFDP-2A and DFDP-2B Technical Completion Report, GNS Science Report 2015/50.
- Sutherland, R., Kim, K., Zondervan, A., McSaveney, M. 2007. Orbital forcing of mid-latitude Southern Hemisphere glaciation since 100 ka inferred from cosmogenic nuclide ages of moraine boulders from the Cascade Plateau, southwest New Zealand. *GSA Bulletin* 119: 443-451.
- Sutherland, R.S., Toy, V.G., Townend, J. et al. 2012. Drilling reveals fluid control on architecture and rupture of the Alpine Fault, New Zealand. *Geology* 40, 1143-1146.
- Swanson, M. T. 1992. Fault structure, wear mechanisms and rupture processes in pseudotachylite generation. *Tectonophysics* 204, 223-242.
- Tippert, J. M. and Kamp, P. J. J. 1993. Fission track analysis of the late Cenozoic vertical kinematics of continental Pacific crust, South Island, New Zealand. *Journal of Geophysical Research* 98, 16119-16148.
- Townend, J., Sutherland, R., Toy, V.G., Eccles, J., Boulton, C., Cox, S., MacNamara, D. 2013. Late-interseismic state of a continental plate-bounding fault: petrophysical results from DFDP-1 wireline logging and core analysis, Alpine Fault, New Zealand. *Geochemistry, Geophysics, Geosystems* 14(9), 3801-3820. doi: 10.1002/ggge.20236.
- Toy, V. G. 2008. Rheology of the Alpine fault mylonite zone: deformation processes at and below the base of the seismogenic zone in a major plate boundary structure. Unpublished PhD thesis, University of Otago.

- Toy, V.G., Boulton, C.J., Sutherland, R., Townend, J., Norris, R.J., Little, T.A., Prior, D.J., Mariani, E., Faulkner, D., Menzies, C.D., Scott, H., Carpenter, B.M. 2015. Fault rock lithologies and architecture of the central Alpine Fault, New Zealand, revealed by DFDP-1 drilling. *Lithosphere* 7(2), 155-173. doi:10.1130/L395.
- Toy, V.G., Craw, D., Cooper, A.F., Norris, R.J. 2010. Thermal regime in the central Alpine Fault zone, New Zealand: Constraints from microstructures, biotite chemistry, and fluid inclusion data. *Tectonophysics* 485, 175-189. doi: 10.1016/j.tecto.2009. 12.013.
- Toy, V.G., Norris, R.J., Prior, D.J., Cooper, A.F., Walrond, M. 2013. How do lineations reflect the strain history of transpressive shear zones? The example of the active Alpine Fault Zone, New Zealand. *Journal of Structural Geology* 50, 187-198. doi: 10.1016/j.jsg.2012.06.006.
- Toy, V. G., Prior, D. J. and Norris, R. J. 2008. Quartz textures in the Alpine fault mylonites: influence of pre-existing preferred orientations on fabric development during progressive uplift. *Journal of Structural Geology* 30(1), 602-621.
- Toy, V.G., Prior, D.J., Norris, R.J., Cooper, A.F. 2012. Relationships between kinematic indicators and strain during syn-deformational exhumation of an oblique slip, transpressive, plate boundary shear zone: the Alpine Fault, New Zealand. *Earth and Planetary Science Letters* 333-334, 282-292. doi: 10.1016/j.epsl.2012.04.037.
- Turnbull, I.M., Mortimer, N., Craw, D. 2001. Textural zones in the haast Schist – a reappraisal. *New Zealand Journal of geology & Geophysics* 44(1), 171-183, doi: 10.1080/00288306.2001.9514933.
- Vry, J. K., Baker, J., Maas, R., Little, T. A., Grapes, R. and Dixon, M. 2004. Zoned (Cretaceous and Cenozoic) garnet and the timing of high-grade metamorphism, Southern Alps, New Zealand. *Journal of Metamorphic Geology* 22, 137-157.
- Waight, T. E., Weaver, S. D., Ireland, T. R., Maas, R., Muir, R. J. and Shelley, D. 1997. Field characteristics, petrography, and geochronology of the Honhu Batholith and the adjacent Granite Hill Complex, North Westland, New Zealand. *New Zealand Journal of Geology and Geophysics* 40, 1-17.
- Warr, L. N., van der Pluijm, B. A. and Tourscher, S. 2007. The age and depth of exhumed friction melts along the Alpine Fault, New Zealand. *Geology* 35(7), 603-606.
- Warr, L. N., van der Pluijm, B. A., Peacor, D. R. and Hall, C. M. 2003. Frictional melt pulses during a 1.1 Ma earthquake along the Alpine Fault, New Zealand. *Earth and Planetary Science Letters* 209, 39-52.
- Warren, G. 1967. Sheet 17 – Hokitika. In: *Geological Map of New Zealand 1:250,000*. DSIR, Wellington, New Zealand.
- Wells, A., Yetton, M. D., Duncan, R. P. and Stewart, G. H. 1999. Prehistoric dates of the most recent Alpine fault earthquakes, New Zealand. *Geology* 27(11), 995-998.
- Wightman, R. H. and Little, T. A. 2007. Deformation of the Pacific Plate above the Alpine Fault ramp and its relationship to expulsion of metamorphic fluids: An array of backshears. In: *Tectonics of a Continental Transform Plate Boundary: The South Island, New Zealand* (edited by Davey, F., Okaya, D. and Stern, T.). American Geophysical Union, Washington, D.C.

- Wightman, R., Prior, D., and Little, T. A. 2006. Quartz veins deformed by diffusion creep-accommodated grain boundary sliding during a transient, high strain-rate event in the Southern Alps, New Zealand, *Journal of Structural Geology*, 28, 902-918.
- Wright, C. A. 1994. Alpine Fault and Related Geology of the Kokatahi Valley, Westland, New Zealand. Unpublished BSc(Hons) thesis, University of Otago.
- Wright, C. A. 1998a. Geology and Palaeoseismology of the Central Alpine Fault, Westland, New Zealand. Unpublished MSc thesis, University of Otago.
- Wright, C. A. 1998b. The AD930 log-runout Round Top debris avalanche, Westland, New Zealand. *New Zealand Journal of Geology and Geophysics* 41(4), 493-497.
- Yetton MD, 2000. The probability and consequences of the next Alpine Fault earthquake, South Island, New Zealand. Doctor of Philosophy thesis, University of Canterbury.
- Yetton, M., Wells, A. and Traylen, N. J. 1998. The probability and consequences of the next Alpine Fault earthquake. In: EQC Research Report 95/193.